REDUCTION OF RUBISCO ACTIVASE LEVELS IN TOBACCO USING ANTISENSE RNA

A thesis submitted by Colleen Mate for the degree of Doctor of Philosophy of the Australian National University

Molecular Plant Physiology

Research School of Biological Sciences

May 1994

CANDIDATE'S STATEMENT

This thesis embodies independent research carried out in the laboratory of Dr. T.J. Andrews, Molecular Plant Physiology, Research School of Biological Sciences. The production of the tobacco and spinach *rca* cDNAs, and the construction of the plasmids pTACT2 and pαTACT described in Chapter 2 was the work of Yvonne Arvidsson and Graham Hudson. The determination of T-DNA copy number using inverse PCR was carried out by Graham Hudson (described in Chapter 2). The anti-SSU plants used in experiments described in Chapters 5 & 6 were produced by Graham Hudson.

The information presented in this thesis has not been submitted for the purposes of obtaining a higher degree at any other university.

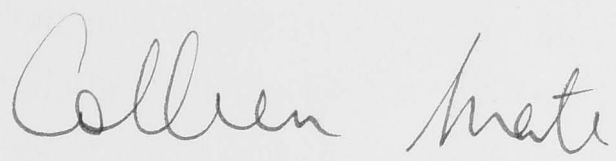

Colleen Mate

ACKNOWLEDGEMENTS

Thankyou to John A., Susanne, Graham H. and John E.

Special thanks to Heather, Nerida, Yvonne and Barbara for their assistance and encouragement, and to Steve for his support and cups of tea.

ABSTRACT

Rubisco (ribulose-1,5-bisphosphate carboxylase/oxygenase) catalyses the carboxylation and oxygenation of ribulose-1,5-bisphosphate (RuBP), reactions central to the photosynthetic carbon reduction (PCR) and the photorespiratory carbon oxidation (PCO) cycle, respectively. Fixation of atmospheric CO_2 by Rubisco's carboxylation of RuBP is the only reaction which results in net acquisition of organic carbon by plants. A two-step activation must occur before Rubisco can catalyse the carboxylation or oxygenation of RuBP. Firstly, the site is carbamylated by addition of an activator CO_2 molecule to lysine residue 201, and then activation is completed by the binding of a Mg^{2+} ion to the carbamylated site. *In vitro* kinetics of activation imply that Rubisco would be only 30-35% active at *in vivo* pH and concentrations of CO_2 and Mg^{2+} (reviewed in Andrews and Lorimer, 1987). These studies, together with other observations showing that RuBP binds so tightly to Rubisco's inactive sites that it blocks carbamylation (Jordan and Chollet, 1983), raised questions about how carbamylation is facilitated *in vivo*. The analysis of a mutant of *Arabidopsis thaliana* that required high CO_2 for growth (Somerville et al., 1982) lead to the identification of a protein, Rubisco activase, with a critical role in the activation of Rubisco *in vivo* (Salvucci et al., 1985). *In vitro* studies showed that activase removes sugar phosphates from Rubisco's catalytic sites, thereby relieving the tight binding of RuBP to Rubisco's inactive sites (Portis, 1990) and that in the presence of RuBP, activase stimulates full carbamylation of Rubisco at *in vivo* pH and concentrations of CO_2 and Mg^{2+} (Portis et al., 1986).

In this study, activase levels were reduced in tobacco *(Nicotiana tabacum)* by transformation with an antisense gene directed against the mRNA for activase. These activase-deficient plants were used to investigate the roles and mechanism of activase *in vivo*. High CO_2 concentrations were required for survival of anti-activase primary transformants after transfer from tissue culture to soil. Immunoblotting of leaf extracts from eighteen primary transformants indicated a range of activase levels. Two of the primary transformants had activase levels that were less than 50% of wild-type and one primary transformant (#52) had activase levels that were less than 25% of wild-type. Inverse PCR analysis indicated that plant #52 had two T-DNA copies inserted into its genome, and the self-progeny of this plant were used exclusively in subsequent experiments. Approximately 25% of the R_1 progeny of anti-activase plant #52 died when raised at atmospheric CO_2 (0.03%), and only 25% of the progeny had

reasonable growth rates. Growth at high CO_2 (0.3%) ensured survival of all R_1 progeny.

The anti-activase R_1 progeny of plant #52 had a range of photosynthetic rates. The Rubisco carbamylation level in photosynthetically impaired plants declined upon illumination. By contrast, illumination increased the carbamylation level in the control plants. The reduction in Rubisco carbamylation level in the anti-activase plants was accompanied by a two-fold increase in the RuBP / PGA ratio, compared to the controls.

Carboxyarabinitol-1-phosphate (CA1P) binds very tightly to Rubisco's catalytic sites, because of its similarity to the six-carbon intermediate of the carboxylase reaction. It accumulates in the darkened leaves of some plants species, including tobacco (Seemann et al., 1985). CA1P binding results in a decrease in the maximum catalytic turnover rate (k_{cat}) of Rubisco. The dark-to-light increase in k_{cat} that accompanies CA1P release occurred to similar extents in antisense and control plants, indicating that normal levels of activase were not essential for CA1P release from Rubisco in the antisense plants. However, CA1P was released in the antisense plants at less than one-quarter of the rate that it was released in the control plants, suggesting a role for activase in accelerating the release of CA1P.

A new, sensitive method for the quantitation of activase protein was developed using immunological techniques. The fusion protein, glutathione *S*-transferase - spinach activase, was purified from *E.coli* and used to obtain activase-specific polyclonal antiserum from rabbits. The antiserum was used in a quantitative immunoblot procedure. The activase bands on the immunoblots were visualised by enhanced chemiluminescence (ECL) and quantified by densitometry. The ECL detection system was very sensitive - 5 ng of activase could be detected reliably - and it responded linearly up to 100 ng. The average activase concentration in leaves of wild-type plants was 42 mg m^{-2}, and their activase to Rubisco stoichiometry was approximately one activase tetramer for every ten octamers of Rubisco. Analysis of air-grown anti-activase plants demonstrated that very low activase concentrations (<5% of wild-type) could support wild-type levels of Rubisco carbamylation and photosynthetic rate under steady-state conditions. These results prove that equimolar concentrations of activase and Rubisco are not required for maintenance of Rubisco carbamylation levels. Thus we conclude that activase does not interact with Rubisco as a ligand or missing subunit, but rather as a catalyst of sugar phosphate release.

There was a reduction in the photosynthetic rate of all air-grown anti-activase plants when activase concentrations decreased below a threshold level, which was approximately 4.5% of wild-type. The range of photosynthetic rates in these plants was proportional to their content of carbamylated Rubisco sites. However, the photosynthetic rates of the high-CO_2-grown anti-activase plants were lower then expected based on measures of Rubisco carbamylated site content. Several possible explanations for this disparity between observed and expected photosynthetic rate in the high-CO_2-grown plants are discussed.

The Rubisco content and the fraction of total leaf protein partitioned into Rubisco in the activase-deficient plants increased above control levels during plant development. These increases were greatest in the plants grown in CO_2-enriched atmospheres. The Rubisco content of the youngest, fully expanded leaves in these plants increased from an average of 1.5 g m^{-2} to 1.8 g m^{-2} during development and, due to the decline in total leaf protein over this period, their protein partitioning into Rubisco increased from 0.27 g g^{-1} to 0.60 g g^{-1}. It appears that the low Rubisco carbamylation level in these plants has lead to an increase in Rubisco concentration This raises the interesting possibility that Rubisco levels may be governed in the long term according to photosynthate supply or the balance between photosynthate supply and demand.

ABBREVIATIONS

ATP	adenosine triphosphate
BSA	bovine serum albumin
CA1P	2'-carboxy-D-arabinitol 1-phosphate
CABP	2'-carboxy-D-arabinitol 1,5-bisphosphate
Chl	chlorophyll
CaMV	cauliflower mosaic virus
CPBP	2'-carboxy-D-pentitol 1,5-bisphosphate
cDNA	complementary deoxyribonucleic acid
DNA	deoxyribonucleic acid
dNTPs	deoxynucleotide triphosphates
DTT	dithiothreitol
[E]	inactive Rubisco
[ER]	inactive Rubisco with RuBP bound
[ECM]	carbamylated Rubisco
ECL	enhanced chemiluminescence
EDTA	ethylenediamine tetraacetic acid
ELISA	enzyme-linked immunosorbent assay
EPPS	*N*-[2-hydroxyethyl]-piperazine-*N'*-[3-propanesulfonic acid]
ϕPSII	Quantum yield of PSII
$\Gamma*$	CO_2 compensation point (CO_2 concentration at which acquisition of carbon in photosynthesis is equivalent to respiratory loss)
GST-activase	glutathione *S*-transferase conjugated to spinach activase
Hepes	*N*-[2-hydroxyethyl]-piperazine-*N'*-[2-ethanesulfonic acid]
IgG	immunoglobulin class G
kb	kilo base pairs
k_{cat}	moles of substrate converted site^{-1} s^{-1} (at saturating substrate concentrations)
K_m	Michaelis constant, that substrate concentration at which the rate of the reaction is half its maximum rate
K_m (CO_2)	Michaelis constant for the carboxylating CO_2 molecule
K_{act} (CO_2)	Michaelis constant for the activating CO_2 molecule
K_d	dissociation constant
L_8S_8	hexadecameric form of Rubisco
mRNA	messenger ribonucleic acid

NAD^+	nicotinamide adenine dinucleotide
NADH	nicotinamide adenine dinucleotide (reduced)
$NADP^+$	nicotinamide adenine dinucleotide phosphate
NADPH	nicotinamide adenine dinucleotide phosphate (reduced)
PCO	photorespiratory carbon oxidation
PCR	photosynthetic carbon reductuion
PGA	phosphoglycerate
p_i	intercellular CO_2 partial pressure
PMSF	phenylmethanesulfonyl flouride
PRK	phosphoribulokinase
PVC	polyvinyl chloride
PSII	photosystem II
R_1	first generation of primary tranformant
rca	regulation of carboxylase activation
RIE	rocket immunoelectrophoresis
RNA	ribonucleic acid
Rubisco	ribulose-1,5-bisphosphate carboxylase / oxygenase
RuBP	D-ribulose-1,5-bisphosphate
SSU	small subunit of ribulose-1,5-bisphosphate carboxylase / oxygenase
SDS	sodium dodecyl sulphate
TBS	Tris-buffered saline
TTBS	Tris-buffered saline plus 0.05% Tween
T-DNA	region of plasmid DNA transferred to plant genome
Tricine	*N*-Tris [hydroxymethyl] methylglycine
Tris	tris(hydroxymethyl) aminomethane
$V_{C\ max}$	maximum velocity of carboxylation (k_{cat} x carbamylated sites)
XuBP	D-xyulose 1,5-bisphosphate

Amino Acids and their Symbols:

Alanine (A)	Isoleucine (I)	Arginine (R)
Cysteine (C)	Lysine (K)	Serine (S)
Aspartic acid (D)	Leucine (L)	Threonine (T)
Glutamic acid (E)	Methionine (M	Valine (V)
Phenylalanine (F)	Asparagine (N)	Tryptophan (W)
Glycine (G)	Proline (P)	Tyrosine (Y)
Histidine (H)	Glutamine (Q)	

TABLE OF CONTENTS

TABLE OF FIGURES

CHAPTER 5

CHAPTER 6

LIST OF TABLES

CHAPTER 2

CHAPTER 3

CHAPTER 1: Literature review

1.1 BACKGROUND

Photosynthesis is the process whereby plants capture light energy and atmospheric carbon dioxide in order to synthesise sugars *de novo*. Sugars produced in photosynthesis are the basis of all organic compounds. The light reactions of photosynthesis yield high energy compounds, such as ATP and reducing equivalents, and these compounds are used by the dark reactions to reduce carbon dioxide to simple sugars. Hence the dark reactions are collectively known as the photosynthetic carbon reduction (PCR) cycle.

Ribulose-bisphosphate carboxylase/oxygenase (Rubisco, EC 4.1.1.39) is a key photosynthetic enzyme of the PCR cycle. It catalyses the carboxylation reaction by which atmospheric carbon dioxide is fixed to form the carbon 'backbone' of sugars, and physiological analysis has shown that this is a major rate-limiting step in the photosynthetic carbon reduction cycle (von Caemmerer and Farquhar, 1981; Woodrow and Berry, 1988). If Rubisco activity is limiting the photosynthetic rate, then we would expect changes in Rubisco activity to be accompanied by proportional changes in photosynthetic rate. von Caemmerer and Farquhar (1981) manipulated Rubisco carboxylase activity *in vivo* in the short-term by changes in CO_2 and O_2 and in the long-term by nitrogen nutrition, development and various other conditions. Their biochemical and physiological analysis of these plants demonstrated that changes in Rubisco activity produced proportional changes in photosynthetic rate (von Caemmerer and Farquhar, 1981).

The carboxylation reaction catalysed by Rubisco involves the addition of carbon dioxide to the enediol form of ribulose bisphosphate (RuBP) to produce a six carbon reaction intermediate which is hydrated and cleaved to form two molecules of 3-phosphoglycerate (Andrews and Lorimer, 1987; Figure 1.1). The production of sugars by the PCR cycle is completed by the phosphorylation and reduction of phosphoglycerate, producing glyceraldehyde-3-phosphate (Figure 1.2). Two molecules of glyceraldehyde-3-phosphate are used to produce one molecule of the six carbon sugar, fructose-1,6-bisphosphate. Some glyceraldehyde-3-phosphate molecules are converted to RuBP, thereby providing or "regenerating" carboxylase substrate (Figure 1.2).

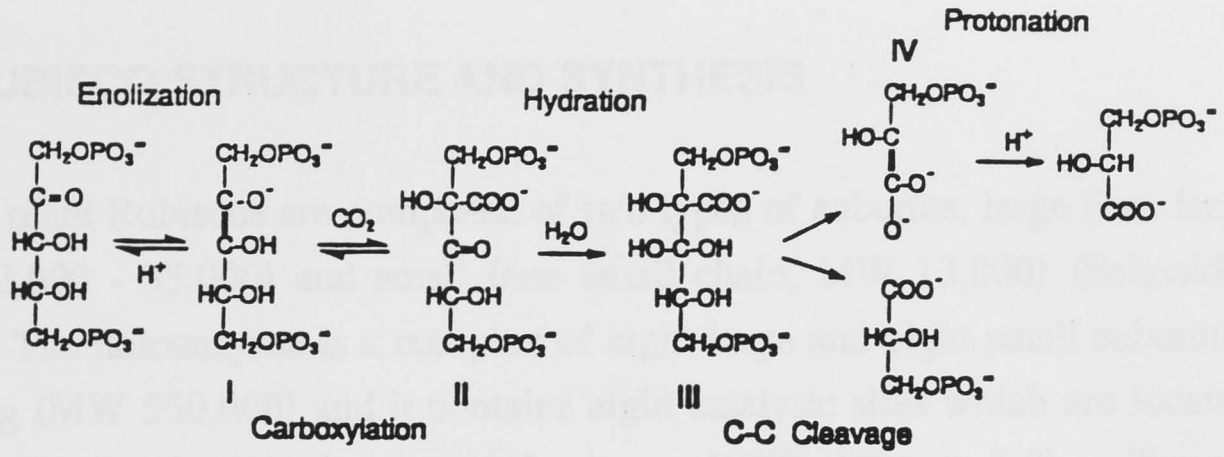

FIGURE 1.1: The carboxylation of RuBP catalysed by Rubisco. I, the 2,3-enediol(ate) of RuBP; II, 2'-carboxy-3-keto-arabinitol-1,5-bisphosphate; III, hydrated *gem*-diol form of II; IV, *aci*-carbanion form of PGA.

Rubisco also has an oxygenase activity which utilises RuBP as the substrate and produces one molecule each of phosphoglycerate and phosphoglycolate. At physiological O_2 and CO_2 concentrations, approximately one oxygenation occurs for every 3 carboxylations (Andrews and Lorimer, 1987). Phosphoglycolate cannot be metabolised in the PCR cycle and as a result it is exported to the peroxisome, and subsequently to the mitochondria, where it is consumed in photorespiration (C_2 cycle) (Figure 1.2). Three-quarters of the carbon lost from the PCR cycle as phosphoglycolate is returned via the photorespiratory pathway. Reducing equivalents and ATP produced by the light reactions of photosynthesis are required to fuel this process (reviewed in Andrews and Lorimer, 1987). This diversion of reducing equivalents and ATP away from the PCR cycle reduces the light-use efficiency of photosynthesis. Therefore, RuBP oxygenation and the consequent photorespiratory cycle seem a rather wasteful use of light energy. Although this energy loss may be beneficial under conditions of photoinhibition where excess photosynthetic reductant is present (Osmond, 1981), it limits the efficiency of photosynthesis at lower light levels.

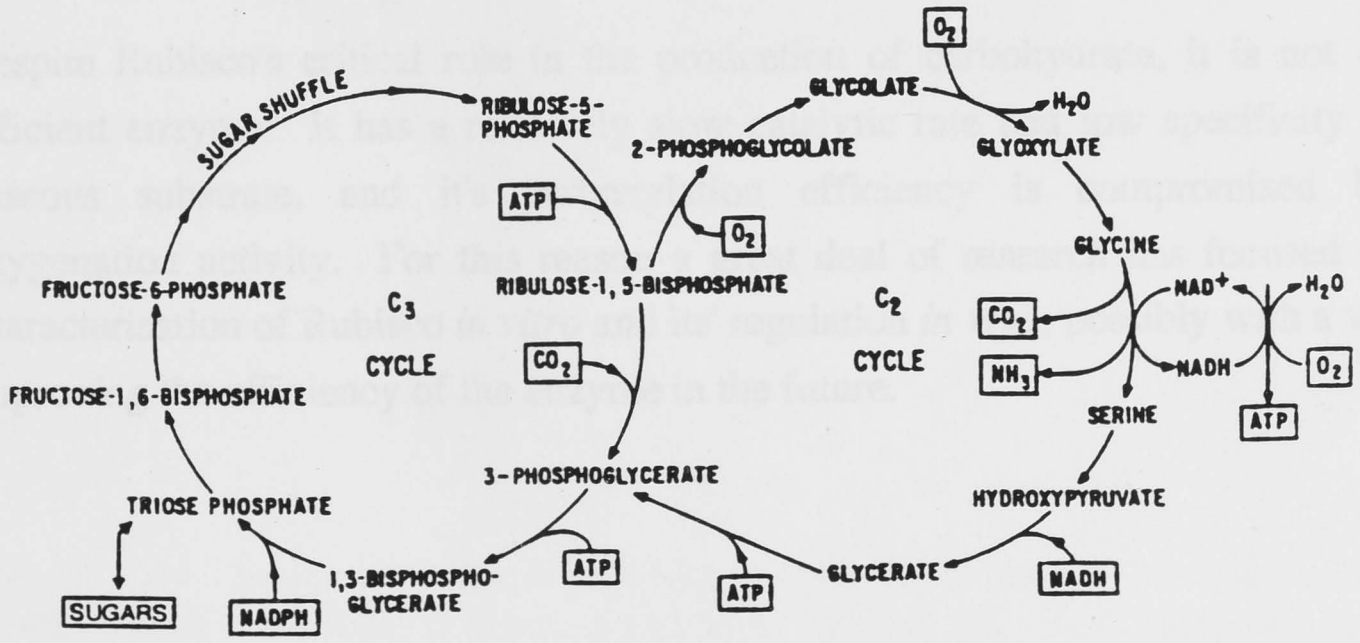

FIGURE 1.2: The photosynthetic carbon reduction (C_3) and photorespiratory carbon oxidation (C_2) cycles. Rubisco catalyses both the carboxylation and oxygenation of RuBP, the initial reactions of the respective pathways.

1.2 RUBISCO STRUCTURE AND SYNTHESIS

Higher plant Rubiscos are composed of two types of subunits, large (one large chain, MW 52,000 - 55,000) and small (one small chain, MW 13,000) (Schneider et al., 1992). The holoenzyme is a complex of eight large and eight small subunits, known as L_8S_8 (MW 550,000) and it contains eight catalytic sites which are located within the large subunits (Andrews and Lorimer, 1987) (Figure 1.3). Photosynthetic microorganisms also contain L_8S_8 Rubisco; however some, such as the photosynthetic bacteria *Rhodospirillum rubrum* and *Rhodobacter sphaeroides,* contain Rubisco in an L_2 structure (reviewed in Schneider et al., 1992).

The genes for the large subunits of higher plant Rubiscos are located in the chloroplast genome, whereas the small subunits are encoded by a family of highly homologous genes located in the nuclear genome (reviewed in Andrews and Lorimer, 1987). The small subunits are translated as a preprotein, with an extra peptide at the amino end of the polypeptide chain. This extra peptide directs transport of the small subunit into the chloroplast, after which the peptide is cleaved off and degraded (Andrews and Lorimer, 1987). A chaperone protein is involved in the assembly of Rubisco within the chloroplast, but the *E.coli* protein GroEL can be substituted when assembling *in vitro* (Schneider et al., 1992). These chaperonin molecules seem to be important in facilitating the correct folding of the large sub-unit monomers.

1.3 THE COST OF RUBISCO'S INEFFICIENCY

Despite Rubisco's critical role in the production of carbohydrate, it is not a very efficient enzyme. It has a relatively slow catalytic rate and low specificity for its gaseous substrate, and it's carboxylation efficiency is compromised by its oxygenation activity. For this reason a great deal of research has focused on the characterisation of Rubisco *in vitro* and its' regulation *in vivo*, possibly with a view to improving the efficiency of the enzyme in the future.

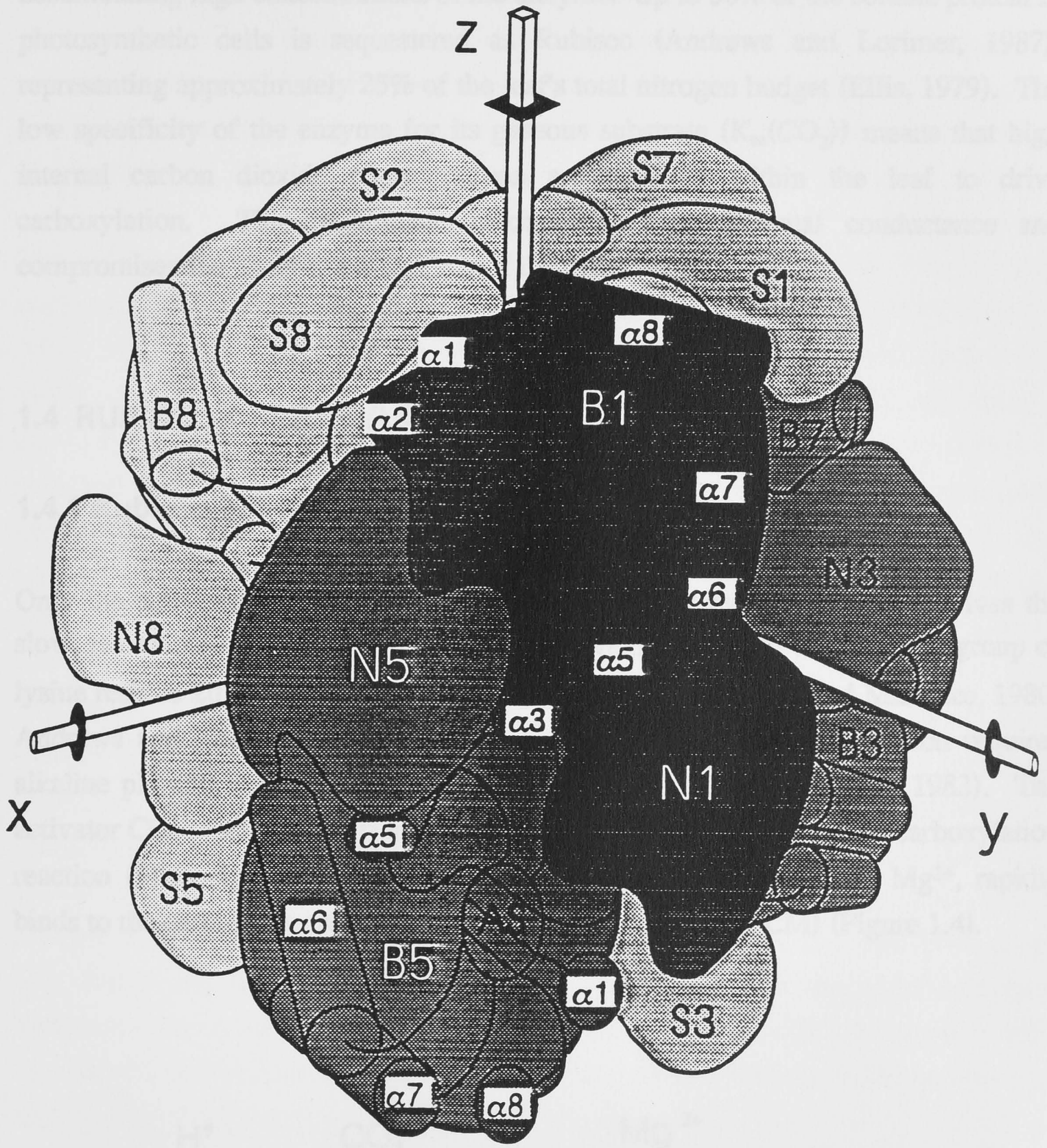

FIGURE 1.3: The hexadecameric (L8S8) structure of Rubisco. The two active sites formed between large subunit dimers 1 and 5 are labelled AS. N, N-terminal domain; B, barrel domain; S, small subunit; α, α-helix (reproduced from Curmi et al., 1991).

Rubisco has a relatively low k_{cat}/K_m (CO_2) ratio (Morell et al., 1992). The rate of turnover at the catalytic site (k_{cat}) is less than one-thousandth of the rate at which the substrates diffuse into the catalytic site. Plants compensate for slow catalysis by accumulating high concentrations of the enzyme. Up to 50% of the soluble protein in photosynthetic cells is sequestered as Rubisco (Andrews and Lorimer, 1987), representing approximately 25% of the leaf's total nitrogen budget (Ellis, 1979). The low specificity of the enzyme for its gaseous substrate ($K_m(CO_2)$) means that high internal carbon dioxide concentrations are required within the leaf to drive carboxylation. This requirement necessitates high stomatal conductance and compromises the water-use efficiency of the plant.

1.4 RUBISCO CARBAMYLATION

1.4.1 Rubisco activation

Only the activated form of Rubisco has catalytic activity. Activation involves the slow, reversible reaction of a molecule of activator CO_2 with the ε-amino group of lysine residue 201 within the inactive catalytic site (E) (Lorimer and Miziorko, 1980; Andrews and Lorimer, 1987), forming a carbamate (EC). This reaction requires alkaline pH and is rate-limiting for activation (Miziorko and Lorimer, 1983). The activator CO_2 molecule is different to the substrate CO_2 involved in the carboxylation reaction (Miziorko, 1979; Lorimer, 1979). The divalent metal ion, Mg^{2+}, rapidly binds to the carbamate, creating an active ternary complex (ECM) (Figure 1.4).

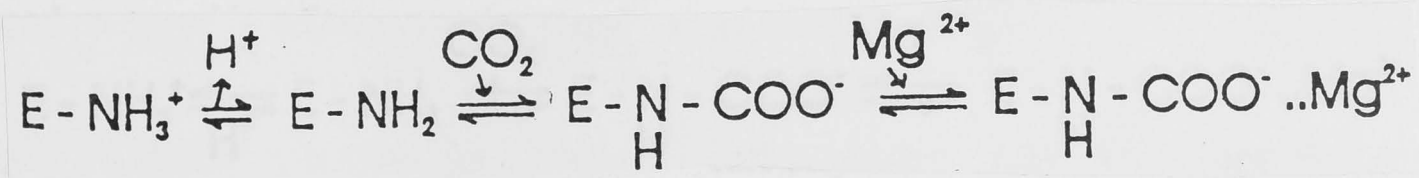

FIGURE 1.4: Rubisco carbamylation reaction

1.4.2 Light-regulation of Rubisco carbamylation

Rubisco carbamylation levels (Mächler and Nösberger, 1980; Perchorowicz et al., 1981; Salvucci et al., 1986; von Caemmerer and Edmondson, 1986) and stromal RuBP concentrations (Badger et al., 1984; Perchorowicz et al., 1981; von Caemmerer and Edmondson, 1986) both change in response to changes in irradiance. This raises questions about how RuBP concentration and carbamylation level may be involved in the regulation of Rubisco activity *in vivo*.

The RuBP concentration in the chloroplast stroma exceeds the Rubisco catalytic site concentration at both high and low light under steady-state conditions (Perchorowicz et al., 1981; Badger et al., 1984; von Caemmerer and Edmondson, 1986; Sage et al., 1990). *Chenopodium album* plants sampled at atmospheric CO_2, had approximately 2.5 - 3 RuBP molecules per Rubisco catalytic site at high light (1750 μmol quanta m^{-2} s^{-1}), and at low light (150 μmol quanta m^{-2} s^{-1}) there were 1.5 - 2 RuBP molecules per catalytic site (Sage et al., 1990). Recent analysis of transgenic plants, containing an antisense gene directed against the chloroplast glyceraldehyde 3-phosphate dehydrogenase, indicates that RuBP concentrations limit the rate of CO_2 assimilation rate when they fall below 1.5 - 2.0 molecules of RuBP per catalytic site (Price et al. - in press). These results indicate that RuBP concentration probably does not limit the rate of steady-state photosynthesis at atmospheric CO_2, except at very low light intensities. However, RuBP concentrations are low (below site concentration) and probably limit the rate of carboxylation during the first few minutes following a high-to-low light transition (Perchorowicz et al., 1981; Mott et al., 1984), after which changes in Rubisco carbamylation occur and Rubisco activity becomes co-limiting with RuBP regeneration. These results are consistent with the hypothesis that Rubisco's carbamylation level is adjusted to match the rate of RuBP consumption with the rate of RuBP regeneration, thereby maintaining a site-saturating RuBP pool over a broad range of irradiances under steady-state conditions.

Light-regulated changes in Rubisco carbamylation may have an important physiological role. The ratio of RuBP:PGA in the chloroplast stroma influences stromal pH because two protons are produced for each molecule of RuBP converted to PGA. High rates of RuBP regeneration relative to consumption increase the RuBP:PGA ratio, resulting in stromal alkalinization. Alternatively, decreases in the rate of RuBP regeneration relative to consumption results in over-production of

phosphoglycerate and concomitant stromal acidification. Changes in Rubisco carbamylation may buffer these fluctuations in stromal pH (Andrews and Lorimer, 1986).

Changes in CO_2 concentration can also result in changes in Rubisco carbamylation level. Past studies have shown that the Rubisco carbamylation level in *Raphanus sativus* (von Caemmerer and Edmondson, 1986) and *Chenopodium album* (Sage et al., 1990) decreased from 100 to 80% when the CO_2 concentration was increased from ambient to 3-4 times ambient. Initially this result seems surprising since high CO_2 concentrations *in vitro* stimulate Rubisco carbamylation. However, at high CO_2 concentrations, the rate of RuBP carboxylation is faster, and as a result, RuBP would be consumed more quickly, thereby depleting the RuBP pool. Under these conditions the RuBP concentration in the chloroplast stroma may limit Rubisco activity. A reduction in Rubisco carbamylation would reduce the rate of catalytic turnover, possibly matching RuBP consumption with the capacity for regeneration. Rubisco decarbamylation is also observed at low CO_2 concentrations (von Caemmerer and Edmondson, 1986; Sage et al., 1990); but this may reflect the CO_2 requirement of the carbamylation reactions rather than a physiological response to the rates of RuBP regeneration and consumption.

1.4.3 *In vitro* kinetics

In vitro studies indicate that Rubisco carbamylation is favoured at alkaline pH, whereas decarbamylation occurs at acidic pH (Lorimer et al., 1976); this reflects the carbamylation reaction's requirement for a neutral lysyl residue (Figure 1.4). The effect of the RuBP:PGA ratio on pH would result in stromal alkalinization during low-to-high light conversions, and stromal acidification during high-to-low light conversions. On initial glance it seems that stromal pH could provide a direct means of regulating Rubisco's activity according to the availabilty of RuBP and the demand for phosphoglycerate (Andrews and Lorimer, 1987). The observation of light-modulated increases in stromal pH and Mg^{2+} in chloroplasts appeared to substantiate this model of regulation (as reviewed in Jensen and Bahr, 1977). However, further analysis showed that stromal alkalinization and Mg^{2+} efflux saturated at lower light intensities than did Rubisco activation (Heber et al., 1982). These results indicated that the pH regulation model was an over-simplification of what was occurring *in vivo*. This was confirmed by *in vitro* studies examining the pH, Mg^{2+}, and CO_2 dependence of spontaneous activation. *In vitro* analysis of the kinetics of Rubisco

carbamylation indicates that the addition of the activator CO_2 molecule to a lysyl residue within the catalytic site proceeds slowly at atmospheric CO_2 concentrations, whereas the addition of Mg^{2+} is relatively quick (Laing and Christeller, 1976). The K_{act} (CO_2)[1] was determined to be in the range of 25 to 30 μM (Lorimer et al., 1976; Jordan and Ogren, 1981). This means that only 30-35% of Rubisco would be carbamylated at 10 μM CO_2, which is the concentration thought to prevail in the chloroplast in air. These results are not consistent with high levels of Rubisco carbamylation *in vivo*.

1.4.4 The interaction between sugar phosphates and Rubisco

1.4.4.1 Positive and negative effectors of carbamylation

Phosphorylated compounds, such as RuBP and other PCR cycle intermediates, bind to Rubisco and perturb the equilibrium between the carbamylated and decarbamylated forms *in vitro*. Hatch and Jensen (1980) classified these phosphorylated compounds into two groups. Positive effectors, such as NADPH and 6-phosphogluconate, that promote carbamylation, and negative effectors, like RuBP and ribose 5-phosphate, which favour the decarbamylated state. Given that effectors can bind to both decarbamylated and carbamylated enzyme, Badger and Lorimer (1981) proposed that positive effectors bind more tightly to carbamylated enzyme than they do to decarbamylated enzyme, thereby stabilising Rubisco in its carbamylated form. The reverse was thought to apply to negative effectors. Later studies carried out by Jordan et al. (1983) established that most positive effector compounds elicited their effect by alterations to the relative rates of activation and deactivation. Preferential binding to the carbamylated enzyme was only demonstrated for ribose 5-P.

1.4.4.2 Cooperativity

A regulatory role for positive effector compounds, such as 6-phosphogluconate, was initially ruled out due to their low concentration in the chloroplast stroma. However, it later became apparent that even at very low concentrations these compounds could still have an effect on carbamylation levels (reviewed in Andrews and Lorimer, 1987). For example, *in vitro* studies have shown that decarbamylation is retarded even if only one site out of eight on the Rubisco molecule has 6-phosphogluconate

---

[1] Assayed at *in vivo* concentrations of Mg^{2+} (5-10 mM $MgCl_2$), in vivo pH (approximately 8.0), and 25 C.

bound (Jordan et al., 1983). It is interesting to note that the binding of 6-phosphogluconate to the first carbamylated site is considerably stronger than binding to subsequent sites (Andrews and Lorimer, 1987). Therefore, the sites do not behave independently, instead there is a cooperative interaction. Cooperativity between sites may enable positive effector compounds to have a physiological role even when present at sub-stoichiometric concentrations. An obvious side-effect of positive effector binding is the loss of catalytic activity at one active site. This loss may be the price paid to enable Rubisco carbamylation at *in vivo* concentrations of CO_2 and Mg^{2+}.

1.4.4.3 Inhibitors of Rubisco carbamylation and catalysis

RuBP. The discovery of positive effector compounds seemed to provide an explanation of how carbamylation was facilitated at *in vivo* pH, and CO_2 and Mg^{2+} concentrations. However, the concurrent discovery that RuBP was a potent inhibitor of the activation process raised more questions. *In vitro* studies indicated that RuBP binds very tightly to the decarbamylated catalytic site. The K_d for decarbamylated sites (approximately 20 nM), appeared to be three orders of magnitude lower than the K_m of carbamylated sites (approximately 20 μM) (Jordan and Chollet, 1983). If this situation prevailed *in vivo*, where RuBP saturates the Rubisco catalytic site concentration under steady-state conditions at both high and low light intensities (Badger et al., 1984; Perchorowicz et al., 1981; von Caemmerer and Edmondson, 1986), then carbamylation would be blocked and photosynthesis would never occur (Andrews and Lorimer, 1987).

Fallover inhibitors. The carboxylation reaction catalysed by Rubisco has several side reactions which produce compounds that bind to Rubisco's active sites and block catalysis. The first step in the Rubisco reaction mechanism is the removal of a proton from RuBP to form the 2,3-enediol; this reaction is readily reversible. Incorrect reprotonation of the enediol at carbon-2 or carbon-3 results in the formation of XuBP or 3-keto-D-arabinitol-1,5-bisphosphate (Edmondson et al., 1990a; Zhu and Jensen, 1991). These misprotonation products can accumulate at Rubisco's active sites, thereby inhibiting catalysis. The inhibition of Rubisco by these compounds has been observed *in vitro* as a progressive decline in Rubisco activity over time, this

phenomenon has been called fallover (Edmondson et al., 1990a; Edmondson et al., 1990b).

Analysis of Rubisco that has been modified by site-directed mutagenesis has lead to the identification of another possible side-reaction compound. Morell et al. (in press) observed that the production of a monophosphorylated compound increased when they substituted Rubisco's threonine 65 with serine. They have tentatively identified this compond as 1-deoxy-D-glycero-2,3-pentodiuolose-5-phosphate, produced by the β-elimination of the 2,3-enediol. This compound may bind to Rubisco's active sites and block catalysis. If this compound is also produced by the wild-type Rubisco it could also contribute to the decrease in Rubisco activity observed over time *in vitro*, known as fallover.

CA1P. The catalytic activity of Rubisco can be modulated *in vivo* by the inhibitor carboxyarabinitol-1-phosphate (CA1P), which binds to the carbamylated active sites of Rubisco by virtue of its similarity to the six-carbon intermediate of the carboxylase reaction. It accumulates in the leaves of some plant species in the dark and at low light intensities (Vu et al., 1984; Seemann et al., 1985; Servaites, 1990). With the onset of illumination, CA1P is released from the active site and degraded by a specific phosphatase (Seemann et al., 1990), resulting in an increase in carboxylase activity (Vu et al. 1983).

The strong inhibition of carbamylation by RuBP, and the ability of the fallover compounds to block catalysis at Rubisco's active sites *in vitro*, are not consistent with high levels of Rubisco carbamylation and activity *in vivo*. Also, the discovery of CA1P raised questions about the mechanisms involved in the release of this compound from Rubisco's catalytic sites with the onset of illumination. The subsequent discovery of the stromal protein, Rubisco activase, has provided some explanations for how Rubisco carbamylation and activity are maintained *in vivo*.

1.5 DISCOVERY OF RUBISCO ACTIVASE

Analysis of an unusual mutant of *Arabidopsis thaliana* that required high CO_2 for growth (Somerville et al., 1982) lead to the identification of a protein that was critical in the carbamylation of Rubisco *in vivo* (Salvucci et al., 1985). The mutant had an impaired photosynthetic rate at atmospheric CO_2,which could not be attributed to reduced stomatal conductance or availability of light reaction products. Labelling experiments at high CO_2 indicated that all Calvin cycle enzymes were functional. However, at low CO_2 a large proportion of the radioactive label accumulated as RuBP, suggesting reduced Rubisco activity due to a changed affinity for CO_2. Purification and *in vitro* analysis of Rubisco from the *A. thaliana* mutant indicated that the kinetic and isoelectric characterisitics were not altered in the mutant. Rapid release and assay of Rubisco from leaves, protoplasts and isolated chloroplasts indicated that carbamylation was reduced in the mutant. Consequently, the phenotype of the *A. thaliana* mutant was attributed to a lesion in the tentatively named *rca* (regulation of carboxylase activation) gene (Somerville et al., 1982).

Subsequent analysis of the soluble protein content of *Arabidopsis* showed that two polypeptides of approximately 47 and 50 kD molecular weight were missing from the *rca* mutant (Salvucci et al., 1985). Inheritance studies, crossing a high-CO_2-requiring photorespiratory mutant with the *rca* mutant, proved that the Rubisco-activation-mutation was linked to the absence of the two polypeptides. The critical role of these polypeptides was demonstrated when Rubisco was activated using a reconstituted light activation system of soluble chloroplast extract (containing the 47 and 50 kD polypeptides), thylakoid membranes, RuBP and purified spinach Rubisco. The inclusion of leaf extract from the *rca* mutant in this assay system had no effect on Rubisco activation. These results proved that it was the absence of an activator and not the presence of an inhibitor that was responsible for the *rca* mutant phenotype (Salvucci et al., 1985). The polypeptides involved in Rubisco carbamylation are now known as Rubisco activase.

1.6 WHAT DOES ACTIVASE DO?

1.6.1 Removal of sugar phosphates

In vitro studies have provided some insight into how activase interacts with the inactive and carbamylated sites of Rubisco. Activase appears to facilitate the release of RuBP from Rubisco's inactive catalytic sites, thereby enabling carbamylation to occur (Figure 1.5(1)). Studies carried out by Portis (1990) have shown that activase accelerates the rate at which ^{3}H-RuBP bound to inactive Rubisco is exchanged with a pool of unlabelled RuBP. This exchange between bound and unbound RuBP was quickly followed by carbamylation and catalysis.

Other studies established that Rubisco activase also facilitated the release of the nocturnal inhibitor to Rubisco, carboxyarabinitol 1-phosphate (CA1P) (Robinson and Portis, 1988a) (Figure 1.5(2)), and prevented inhibition of Rubisco by the fallover compounds *in vitro* (Robinson and Portis, 1989a). In these experiments, both CA1P and the fallover compounds were bound to the carbamylated active site of Rubisco, thereby blocking RuBP binding and catalysis. The ability of Rubisco activase to relieve this inhibition, and to release RuBP from Rubisco's inactive sites indicates that it interacts with both the E and ECM forms of Rubisco.

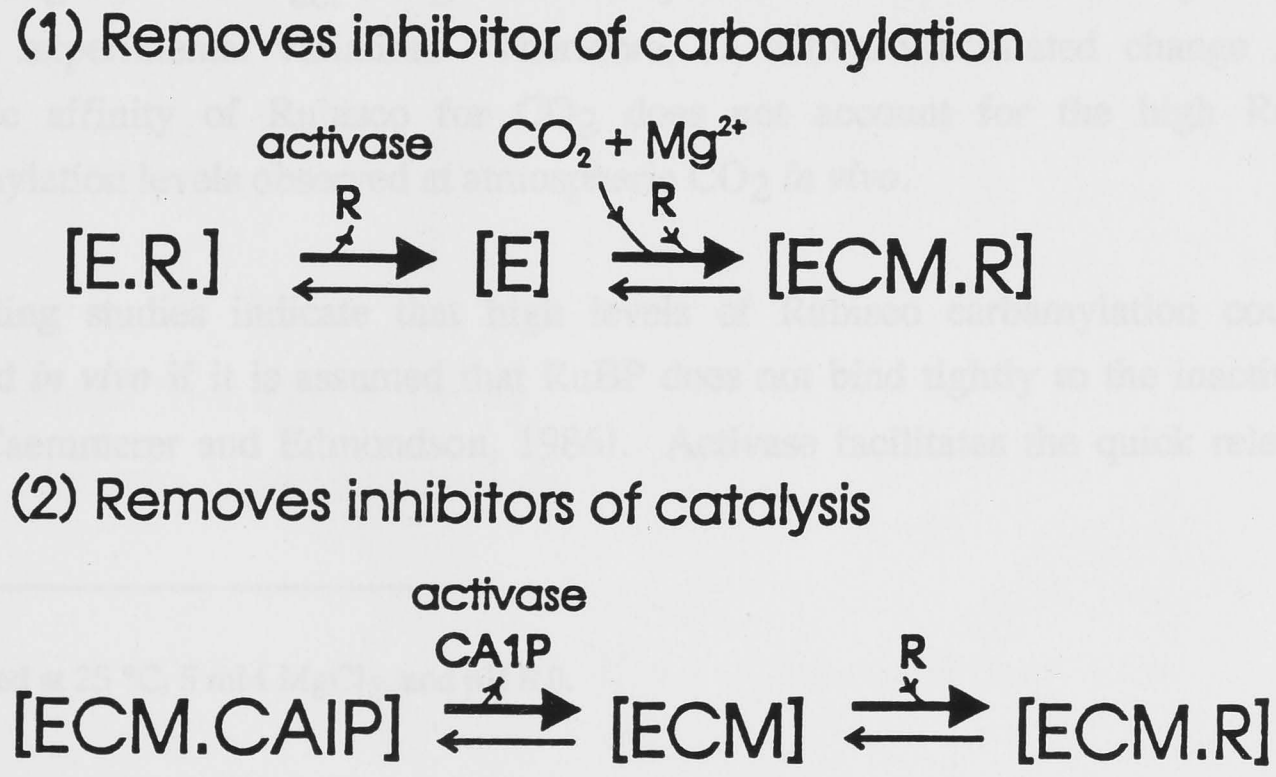

FIGURE 1.5: Activase removes sugar phosphates

1.6.2 Enables full carbamylation of Rubisco at atmospheric CO_2

The inclusion of activase and ATP in *in vitro* assays of Rubisco enabled full carbamylation of Rubisco at atmospheric CO_2 concentrations. However, Rubisco activase did not stimulate Rubisco carbamylation in the absence of RuBP. The $K_{act}(CO_2)^2$ of carbamylation in the presence of activase and absence of RuBP was 23 μM (Portis et al., 1986). This is very similar to the $K_{act}(CO_2)^3$ in the absence of activase (25 to 30 μM; Lorimer et al., 1976; Jordan and Ogren, 1981). Portis et al. (1986) observed that the activase-facilitated carbamylation of Rubisco *in vitro* was dependent on RuBP concentration, and in the presence of 0.9 mM RuBP activase could reduce the $K_{act}(CO_2)^4$ of carbamylation from 23 to 4 μM. In this system, Rubisco would be fully carbamylated at 10 μM CO_2. These results indicate that activase enables RuBP to perturb the equilibrium of the carbamylation reaction toward the carbamylated form.

It seems unlikely that activase is increasing the intrinsic affinity of Rubisco for the activating CO_2 molecule because, if this was the case, we would expect activase to stimulate Rubisco activity even in the absence of RuBP. However, the K_{act} (CO_2) for Rubisco carbamylation in the presence of activase, and the absence of RuBP is only slightly lower than values of K_{act} (CO_2) obtained previously in the absence of activase (see previous paragraph for values). Rubisco activase could be responsible for the slightly lower K_{act} (CO_2) obtained by Portis et al.(1986), or it may simply be due to experimental variation. Therefore, an activase-facilitated change in the intrinsic affinity of Rubisco for CO_2 does not account for the high Rubisco carbamylation levels observed at atmospheric CO_2 *in vivo*.

Modelling studies indicate that high levels of Rubisco carbamylation could be attained *in vivo* if it is assumed that RuBP does not bind tightly to the inactive site (von Caemmerer and Edmondson, 1986). Activase facilitates the quick release of

---

[2] Assayed at 25 °C, 5 mM $MgCl_2$, and pH 8.0.

[3] Assayed at *in vivo* concentrations of Mg^{2+} (5-10 mM $MgCl_2$), *in vivo* pH (approximately 8.0), and 25°C.

[4] Assayed at 25 °C, 5 mM $MgCl_2$, and pH 8.0.

RuBP from Rubisco's inactive sites (Portis, 1990), and this increase in the apparent rate of dissociation could result in a decrease in the affinity of RuBP for the inactive site (Figure 1.6). If this was the case, the activator CO_2 molecule could displace RuBP from the inactive site, enabling carbamylation and subsequent catalysis of RuBP. The RuBP concentration in the chloroplast stroma exceeds the Rubisco catalytic site concentration over a wide range of light intensities (Perchorowicz et al., 1981; Badger et al., 1984; von Caemmerer and Edmondson, 1986). This high concentration and Rubisco's relatively low K_m for RuBP (20 μM) ensures that carbamylation will be followed rapidly by RuBP binding *in vivo*. If binding of RuBP to Rubisco's carbamylated sites [ECM] is fast, compared to catalytic turnover, then [ECM] will be small compared to [ECM.R]. Since, only [ECM] can decarbamylate, RuBP will therefore supress decarbamylation. This has been demonstrated *in vitro*, where RuBP severely inhibits the rate of activity loss when CO_2 and Mg^{2+} concentrations are reduced (Jordan et al., 1983). Essentially, in the presence of activase, RuBP has a greater affinity for Rubisco's active sites than it does for its inactive sites. Consequently, it changes from being a negative effector of Rubisco carbamylation to being a positive effector (Portis, 1990). The ability of positive effectors to reduce the CO_2 dependence of carbamylation has been demonstrated previously (Hatch and Jensen, 1984). Therefore, this model seems to provide an explanation for the carbamylation of Rubisco at atmospheric CO_2, and in the presence of RuBP.

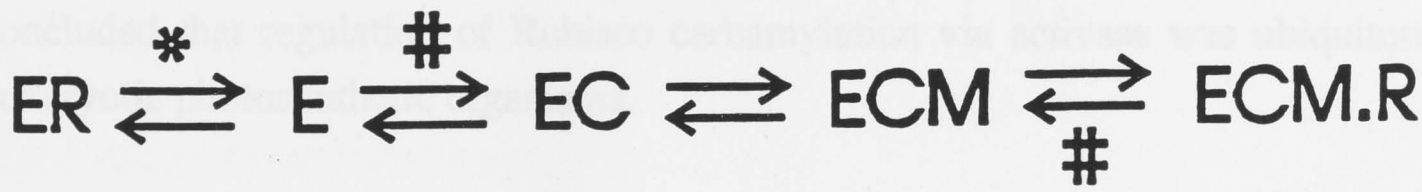

* Rate altered by activase

\# Not rate-altered by activase

FIGURE 1.6: The effect of activase on Rubisco carbamylation

1.7 PURIFICATION AND SPECIES DISTRIBUTION OF RUBISCO ACTIVASE

The identification of activase's role in carbamylation *in vivo* initiated a great deal of interest in working with the purified form of the enzyme. A purification scheme was devised based on the fractionation of spinach chloroplast stromal extracts by ion exchange followed by gel filtration (Salvucci et al., 1987). Polyacrylamide gel electrophoresis of the spinach preparation indicated the presence of two major polypeptides at 45 and 47 kD, consistent with the absence of 43 and 47 kD polypeptides in the *Arabidopsis rca* mutant (Portis, 1990).

1.7.1 Species distribution

Activase polypeptides purified from spinach were used to raise antibodies in tumor-induced mouse ascites. These antibodies were used as probes for activase on immunoblots of soluble proteins from a number of species, including representatives with C_3 and C_4 photosynthesis and plants containing CA1P (Salvucci et al., 1987). One or both of the activase polpeptides were recognised in all higher plant species examined, including *Arabidopsis thaliana*, soybean, kidney bean, pea, tobacco, maize, oat, barley, celery, tomato, pigweed, purslane, dandelion, sorghum and crabgrass. The activase polypeptides were also detected in cell extracts of the green alga *Chlamydomonas reinhardii.* Based on these results, Salvucci et al. (1987) concluded that regulation of Rubisco carbamylation via activase was ubiquitous in eukaryotic photosynthetic organisms.

1.7.2 Purification from spinach

Rubisco activase prepared using the method outlined by Salvucci at al. (1987) was found to be unstable and sometimes extensive proteolysis occurred (Portis, 1990). Subsequent studies showed that the addition of ATP during purification and storage was necessary to maintain activity, and this led to the development of a better purification procedure. Using the new method, Rubisco activase was purified from spinach extract by a 0-35% ammonium sulfate step, followed by ion exchange fast protein liquid chromatography (Robinson et al., 1988).

1.7.3 Purification from tobacco

More recently a method for purification of tobacco activase has also been developed (Wang et al., 1992). This procedure also utilizes an initial 0-35% ammonium sulfate precipitation, followed by an 18% PEG precipitation to pellet activase protein. The activase protein is then isolated by anion exchange, using Q-sepharose. ATP is included in the extraction buffer, and is present during the ammonium sulfate and PEG precipitations. However, it is not added to the fractions collected from the Q-sepharose column. This is because the protein is relatively stable when stored at high concentrations, even in the absence of ATP (Portis- pers. comm.).

1.8 PRIMARY STRUCTURE AND SYNTHESIS OF RUBISCO ACTIVASE

1.8.1 Two forms of Rubisco activase

Two forms of Rubisco activase cDNA have been recovered from spinach, *Arabidopsis* (Werneke et al., 1988) and barley cDNA libraries (Rundle and Zielenski, 1991). For spinach, a comparison of the polypeptide sequences deduced from the two cDNAs showed that they were identical, except that the larger polypeptide contained an additional 37 amino acids at the C-terminal end. The Rubisco activase proteins have little sequence homology with other known proteins, except for the two short regions associated with nucleotide binding (Werneke et al., 1988).

1.8.2 Alternative mRNA splicing

Southern blot analysis indicated that there was only a single Rubisco activase gene in both *Arabidopsis* and spinach (Werneke et al., 1989). Analysis of the structure of the genomic clones of spinach and *Arabidopsis* provided an explanation. Werneke et al. (1989) identified an intron at the 3' end of the gene which could produce two mRNAs, of the appropriate sizes, by an alternative splicing process. This process is not associated with developmental-specific (Zielenski et al., 1989) or tissue-specific (Werneke, 1989) expression of the two different forms of the Rubisco activase polypeptide. This is contrary to the majority of examples in animal systems (Leff et al., 1986). Therefore, the signifigance of this process remains unknown.

Interestingly, the gene encoding activase in *Nicotiana tabacum* does not contain an alternative splicing site (Qian and Rodermel, 1993). Therefore, only one activase polypeptide is found in tobacco.

1.8.3. Synthesis of Rubisco activase

Rubisco activase is a chloroplast protein which is encoded by a nuclear gene, synthesized on cytoplasmic ribosomes, and imported into the chloroplast (Werneke et al., 1988; Werneke, 1989). The precursor polypeptide of Rubisco activase contains an N-terminal transit peptide of 58 amino acids that enables chloroplast importing and processing (Werneke et al., 1988).

1.8.4. Functional structure of Rubisco activase

The isolation of the cDNA sequences of Rubisco activase confirmed the initial indications that Rubisco activase consists of two polypeptides in the range 40-47 kD (Portis, 1990). Shen et al. (1991) expressed each polypeptide separately in *E.coli* and as a result they were able to demonstrate that either polypeptide is capable of independently activating Rubisco. Therefore, the two polypeptides are not essential components of an active holoenzyme. The absence of an alternative mRNA splicing site in the tobacco activase gene (Qian and Rodermel, 1993) provides further evidence that each activase polypeptide is independently active.

1.9 CHARACTERISATION OF RUBISCO ACTIVASE *IN VITRO*

1.9.1 ATPase activity

1.9.1.1 Activase requires ATP

Early studies on the light-regulation of activase, carried out by Salvucci et al. (1985) used RuBP which was contaminated by adenine nucleotides (Portis et al., 1986), obscuring the vital role of this compound in activase-facilitated Rubisco carbamylation (Streusand and Portis, 1987; Parry et al., 1988). In early experiments, chloroplast thylakoids and light were essential components of the *in vitro* activase

system used to carbamylate Rubisco (Salvucci et al., 1985; Portis et al., 1986). However, Streusand and Portis (1987) later found that Rubisco could be carbamylated by activase in the absence of thylakoids and light as long as ATP was enzymatically regenerated in order to maintain very high ATP / ADP ratios. Subsequent studies by Robinson and Portis (1988b) showed that Rubisco carbamylation levels changed when they manipulated the stromal ATP and ADP/P_i content of isolated spinach chloroplasts. Activase-facilitated Rubisco carbamylation was stimulated by high ATP concentrations and was inhibited by high ADP concentrations.

1.9.1.2 Characteristics of the ATPase

The development of a refined purification procedure for Rubisco activase enabled the characterisation of the protein's ATPase activity *in vitro* (Robinson and Portis, 1989b). Purified Rubiso activase hydrolyzed ATP with a specific activity of 1.5 μmol min^{-1} mg^{-1}, and the reaction was highly specific for Mg^{2+} and it had a broad pH optimum with maximum activity at pH 8-8.5. The ATPase activity was independent of Rubisco activation state and the presence of Rubisco, and the addition of Rubisco in either the active or inactive form had no effect on the rate of hydrolysis. The ATPase activity was not affected by typical phosphatase and ATPase inhibitors, and the ATPase and Rubisco carbamylation activities of activase were heat labile to the same extent and showed the same sigmoidal response to ATP concentration (Robinson and Portis, 1989b). These results provided substantial evidence that ATP hydrolysis is an intrinsic property of Rubisco activase and is part of the overall activation process (Portis, 1990).

The intrinsic ATPase activity of Rubisco activase was confirmed when Werneke et al. (1988) identified nucleotide binding domains within the activase poypeptides that had a high sequence homology with other well known ATPase proteins.

1.9.1.3 The ATPase and Rubisco activation activities are at different ends of the activase protein

The hydrolysis of ATP and Rubisco carbamylation activities of activase seem to occur within different areas of the activase protein. Trypsin digestion of spinach

Rubisco activase resulted in the cleavage of the protein at the N-terminal end (Esau et al., 1991). This cleavage caused a much greater decrease in Rubisco-RUBP activation than ATP hydrolysis. Subsequent construction and analysis of spinach activase deletion mutants demonstrated that the twelve N-terminal residues are essential for Rubisco activation activity but not ATP hydrolysis. In contrast, a 50% reduction of ATPase activity by deletion of 30 residues at the C-terminal end of the protein left the Rubisco activation activity unaffected. These results indicate that the two activities depend on opposite ends of the polypeptide.

1.9.1.4 What is the purpose of ATP hydrolysis?

The essential role of ATP hydrolysis in Rubisco activation, and the possible two domain structure, raises the possibility that Rubisco activase is similar in structure and mechansim to chaperonins, such as heat shock protein 70 (hsp 70). Hsp 70 hydrolyses ATP to drive the energetically unfavourable release of clathrin molecules from coated vesicles (Brändén, 1990). The ATPase activity and the clathrin-binding function of this enzyme reside in two different domains of the polypeptide chain. Flaherty et al. (1990) have proposed a possible route for the transduction of the energy of ATP hydrolysis to a bound substrate. They suggest that changes in the ATPase fold of the hsp 70, caused by ATP hydrolysis, are transmitted to the clathrin-binding domain and induce a conformational change in the target substrate so that clathrin is released. At the moment, the pathway by which ATP hydrolysis is harnessed to facilitate the removal of sugar phosphates from Rubisco's active site is unknown. However, the possible two domain structure of activase (Esau et al., 1991) indicates that it may operate in a similar way to hsp 70. Future analysis of the crystal structure of Rubisco activase, with and without its substrates bound, will help to clarify the mechansims by which activase facilitates RuBP release.

1.9.2 Activase self-associates

The initial purification scheme for spinach activase involved a gel filtration step (Salvucci et al., 1987). Using this technique the molecular mass of Rubisco activase was estimated to be 200 kD. Subsequent assays of molecular mass were carried out with protein that was purified using the refined procedure outlined above (Robinson et al., 1988). Gel filtration of a Rubisco activase preparation isolated in the presence of ATP and protease inhibitors, resulted in an assymetric peak with a maximum suggesting a molecular mass of about 500 kD (Robinson and Portis, unpublished results, as cited in Portis, 1990). Similarly, broad bands were obtained when the protein was electrophoresed on nondenaturing gels (Portis, 1990). It is apparent from these results that activase self-associates, making the functional size of the protein difficult to estimate.

Tobacco activase also self-associates, but not to the same extent. There is only one tobacco activase polypeptide; it has a MW of 42 kD (Wang et al., 1991). The molecular mass of the tobacco activase native protein as determined by elution on a Superose 12-B gel permeation column is approximately 170 kD, indicating that the polypeptides form a tetramer (Wang et al., 1991).

I have described above how purified tobacco activase does not require ATP to be present during storage as long as the protein concentration is high (1.0-1.5 mg mL^{-1}). At high concentrations the polypeptides would aggregate. Therefore, it seems that the aggregated form of Rubisco activase is the most stable. This is hardly surprising since activase protein would be present in high concentrations in the chloroplast stroma. Based on the recovery of purified activase from spinach leaves, Robinson et al. (1988) estimated that Rubisco activase accounts for approximately 2% of total soluble protein, this means the activase concentration would be approximately 10 mg mL^{-1} in the stroma.

Recent work carried out by Salvucci (1992) indicates that not only is activase more stable in its aggregated form, but it is also more active. The self-association of Rubisco activase, which probably occurs in the chloroplast stroma *in vivo*, may be promoted *in vitro* by the addition of polyethylene glycol (PEG) (Salvucci, 1992). Solvent-excluding reagents, such as PEG, increase the effective concentration of proteins, thereby driving self-association. The inclusion of PEG in the assay mixture increased all known activities of Rubisco activase. Rubisco activase had higher

ATPase and Rubisco carbamylation activities, concomitant with increased apparent affinity for ATP and Rubisco; and also, the ability of Rubisco activase to facilitate dissociation of the tight-binding inhibitor, 2-carboxyarabinitol 1-phosphate (CA1P), from carbamylated Rubisco was increased in the presence of PEG (Salvucci, 1992). Based on these results, Salvucci (1992) concluded that high concentrations of activase protein in the chloroplast stroma would provide an environment conducive to self-association, and association with Rubisco, and cause expression of properties that would enhance its ability to function *in vivo*.

The characterisation of Rubisco activase's increased activity in its aggregated form provides an explanation for the relatively large amounts of Rubisco activase relative to Rubisco required to facilitate Rubisco carbamylation *in vitro* (Portis, 1990). It seems likely that the high concentrations of Rubisco activase required in these assays are necessary to drive aggregation.

1.9.3 Species specificity of Rubisco activase

If an intimate protein-protein interaction between Rubisco and Rubisco activase is required in the release of inhibitors from Rubisco's catalytic sites, we might expect that any functional, species-dependent differences in the amino acid sequence of Rubisco would be accompanied by species-dependent differences in the amino acid sequence of Rubisco activase. Wang et al. (1992) have observed that Rubisco activase, purified from *Solanaceae* species, stimulated 75-100% Rubisco carbamylation of *Solanaceae* Rubisco, but only 10 to 25% carbamylation of Rubisco from other species. Rubisco activase from the other species supported 50 to 100% carbamylation of their endogenous Rubiscos, but only 10 to 35% in the *Solanaceae*. Therefore, the interaction between substrate-bound Rubisco and Rubisco activase is species dependent. The amino acid sequence of the two Rubisco subunits differ between the *Solanaceae* and the non-*Solanaceae* species that were used in this experiment. Wang et al. (1992) propose that Rubisco and Rubisco activase have co-evolved within these divergent groups, thereby maintaining a physical interaction between these two proteins. This result indicates that activase faciltates carbamylation and sugar phosphate release by binding directly onto Rubisco.

1.10 LIGHT-REGULATION OF RUBISCO CARBAMYLATION

1.10.1 Activase is light-regulated

Early *in vitro* studies on activase established a requirement for light and thylakoids in the activase-facilitated carbamylation of Rubisco (Salvucci et al., 1985). This raised the possibility that activase was involved in modulating changes in Rubisco carbamylation level in response to changes in light intensity. There are several PCR cycle enzymes, such as phosphoribulokinase and fructosebisphosphatase, which are light-regulated by the ferredoxin/thioredoxin system (Buchanan, 1980). However, activase is regulated by a different system (Campbell and Ogren, 1990).

ATP hydrolysis by activase is an essential step in activase-facilitated Rubisco carbamylation (Section 1.9.1). Studies carried out by Robinson and Portis (1988b) showed that Rubisco carbamylation levels changed when they manipulated the stromal ATP and ADP/P_i content of isolated spinach chloroplasts; activase-facilitated Rubisco carbamylation was stimulated by high ATP concentrations and was inhibited by high ADP concentrations. On the basis of these results, Robinson and Portis (1988b) proposed a simple model for the regulation of activase activity and thereby Rubisco carbamylation *in vivo*. They proposed that increases in light intensity would produce an increase in ATP concentration and ATP/ADP ratio, which as a result would increase activase activity and Rubisco carbamylation. Conversely, reductions in light intensity would produce a decrease in ATP concentration and the ATP/ADP ratio, resulting in a decrease in activase activity and Rubisco carbamylation. However subsequent studies carried out by Campbell and Ogren (1990a, 1990b) have shown that several processes are involved in the regulation of activase activity. They used a lysed chloroplast system, in the presence of saturating ATP with a regenerating system, and physiological concentrations of CO_2. Under these conditions they observed a stimulation of Rubisco carbamylation by light (Campbell and Ogren, 1990a), indicating that other reactions or metabolites were involved in the light-activation process in addition to ATP. Campbell and Ogren (1990b) used electron transport inhibitors, and artificial electron donors and acceptors, and the reconstituted system outlined in Campbell and Ogren (1990a) to identify the region of the electron transport chain that was involved in this light-dependent reaction. They observed that stimulation of light activation of Rubisco by activase required electron flow through PS I but not PS II, and that this requirement was not to supply the ATP needed by the Rubisco activase reaction. Since PS I is located within the

nonappressed regions of the thylakoids, this arrangement permits access of the soluble stromal components to that region which mediates the stimulation of Rubisco carbamylation (Campbell and Ogren, 1990b). They also observed that a pH gradient across the thylakoid membrane was necessary for maximum light activation of Rubisco, even when ATP was produced exogenously. Therefore, ATP, a transthylakoid pH gradient and electron flow through PSI are all involved in the regulation of activase-facilitated Rubisco carbamylation (Figure 1.7).

The mechanism by which these processes regulate activase activity have not been identified. Woodrow and Mott (1992) have proposed a mechanism for the light-regulation of activase in which activase is converted to its active form by phosphorylation (Figure 1.7). Some preliminary evidence in support of this claim has been obtained but other workers have not been able to repeat these results (Portis - pers. comm.).

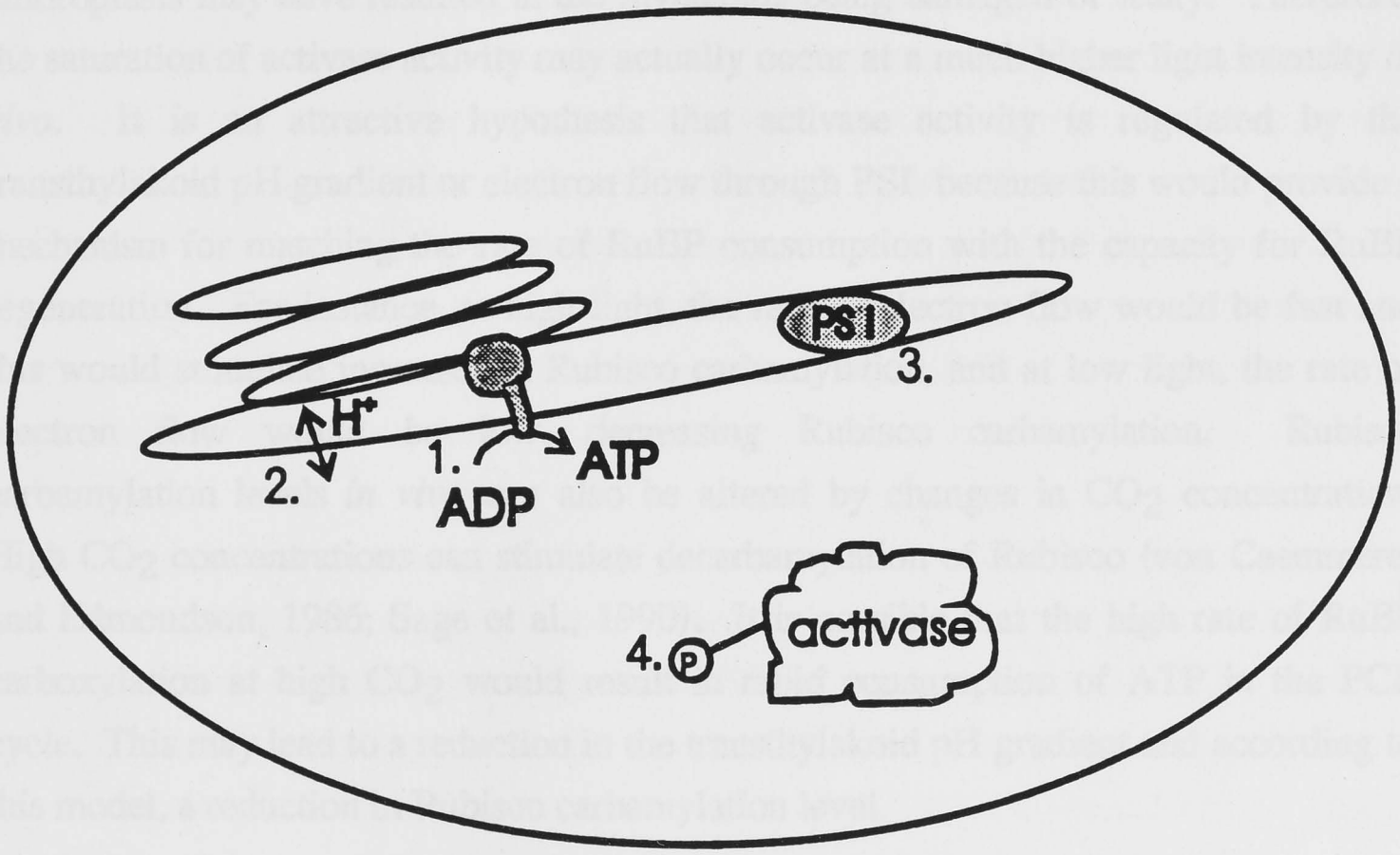

FIGURE 1.7: Possible factors involved in the light-regulation of activase. 1, ATP concentration and the ATP / ADP ratio; 2., the transthylakoid delta pH; 3., Electron flow through photosystem I; 4. Phosphorylation of activase.

1.10.2 Does activase regulate Rubisco carbamylation?

There are *in vitro* and physiological studies that claim to have identified the light intensity at which activase activity saturates, 90 and 200 μmol quanta $m^{-2}s^{-1}$ respectively (Campbell and Ogren, 1992; Woodrow and Mott, 1992). If this was the case we might conclude that activase activity does not limit Rubisco carbamylation level at high light intensities. However, it may be premature to conclude this from the present data.

Campbell and Ogren (1992) have found that the light-activation of Rubisco in their *in vitro* lysed chloroplast - Rubisco activase system saturates at 90 μmol quanta $m^{-2}s^{-1}$. This was assayed in the presence of exogenously supplied, saturating concentrations of ATP. This result demonstrates that the stimulation of activase activity by electron flow through PS I and transthylakoid pH gradient can be saturated. However, it is important to take into account when considering this data that the purification of the chloroplasts may have resulted in the thylakoids being damaged or leaky. Therefore, the saturation of activase activity may actually occur at a much higher light intensity *in vivo*. It is an attractive hypothesis that activase activity is regulated by the transthylakoid pH gradient or electron flow through PSI because this would provide a mechanism for matching the rate of RuBP consumption with the capacity for RuBP regeneration. For instance, at high light, the rate of electron flow would be fast and this would stimulate increases in Rubisco carbamylation, and at low light, the rate of electron flow would be low, decreasing Rubisco carbamylation. Rubisco carbamylation levels *in vivo* can also be altered by changes in CO_2 concentration. High CO_2 concentrations can stimulate decarbamylation of Rubisco (von Caemmerer and Edmondson, 1986; Sage et al., 1990). It is possible that the high rate of RuBP carboxylation at high CO_2 would result in rapid consumption of ATP in the PCR cycle. This may lead to a reduction in the transthylakoid pH gradient and according to this model, a reduction in Rubisco carbamylation level.

Physiological determination of the kinetics of Rubisco activation have lead Woodrow and Mott (1992) to conclude that two processes must take place before an increase in Rubisco activity will occur after a dark-to-light transition. The first process saturates at low light intensity (200 μmol quanta m^{-2} s^{-1}), and the second process saturates in parallel with photosynthesis (Woodrow and Mott, 1992). Analyses of Rubisco and Rubisco activase activities in crude extracts has led them to conclude that the first of these two-processes is the light-dependent activation of activase and the second

process is the carbamylation of Rubisco (Lan et al., 1992). Woodrow and Mott (1992) propose that their biphasic model of Rubisco activation provides an explanation for the observation that low-to-high light increases in Rubisco activity occur more quickly than do dark to light increases in Rubisco activity (Jackson et al., 1991). During dark-to-light conversions, activase must first be "light-activated" and then Rubisco's active sites will be carbamylated, whereas during low to high light conversions, the activase is already fully activated and only carbamylation has to occur.

The two phase activation of Rubisco identified by Woodrow and Mott (1992) is primarily based on gas exchange measures of assimilation rate following changes in light intensity, and on an activase activity assay for crude extract that has several limitations (these are discussed in detail in Chapter 4, Section 4.1). This means their conclusion that activase activity is saturating at low light intensities is currently based on indirect data, and the biochemical processes responsible for the slow increase in photosynthetic rate following dark to high light conversions have not yet been identified. There are several other processes, such as stomatal opening and the build-up of PCR cycle metabolites, which contribute to the slow increase in photosynthetic rate following a dark to high light conversion. Mott and Woodrow (1993) claim to have taken the contribution of these processes into account in their biphasic model. However, it is difficult to resolve the contribution of these processes to the slow increase in photosynthetic rate during dark-to-high light conversions until the mechanism by which activase is light-activated has been positively identified.

If we speculate that activase is fully activated at low light intensities, then what processes are regulating changes in Rubisco carbamylation during low to high light transitions? *In vitro* studies indicated that Rubisco carbamylation could be regulated by ATP / ADP ratios (Streusand and Portis, 1987; Robinson and Portis, 1988b). If this occurred *in vivo* we would expect the ATP / ADP ratios in the chloroplast stroma to change under conditions that are known to alter Rubisco carbamylation level. However, Brooks et al. (1988) found that the ATP / ADP ratio in intact leaves remained relatively constant over a range of irradiance. It is possible that changes in the ATP / ADP ratio in the chloroplast stroma were undetected due to mixing of the stromal pool with adenine nucleotides from the rest of the cell, but this is difficult to prove.

The ability of sugar phosphate compounds to affect the process of Rubisco carbamylation has been discussed previously (Sections 1.4.4). These compounds may have an important role in the regulation of Rubisco carbamylation levels. Low phosphate supplies reduce Rubisco carbamylation in intact plants (Brooks, 1986), and in isolated chloroplasts (Heldt et al., 1978; Mächler and Nösberger, 1984). Portis (1990) attributed this decrease in Rubisco carbamylation to a reduction in the ATP / ADP pools within the chloroplast stroma. However, it is also possible that the low phosphate conditions may have altered the pool size of a sugar phosphate compound that is important in the regulation of Rubisco carbamylation.

If Rubisco carbamylation is controlled by the concentration of a single 'regulator' compound, then the concentration of this compound must change in response to factors which limit the rate of carbon assimilation, such as light intensity and the rate at which the products of the carboxylation are used . The involvement of a phosphate compound or compounds in regulation of carbamylation is an attractive hypothesis, because the concentration of this compound(s) could possibly be regulated by these factors. The concentration of the sugar phosphate could be modulated by light intensity via the availability of ATP, and also by the demand for sugars in the cytoplasm via the rate of orthophosphate import into the chloroplast. For instance, the slight decrease in Rubisco carbamylation at high CO_2 (Section 1.4.2) may be regulated by a decrease in the stromal supply of phosphate brought about by either a depletion of ATP pools and/or a relatively slow rate of orthophosphate import into the chloroplast.

RuBP pool size is a possible regulator of changes in Rubisco carbamylation. *In vitro* studies indicate that activase-facilitated Rubisco carbamylation is dependent on RuBP concentration (Portis et al., 1986). This is consistent with RuBP acting as a positive effector of Rubisco carbamylation in the presence of activase. In this model, an increase in light intensity would produce an increase in the rate of RuBP regeneration relative to consumption, resulting in an increase in RuBP pool size and a consequent increase in Rubisco carbamylation. However, recent results indicate that RuBP pool size is probably not a tight regulator of Rubisco carbamylation. Transgenic plants that contain antisense RNA to glyceraldehyde-3-phosphate dehydrogenase mRNA have a range of steady-state RuBP concentrations when measured at the same light intensity (Price et al., in press). These plants had very similar Rubisco carbamylation levels despite the range in RuBP concentration. It is interesting to note that the RuBP concentration in these transgenic plants did not drop below the

Rubisco catalytic site concentration. This means that it is possible that a reduction in Rubisco carbamylation may have occurrred if the RuBP concentration had decreased below the Rubisco catalytic site concentration.

At the moment the processes involved in the light-regulation of Rubisco and Rubisco activase are not well resolved. Several compounds and processes have been identified as possible regulators of Rubisco carbamylation. It may be that these different processes are important in the regulation of Rubisco carbamylation under different conditions. For instance, electron flow through PS I may regulate changes in Rubisco carbamylation in response to light intensity, and RuBP concentration may modulate changes in Rubisco carbamylation in response to the CO_2 partial pressure.

1.11 STUDYING THE ROLE OF RUBISCO ACTIVASE *IN VIVO*

1.11.1 Rationale

My PhD project has involved the production of tobacco plants which have a range of activase concentrations, using antisense RNA techniques; the analysis of those plants and the development of a quantitative assay for activase content. In this literature review I have outlined the many unknowns in the interaction between activase and Rubisco, and the regulation of Rubisco activity. The analysis of these plants and the application of this assay will enable us to address many of the questions that have been raised. For instance, by studying the requirement for activase *in vivo* we will be able to draw conclusions about the importance of this protein in the maintenance and regulation of Rubisco carbamylation and its role in the removal of inhibitory sugar phosphates, such as CA1P.

1.11.2 Antisense RNA

The activase content of *Nicotiana tabacum* was manipulated using antisense technology. Regulation of expression of specific genes by antisense RNA is a naturally occurring mechanism in bacteria (reviewed in Smith et al., 1988), and antisense genes have been successfully used to inhibit the expression of endogenous genes in transgenic plants (Smith et al., 1988; Rodermel et al., 1988; Hudson et al., 1992b). Transformation with an antisense gene results in decreased levels of mRNA,

and consequently decreased levels of the target protein (Smith et al., 1988). However, it has been difficult to identify the precise mechanism by which antisense genes elicit their effect. The decreased levels of mRNA seemed to indicate that processes occurring in the nucleus, such as interference with transport or transcription, were responsible (Smith et al., 1988). However, subsequent studies have shown that the reduction in target protein by antisense genes is due to an event which occurs after transcription (Grierson, 1993). Therefore, the low levels of mRNA in plants containing antisense genes, are probably caused by the rapid and selective degradation of double-stranded RNA hybrids (Grierson, 1993) (Figure 1.8).

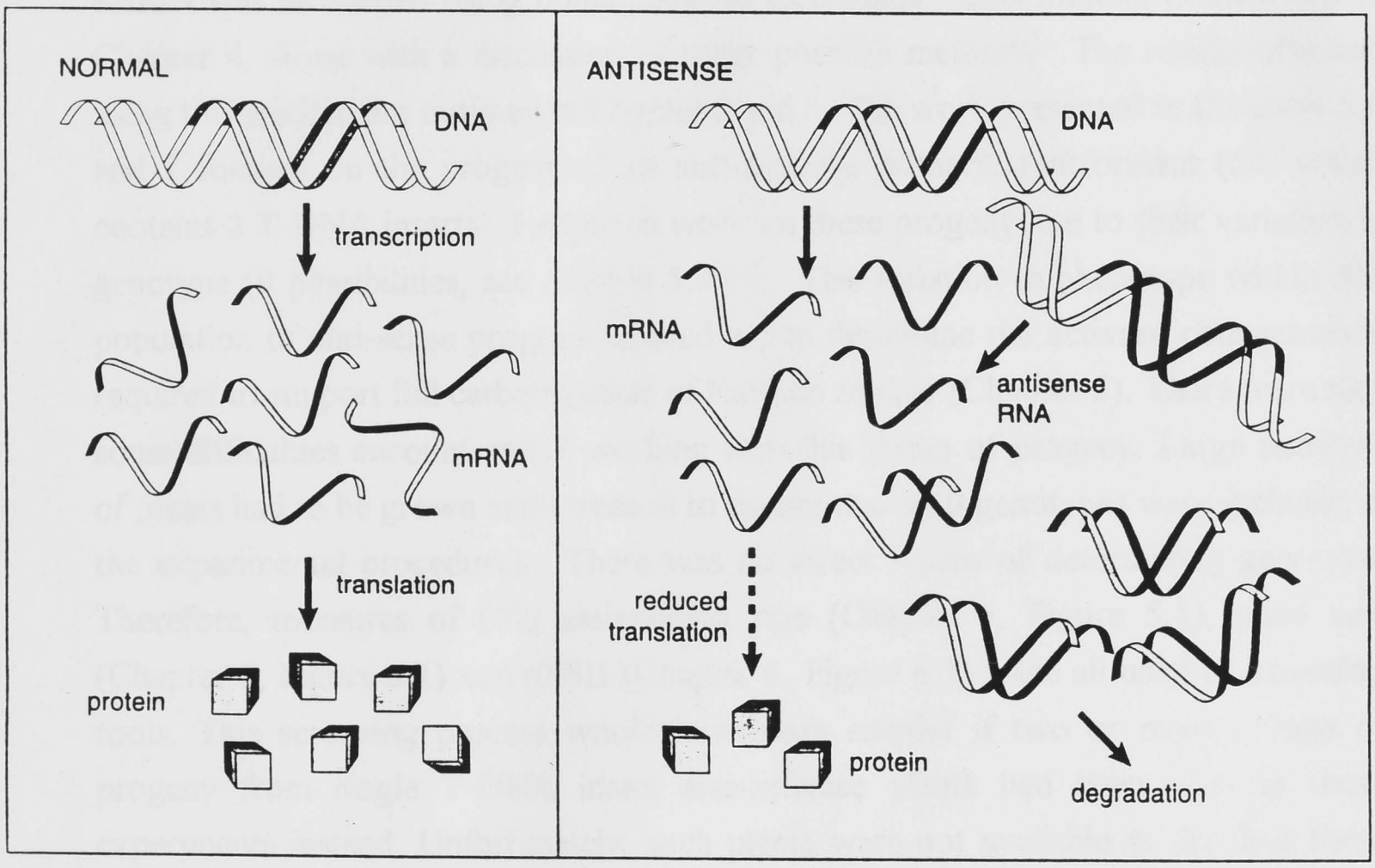

FIGURE 1.8: Effect of antisense RNA

The reduction of activase content *in vivo* is a component of a larger project in which key photosynthetic enzymes are being targeted using antisense techniques. The Rubisco, glyceraldehyde 3-phosphate dehydrogenase, phosphoribulokinase and carbonic anyhdrase content of *Nicotiana tabacum* have also been decreased using antisense RNA, and plans are currently under way to target several other key photosynthetic proteins. The analysis of the anti-activase plants will enable us to investigate the specific roles of activase *in vivo*. Future comparisons between the

anti-activase and other photosynthetically impaired plants will also enable us to investigate other processes, such as the light-regulation of Rubisco.

1.12 OUTLINE OF THESIS

In this thesis I will outline the construction and initial identification of the activase-deficient antisense plants (Chapter 2), followed by an investigation of the effect of activase-deficiency on Rubisco carbamylation and CA1P release after the onset of illumination (Chapter 3). A method for quantifying the activase content within plant extract was developed using immunological techniques. This method is described in Chapter 4, along with a discussion of other possible methods. The results obtained using this method are outlined in Chapter 5 and 6. The work presented in Chapters 5,6 and 7 focuses on the progeny of an anti-activase primary transformant (52) which contains 2 T-DNA inserts. I chose to work on these progeny due to their variation in genotype (9 possibilities, see Section 5.3.1.). The variation in phenotype within this population of anti-sense progeny enabled me to determine the activase concentration required to support full carbamylation of Rubisco *in vivo* (Chapter 5). There were also some difficulties encountered in working with this group of progeny. Large numbers of plants had to be grown and screened to ensure that all 9 genotypes were included in the experimental procedures. There was no direct means of determining genotype. Therefore, measures of CO_2 assimilation rate (Chapter 5, Figure 5.1), plant size (Chapter 5, Figure 5.1) and ϕPSII (Chapter 6, Figure 6.1) were all used as screening tools. This screening process would have been simpler if two or more groups of progeny from single T-DNA insert anti-activase plants had been used in these experiments instead. Unfortunately, such plants were not available at the time these experiments were carried out. In spite of the difficulties in screening the progeny of anti-activase plant 52, these plants have been used successfully to investigate the physiological and biochemical impact of activase-deficiency (Chapters 5, 6 and 7).

CHAPTER 2: The production and identification of activase-deficient tobacco plants

2.1 INTRODUCTION

Our current understanding of activase's role and mechanism *in vivo* has been gleaned from the analysis of the *A.thaliana rca* mutant and from *in vitro* studies on the interaction between Rubisco and activase. However, these methods of investigation have their limitations. The *rca* mutant contains no activase, due to a guanine-to-adenine transition at the 5'-splice junction of intron 3 in the six-intron pre-mRNA (Orozco et al., 1993). Consequently, the *rca* mutant has an absolute requirement for high CO_2 for growth. Growth at high CO_2 can affect several photosynthetic parameters in wild-type plants, such as Rubisco content and carbamylation level, and it can also affect growth rates and lead to the accumulation of high concentrations of starch. Therefore, any experiments comparing control and *rca* mutant *A.thaliana* plants must take into account the confounding effects of growth at high CO_2.

In vitro studies are also limited in the information they can provide about the interaction between Rubisco and activase *in vivo*. Very high ratios of activase to Rubisco have to be used *in vitro* to activate Rubisco, much higher than eight activase dimers per Rubisco (L_8S_8) (Portis et al., 1986; Lan and Mott, 1991). If such high ratios were required *in vivo*, then activase would have to account for approximately 40% of total soluble protein (assuming that Rubisco accounts for approximately 30% of total soluble protein); whereas, purification studies have shown that it accounts for approximately 2% of total soluble protein (Robinson et al., 1988). Therefore, although *in vitro* studies can provide some insight into the interaction between Rubisco and activase, they obviously do not reproduce the interaction that occurs between Rubisco and activase *in vivo*.

In this chapter, I will outline the production and initial analysis of activase-deficient tobacco plants. These plants were transformed with a partial tobacco activase cDNA inserted into the genome in the antisense orientation. Past studies have shown that antisense RNA techniques enable the production of plants that are deficient in a specific protein, and that a group of plants transformed with an antisense construct will usually have a range of target protein concentrations (Smith et al., 1988; Rodermel et al., 1988; Hudson et al., 1992b). The production of activase-deficient plants, with a range of activase levels, enables us to carry out investigations into the roles and mechanisms of activase that were not previously possible. For instance, some of the anti-activase plants can be grown in air, and as a result a comparison of

control and activase-deficient plants can be carried out without the confounding effects of growth at high CO_2. Also, the production of plants with a range of activase levels has enabled us to determine the stoichiometry of activase to Rubisco required to maintain wild-type levels of photosynthesis.

2.2 MATERIALS AND METHODS

2.2.1 Isolation and manipulation of tobacco and spinach *rca* cDNAs

A partial cDNA for tobacco *rca* was isolated from *N. tabacum* cv W38 RNA by the polymerase chain reaction using a specific 5' primer (ACT 5'c) and a general 3' primer (Hudson et al., 1992a). The specific primer 5'-GGGAGGCAAGGGTCAAGGTAA-3' was based on the codons for the amino acid sequence Gly-Gly-Lys-Gly-Gln-Gly-Lys, which is located at the putative ATP-binding site of *S. oleracea* and *A. thaliana* Rubisco activases (Werneke et al., 1988; Werneke and Ogren, 1989). The 1.2 kbp cDNA corresponding to the 3' two-thirds of the *rca* mRNA was cloned into the *Sma*I site of pTZ18R and one clone, pTACT2, was found to have the cDNA inserted in the correct orientation for subcloning. A *Bam*HI - *Kpn*I fragment from pTACT2 encompassing the cDNA was subcloned into pBIN19(CaMV-nos), which is a derivative of pBI121 (Jefferson et al., 1987) without the *uidA* gene. The resulting plasmid, pαTACT, had the cDNA in the antisense orientation with respect to the CaMV 35S promoter.

2.2.2 Sequencing

The putative cDNA of tobacco activase was partially sequenced using the Pharmacia T7 Sequencing kit and the specific 5' primer, ACT 5'c, and fractionated on a 5% sequencing gel.

2.2.3 Transformation and growth of the antisense plants

The T-DNAs of pαTACT and pBI121 (as a control) were introduced into tobacco by the leaf disc method (Herrera-Estrella and Simpson, 1988) and selected on kanamycin-containing medium. Regenerated plantlets were initially transferred into pots of

vermiculite and placed in a growth cabinet. The cabinet temperature was 22°C (day) and 15°C (night), with 60% relative humidity and a 12-h photoperiod. Two series of plantlets were raised in tissue culture; the first series was transferred into the growth cabinets at atmospheric CO_2 and an irradiance of 750 μmol quanta m^{-2} s^{-1}. Approximately 80% of the pαTACT primary transformants died under these conditions. The second series of plants was raised under a higher CO_2 concentration (0.3 to 0.5%) with an initial irradiance of 400 μmol quanta m^{-2} s^{-1}, increasing after seven days to 750 μmol quanta m^{-2} s^{-1}. Under these conditions, the fatality rate was only 7%. The plants were supplied with complete nutrient solution containing 12 mM nitrate three times per week (Hewitt and Smith, 1975). The plants were transferred into three-litre pots containing sterilized garden soil after three weeks, and three weeks later they were screened by immunoblot and biochemical assays for activase and Rubisco carbamylation levels. The primary transformants were allowed to self-fertilize and the R_1 seed was collected and stored at 4°C. The R_1 seedlings were raised in a growth cabinet with a 12-h photoperiod, at 25°C (day) and 17°C (night), 0.3 to 0.5% CO_2, 60% relative humidity and 550 μmol quanta m^{-2} s^{-1}. The plants were grown in five-litre pots and analyzed approximately six to eight weeks after germination.

2.2.4 Sampling procedures

All of the plants were sampled or assayed in the growth cabinets, except those used in the gas exchange analysis. The plants were sampled by taking leaf punches which were collected into liquid nitrogen and stored at -80°C until required. Samples from the primary transformants for immunoblotting were taken six weeks after the plantlets had been removed from tissue culture. Samples for the carbamylation assays were taken in the dark (five min before the photoperiod commenced) and 90-min after the onset of illumination. After the 90-min sample was taken, the CO_2 concentration in the growth cabinets was lowered to 0.03%. The low CO_2 -leaf samples were taken the following day.

The R_1 seedlings were initially screened by chlorophyll fluorescence in the growth cabinet. Measurements were taken at high CO_2 , after which the CO_2 concentration in the growth cabinet was decreased to 0.03% for approximately 24 h before taking the next fluorescence measurements. The growth cabinet was returned to high CO_2 and the plants were sampled for determination of activase levels the following day.

2.2.5 Immunoblotting

Leaf punches (2 cm^2) were extracted in 0.5 mL of buffer (50 mM bis-Tris propane, pH 7.0, 10 mM $MgCl_2$, 1 mM sodium EDTA, 10 mM DTT, 1.5% polyvinylpolypyrrolidone, 1 mM phenyl methyl sulphonyl fluoride). Mercaptoethanol and SDS were added to the extract to 4% [v/v] and 2% [v/v] respectively, before boiling for 10 min. The extract was centrifuged and a sample of the supernatant was separated on a Pharmacia Phastgel (SDS buffer, 12.5% homogenous). The proteins were electroblotted to nitrocellulose, then blocked with 5% milk powder in 20 mM Tris-HCl, pH 8.5, 0.5 M NaCl (TBS) and probed with the following antibodies and reagents in 5% milk powder, 0.05% Triton X100 in TBS: (1) primary antibody, polyclonal rabbit anti-glutathione *S*-transferase / spinach activase fusion protein (for a complete description of the immunogen and antibody refer to Chapter 4); (2) secondary antibody, biotinylated goat anti-rabbit immunoglobulin (Amersham); and (3) streptavidin-alkaline phosphatase (BioRad). The activase bands were visualized by incubation with the substrates 5-bromo-4-chloro-3-indoyl phosphate and nitroblue tetrazolium.

2.2.6 Determination of T-DNA copy number

Leaf DNA was prepared by the hexadecyltrimethylammonium bromide method (Saghai-Maroof et al., 1984). An inverse polymerase chain reaction technique (Does et al., 1991) with α-thio[^{35}S]dATP (Amersham) included in the amplification reaction was used to determine the number of T-DNA copies inserted into the genomes of individual plants. The segregation of kanamycin resistance and sensitivity in the R_1 generation was also used to determine the T-DNA copy number of the primary transformants. Surface-sterilized seeds were germinated on half-strength MS media (Herrera-Estrella and Simpson, 1988) containing 200 µg/mL of kanamycin and 200 µg/mL of cefotaxamine. After 5 weeks in a growth cabinet at 0.5% CO_2 , the kanamycin-sensitive seedlings turned white, whereas the resistant seedlings remained green.

2.2.7 Measurements of CO_2 assimilation rate

Gas exchange measurements were made in an open gas exchange system, as described by Brugnoli et al. (1988) with modifications as outlined by Hudson et al. (1992b). Plants were placed in the gas exchange system in the dark following 12 h of darkness and the first measurements were taken. The lights were switched on to give an irradiance of 1000 μmol quanta m^{-2} s^{-1} and the rate of CO_2 assimilation was followed. The leaf temperature was 25°C, the leaf to air vapour pressure difference was 11 mbar and the CO_2 concentration was 350 μbar. Calculation of gas exchange parameters was made according to the method of von Caemmerer and Farquhar (1981).

Chlorophyll fluorescence was measured with a fluorimeter (Pam 101, Waltz, Effeltrich, Germany) under the growth conditions approximately 90 min after the onset of illumination following 12 h darkness. The steady state fluorescence yield (F_s) was measured under the growth irradiance, and saturating pulses (14,000 μmol quanta m^{-2} s^{-1}) were given at 100-s intervals to determine F_m'. The electron flow through photosystem II per unit quantum flux, ϕPSII, was calculated as (F_m' - F_s)/ F_m' in accordance with Genty et al. (1989).

2.2.8 Biochemical assays

Leaf punches (0.5 cm^2) were rapidly extracted in 1 mL of buffer (50 mM HEPES/KOH, pH 7.1, 5 mM $MgCl_2$, 1 mM sodium EDTA, 10 mM DTT, 20 mM sodium isoascorbate, 1 mM phenyl methyl sulfonyl fluoride and 1.5% polyvinylpolypyrrolidone) on ice. Rubisco carbamylation was measured immediately (within 10-15 s), after which Rubisco content and soluble protein were measured.

The Rubisco catalytic site concentrations and carbamylation levels were measured by the stoichiometric binding of [^{14}C]CABP (Collatz et al., 1978), based on the method of Butz and Sharkey (1989). [*carboxy*-^{14}C]CPBP was prepared as described by Collatz et al. (1978). The catalytic site concentration was determined by measuring the [^{14}C]CABP binding capacity of extract in which the Rubisco had been fully carbamylated by saturating CO_2 and Mg^{2+}. The buffer was 50 mM Bicine [pH 7.8], 20 mM $MgCl_2$, 15 mM $NaHCO_3$, 1 mM sodium EDTA and [^{14}C]CPBP at a ten-fold or greater excess over Rubisco catalytic sites. All buffers used in these experiments were sparged overnight with N_2 to displace any CO_2 present in solution. 50 μL of extract was incubated with 150 μL of the buffer containing [^{14}C]CPBP for 45 min at

25°C, during which time all Rubisco sites were carbamylated and [^{14}C]CABP was bound irreversibly. Rubisco-[^{14}C]CABP complexes were precipitated with bovine serum albumin (2.5 mg mL^{-1}) as carrier by adding polyethylene glycol (4000 to 6000 kD) and $MgCl_2$ to a final concentration of 20%[w/v] and 25 mM, respectively. Precipitation was carried out on ice for 30 min, followed by centrifugation at 4°C for 15 min. The pellet was washed (but not resuspended) three times using 500 µL of 50 mM Bicine, pH 7.8, 15 mM $MgCl_2$, 1 mM sodium EDTA and 20% PEG. Each wash was followed by 5 min of centrifugation at 4°C. The pellet was dissolved in 300 µL of water and transferred to a scintillation vial, and 3 mL of Amersham ACS II fluid was added. The ^{14}C retained within the sample was determined by liquid scintillation counting. It was assumed that eight binding sites occur per 550 kD holoenzyme.

The carbamylation level was determined by exchanging loosely bound [^{14}C]CABP at noncarbamylated catalytic sites with an excess of [^{12}C]CABP (Butz and Sharkey, 1989). Carbamylation levels measured this way correlate with the ratio between initial Rubisco activity after rapid leaf extraction and total Rubisco activity following preincubation with CO_2 and Mg^{2+} (Butz and Sharkey, 1989). Within 10 - 15 s after extraction, 50 µL of extract was added to a 150 µL solution containing buffer (50 mM Bicine, pH 7.8, 5 mM $MgCl_2$, 1 mM sodium EDTA) plus [^{14}C]CPBP (at a ten-fold or greater excess over Rubisco catalytic sites) and incubated on ice for 45 min. Then, [^{12}C]CPBP was added at a 200-fold higher concentration than that of [^{14}C]CPBP, and the extract was incubated at 25°C for 5 min. The Rubisco-CABP complexes were precipitated, washed and counted as outlined above.

Phosphoribulokinase activity and total protein were assayed as described by Hudson et al. (1992b) except the volume was halved for the enzyme assay. A molecular weight of 80 kD and a specific activity of 6800 µmole g^{-1} s^{-1} (Porter et al., 1986) were used to calculate phosphoribulokinase content.

2.3 RESULTS

2.3.1 Production of primary transformants

The identity of the partial tobacco activase cDNA, generated using the polymerase chain reaction, was confirmed by partial DNA sequencing. An open reading frame was revealed with a

predicted amino acid sequence similar to that of the spinach *rca* cDNA (Werneke et al., 1988; Figure 2.1). This reading frame was later found to be identical to the nucleotide sequence of another tobacco *rca* cDNA (Qian and Rodermel, 1993).

```
sp    G G K G Q G K S F Q C E L V F A K L G I N P I M M S A G E L E
tob   . . . . E . . . . . . . . . . R . M . . . . . . . . . . . .
      I  ACT 5'C  I
```

FIGURE 2.1: Homology between the amino acid sequences encoded by spinach activase cDNA (sp) and the partial tobacco activase cDNA (tob) generated by the polymerase chain reaction. A portion of the putative tobacco activase cDNA was sequenced in order to confirm its identity. The sequence shown here starts at the site where the primer ACT 5'C anneals to the encoding cDNA. The ACT 5'C primer binds to the cDNA which encodes for an ATP binding site, approximately 110 amino acids downstream of the amino terminal end of the polypeptide. A dot in the tobacco sequence indicates identity with the spinach residue.

Tobacco was transformed with a T-DNA containing the kanamycin resistance gene linked to either the *uidA* gene for β-glucuronidase (control) or the antisense gene (Figure 2.2). Transformed plants were grown in growth cabinets at high CO_2 and were screened for activase protein by immunoblotting of proteins in leaf extracts. Eighteen anti-activase primary transformants were screened using this technique. Several plants had low to very low levels of activase (Figure 2.3A). Taking into account the sensitivity of the immunoblotting technique, a comparison of the control and anti-activase plants indicated that activase levels had been reduced by at least 50% in plants 38 and 50, and by at least 75% in plant 52. All eighteen plants were grown to seed.

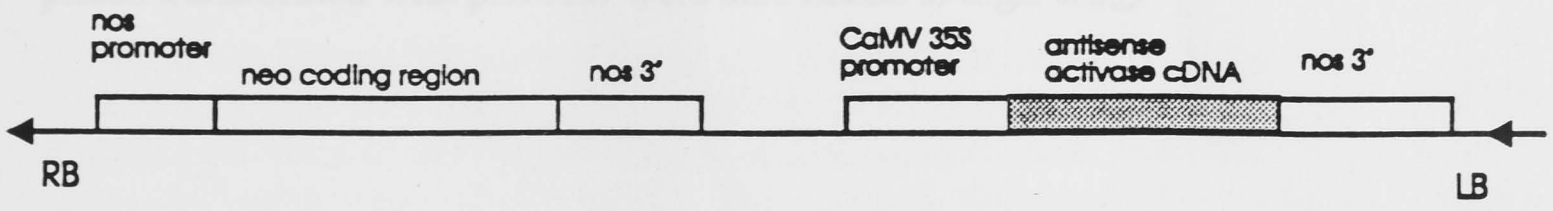

FIGURE 2.2: Map of the T-DNA region from plasmid pαTACT, a derivative of pBIN19. LB and RB, left and right borders, respectively; kbp, kilobase pair. The *neo* gene encodes the neomycin phosphotransferase II protein for kanamycin resistance. Transcription of the *neo* and antisense genes is from left to right.

DNA was prepared from primary transformants 50 and 52, and the number of T-DNA copies inserted into the genome was determined by an inverse PCR method (Does et al., 1991) (Figure 2.3B). Plant 52 had two inserts. The R_1 progeny of plant 52 had a fatality ratio of 59:850 on kanamycin-containing medium, which is consistent with the stable inheritance of two T-DNA inserts (expected fatality rate 1:15). All subsequent results presented in this thesis were obtained from the R_1 progeny of plant 52. Since plant 52 had two inserts, we expected that the R_1 progeny would have a range of zero to four inserts, with activase levels varying inversely with the number of inserts inherited.

2.3.2 Phenotype of the R_1 antisense plants

The R_1 anti-activase plants were grown at high and low CO_2. There were two phenotypes at low CO_2 (ambient) (Figure 2.4, left). Approximately half of the seedlings were yellow-green and the other half were dark green. The dark green phenotype grew more quickly than the yellow-green, but both phenotypes grew slower than the wild-type controls (not shown). Several of the yellow-green phenotype hardly grew at all. At high CO_2, the anti-activase seedlings were initially homogeneous in appearance (Figure 2.4, right) and looked similar to the controls (not shown). Later in development (1 to 2 weeks), some anti-activase plants (approximately 25%) developed veinal chlorosis. All plants assayed by immunoblotting (four of dark green phenotype and five of yellow-green phenotype) had a greater than 75% reduction in activase content compared to the control plants (results not shown). Differences in the activase content of the R_1 progeny could not be detected due to the limitations of the immunoblot technique. Plants from the high CO_2-grown group were used in the experiments. The control plants (R_1 progeny of plants transformed with pBI121) were also raised at high CO_2.

A.

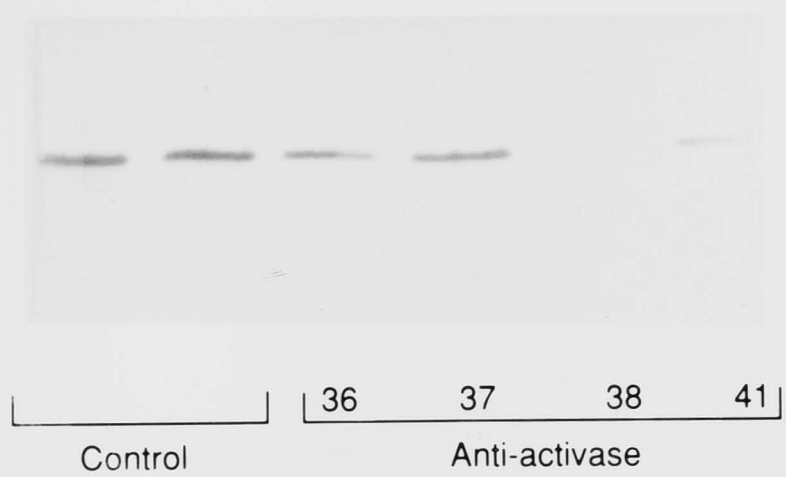

B.

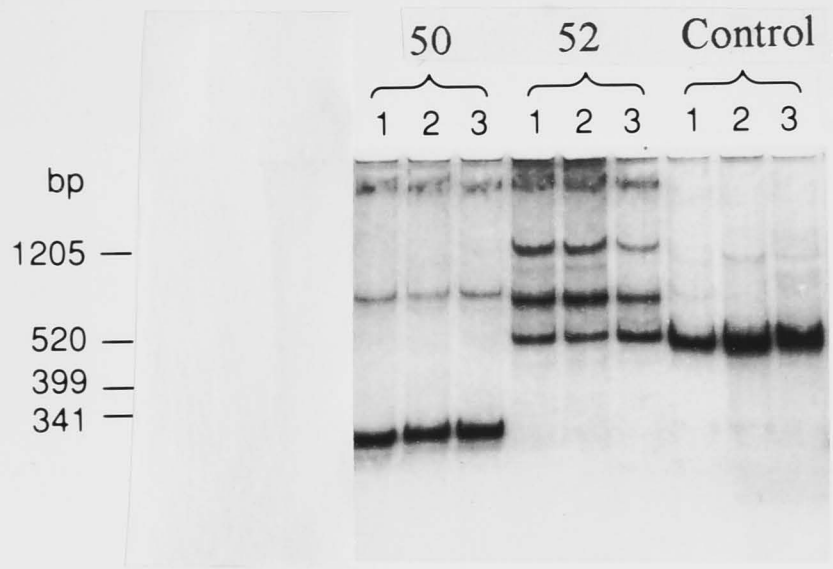

FIGURE 2.3: Characterisation of the primary transformant anti-activase plants.
A. Immunological detection of rubisco activase in tobacco leaf extracts separated by SDS-PAGE. Leaf extracts were obtained from mature tobacco plants that had been transformed with either pBI121 (control) or pαTACT (anti-activase). The numbers refer to individual anti-activase transformants from which the extracts were obtained. B. Inverse polymerase chain reaction assay for determining T-DNA copy number. This technique is based on the varying distance between *Taq*I sites within the *neo* gene of the T-DNA and the tobacco DNA flanking the right border (Does et al., 1991). Shown is an autoradiograph of the radiolabelled amplification products on a 4% sequencing gel. The samples are, from left to right, antisense transformants 50 and 52, and a control transformant. Prior to amplification, the samples were cut with a second enzyme, either *Bsu*361, *Sac*II or *Ssp*I (from left to right), so that three lanes occur for each DNA sample.

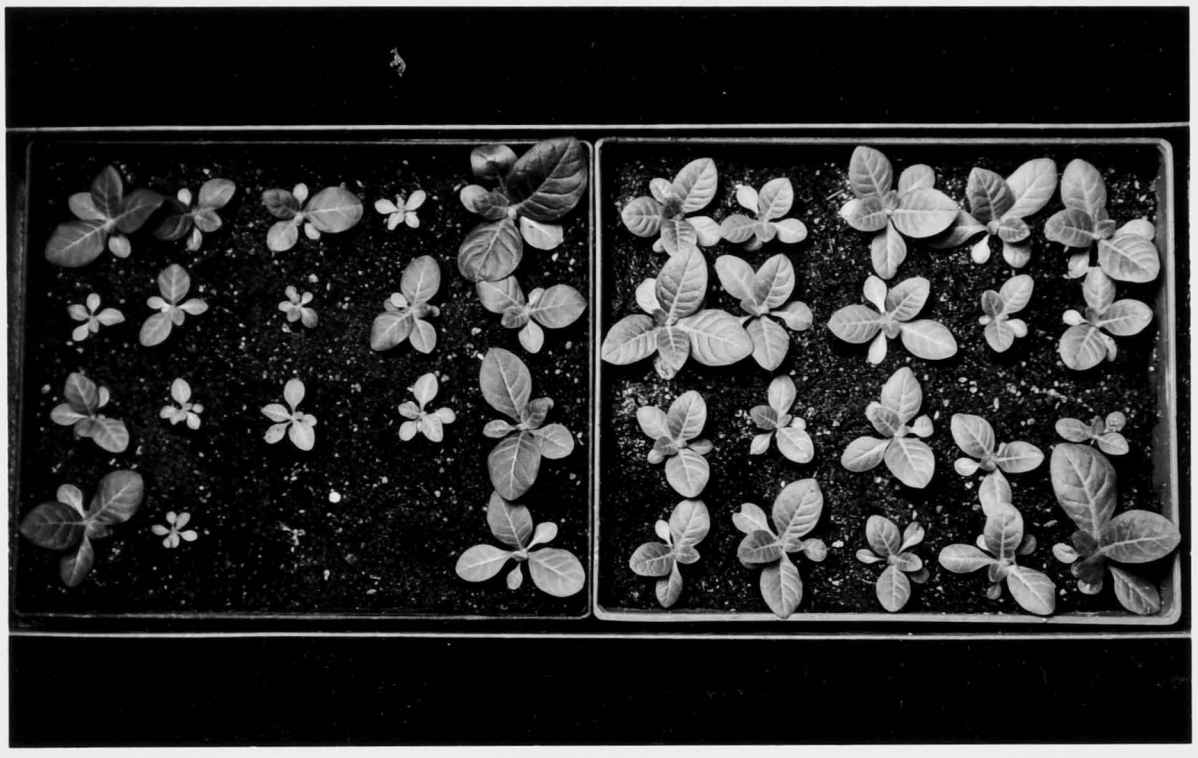

FIGURE 2.4: Anti-activase plants germinated and grown at high (0.3-0.5%, right) and atmospheric (0.03%, left) CO_2. Growth conditions for both CO_2 concentrations were as follows: irradiance 550 μmol quanta m^{-2} s^{-1}, temperature 25° C day / 17° C night, 12 h photoperiod, relative humidity 60%.

2.3.3 Photosynthesis

The chlorophyll fluorescence parameter, ϕPSII, measures the quantum efficiency of photosystem II. ϕPSII reflects the activity of the light reactions and the consumption of their products. Therefore, it provides a quick and useful estimate of light reaction activity and, by inference, photosynthetic rate. Chlorophyll fluorescence was measured in the growth cabinets under high CO_2 growth conditions and again after 24 h of equilibration at ambient CO_2. ϕPSII was quite high in both control and anti-activase plants at high CO_2, indicating healthy rates of photosynthesis. There was no difference between high and low CO_2 measurements for the control plants (Table I), probably due to light limitation of the photosynthetic rate. In contrast, the chlorophyll fluorescence parameter of the anti-activase plants dropped by 40% when transferred from high to low CO_2, reflecting a decrease in the photosynthetic rate.

Table I: *Chlorophyll fluorescence parameter (ϕPSII) of control and R_1 anti-activase plants at high and atmospheric CO_2.* Measurements were taken under the growth conditions according to Hudson e*t al* (1992b) approximately 90 min after the onset of illumination following 12 h of darkness The chlorophyll fluorescence parameter, which represents the quantum efficiency of PS II, was measured on the adaxial surface and calculated according to Genty et al. (1989).

	ϕ PSII	
	High CO_2 (0.35%)	Low CO_2 (0.03%)
Control	0.66 ± 0.001 n=3	0.652 ± 0.001 n=3
Anti-activase	0.58 ± 0.002 n=7	0.327 ± 0.010 n=9

Gas exchange measurements were made on three anti-activase and three control plants. The plants were illuminated at 1000 μmol quanta m^{-2} s^{-1} in the gas exchange system after 12 to 15 h at ambient CO_2 in the dark. After 2h of illumination the assimilation rate of the anti-activase R_1 progeny was approximately half that of the control (Table II). The assimilation rates of primary transformant 52 and a corresponding control were relatively low compared to the R_1 progeny. The lower

rate of the primary transformant control is probably because gas exchange was measured at a later stage in development. This may also be the reason for the lower rate in primary transformant 52. Alternatively, the lower assimilation rate of plant 52, parent of the R_1 progeny, may be due to a higher antisense gene dosage than the R_1 progeny.

The internal partial pressure of CO_2 in the anti-activase plants was higher than that of the control plants (Table II). Therefore, on the basis of this preliminary data we can draw the tenatative conclusion that diffusional resistance did not contribute to the disparity in photosynthetic rate between control and anti-activase plants. The difference in CO_2 assimilation rate was also not due to differences in Rubisco content since assays showed that the anti-activase plants contained, on average, approximately twice as much Rubisco protein as the control plants (Figure 2.5).

Table II: *CO_2 assimilation rate and intercellular CO_2 partial pressure of control and anti-activase plants after 2h of illumination.* The irradiance was 1000 μmol quanta m^{-2} s^{-1}. The leaf temperature was 25°C, the leaf to air vapour pressure difference was 11 mbar and the CO_2 partial pressure was 350 mbar.

	Assimilation rate (μmol m^{-2} s^{-1})	Intercellular CO_2 partial pressure (μbar)
Control (pBI121)		
Primary transformant	9.10 (n=1)	243 (n=1)
R_1	14.63 + 2.37 (n=2)	256.5 + 5.5 (n=2)
Anti-activase (pαTACT)		
Primary transformant 52	0.87 (n=1)	304 (n=1)
R_1	6.29 + 0.09 (n=2)	294 + 10 (n=2)

2.3.4 Rubisco carbamylation levels

Both the primary transformants and the R_1 seedlings were grown at high CO_2 and were sampled for carbamylation assays. The primary transformants were also sampled at low CO_2 . Preliminary results with control and anti-activase (plants 52 and 50) primary transformants showed little difference in Rubisco carbamylation levels between high and low CO_2 (Table III). Therefore, all subsequent leaf samples were taken at high CO_2 in the dark and after 90 min of illumination at 1000 μmol quanta m^{-2} s^{-1}. The Rubisco carbamylation level in the primary transformant

controls was 75% after 90 min of illumination, compared to 30 to 36% in the anti-activase plants. The 90-min leaf samples of the R_1 progeny of plant 52, taken at the same light intensity as the primary transformants, had very similar Rubisco carbamylation levels.

Table III: *Carbamylation level of Rubisco (%) in control and anti-activase tobacco plants in the light and dark at two CO_2 concentrations.* Carbamylation levels in primary transformants (plants 52 and 50) and a selection of R_1 seedlings were measured as described in the methods. Carbamylation level was measured by CABP binding.

	Carbamylation level (%)			
	Primary transformants		R_1 generation	
	Dark	Light[a]	Dark	Light[b,c]
Control				
0.3-0.5% CO_2	55.5 ± 5.5 n=2	74.5 ± 3.5 n=2	41 ± 9 n=2	77.5 ± 3.5[b] n=2
				55.3 ± 0.9[c] n=3
0.03% CO_2	61 ± 5 n=2	74.5 ± 5.5 n=2	–	–
Anti-activase				
0.3-0.5% CO_2	49 ± 1.4 n=2	30.5 ± 0.5 n=2	66.3 ± 1.5 n=3	34.3 ± 1.7[b] n=3
				21.7 ± 1.2[c] n=9
0.03% CO_2	58.5 ± 6.5 n=2	36.5 ± 4.5 n=2	–	–

a Leaves sampled after 90 min at 750 μmol quanta $m^{-2}s^{-1}$
b Leaves sampled after 90 min at 1000 μmol quanta $m^{-2}s^{-1}$
c Leaves sampled after 3 h at 550 μmol quanta $m^{-2}s^{-1}$

The R_1 progeny were also sampled for Rubisco carbamylation after 3 h of illumination at 550 μmol quanta m^{-2} s^{-1} following a 12-h night (Table III). The carbamylation level of the control plants was only 55%, probably due to the low light intensity. Interestingly, there was very little variation in the carbamylation levels among the nine R_1 progeny, which were all around 20%. This result indicates that the R_1 progeny are physiologically similar despite their expected range of genotypes.

2.3.5 Relationship between Rubisco and soluble protein

The anti-activase plants had more soluble protein in their leaves than the control plants (Figure 2.5). A constant relationship between phosphoribulokinase and protein content was observed for both control and anti-activase plants. All points fell on the same line of constant slope drawn through the origin (Figure 2.5A), indicating that a constant proportion of the soluble protein was partitioned into phosphoribulokinase. However, the anti-activase points fell on a line of steeper slope than did the control plants when Rubisco content was plotted against protein (Figure 2.5B). This indicates that a greater amount of protein was partitioned into Rubisco in the anti-activase plants (0.33 g Rubisco per g soluble protein) than in the control plants (0.2 g Rubisco per g soluble protein). The anti-activase plants' soluble protein content was approximately 1.0-1.5 g m^{-2} higher than that of the control plants. Rubisco accounted for most of this increase.

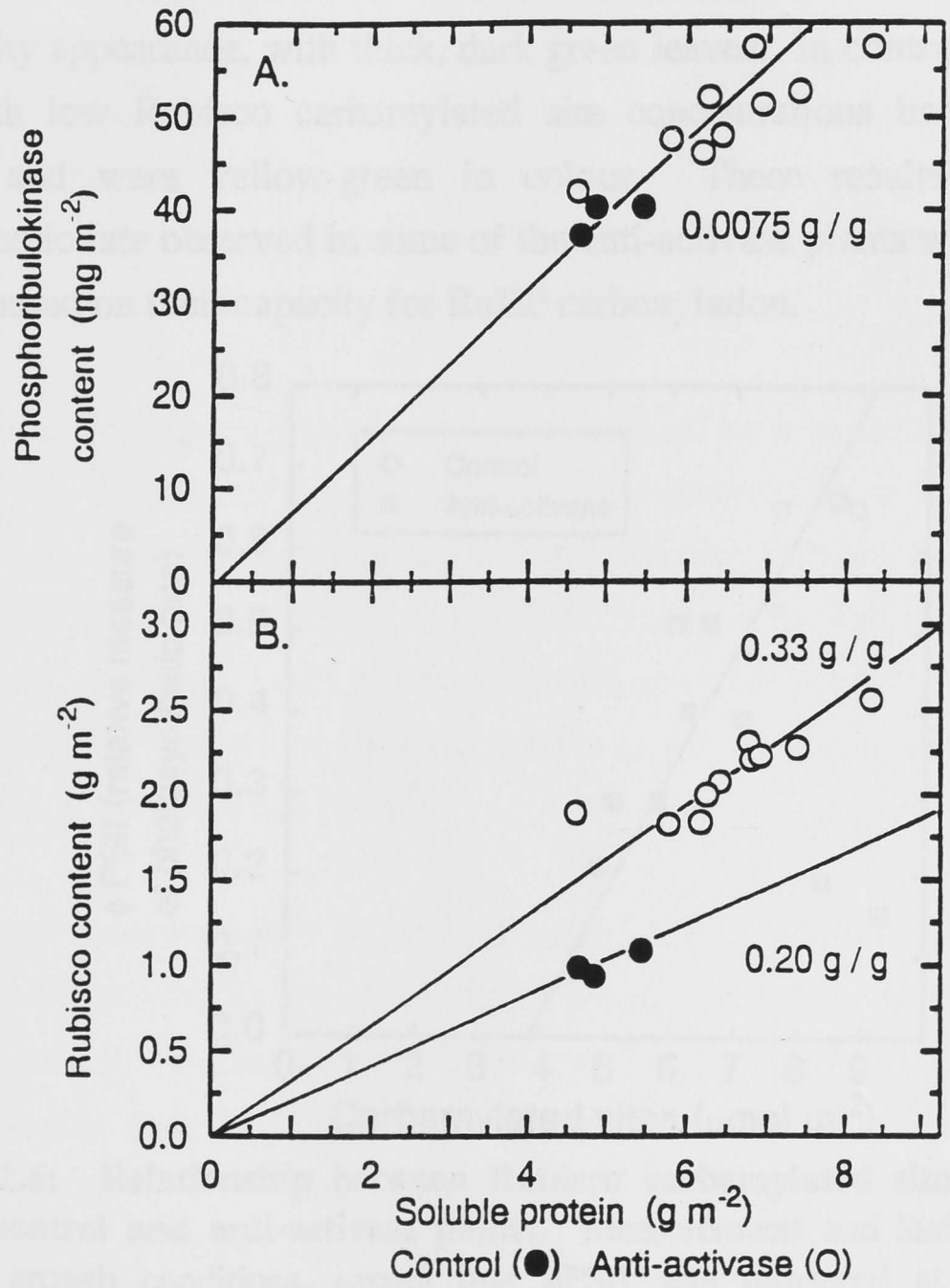

FIGURE 2.5: Protein partitioning in transgenic tobacco plants. Shown are the relationships between soluble protein content, and (A) phosphoribulokinase or (B) Rubisco content.

2.3.6 Repressed Rubisco activity in some anti-activase plants

All the R_1 anti-activase plants had low Rubisco carbamylation levels of approximately 20% when measured under the growth conditions, compared to 55% in the controls. On initial inspection this difference in Rubisco carbamylation seemed to account for the difference in photosynthetic rate (Table I and Table II). However, when the high Rubisco concentration in the anti-activase plants was taken into consideration we found that the reductions in Rubisco carbamylated site concentration did not account for the reductions in photosynthetic rate, as indicated by ϕPSII. For example, one of the anti-activase plants had a ϕPSII that was only 30% of the control plants, but its Rubisco carbamylated site concentration was nearly 60% of that observed in the control plants (Figure 2.6). There were also two outlying points, these plants had the lowest ϕPSII ratios but their Rubisco carbamylated site concentrations were similar to the controls. These plants had a very healthy appearance, with thick, dark green leaves. In contrast, the anti-activase plants with low Rubisco carbamylated site concentrations had developed veinal chlorosis and were yellow-green in colour. These results indicate that the photosynthetic rate observed in some of the anti-activase plants was much lower than expected based on their capacity for RuBP carboxylation.

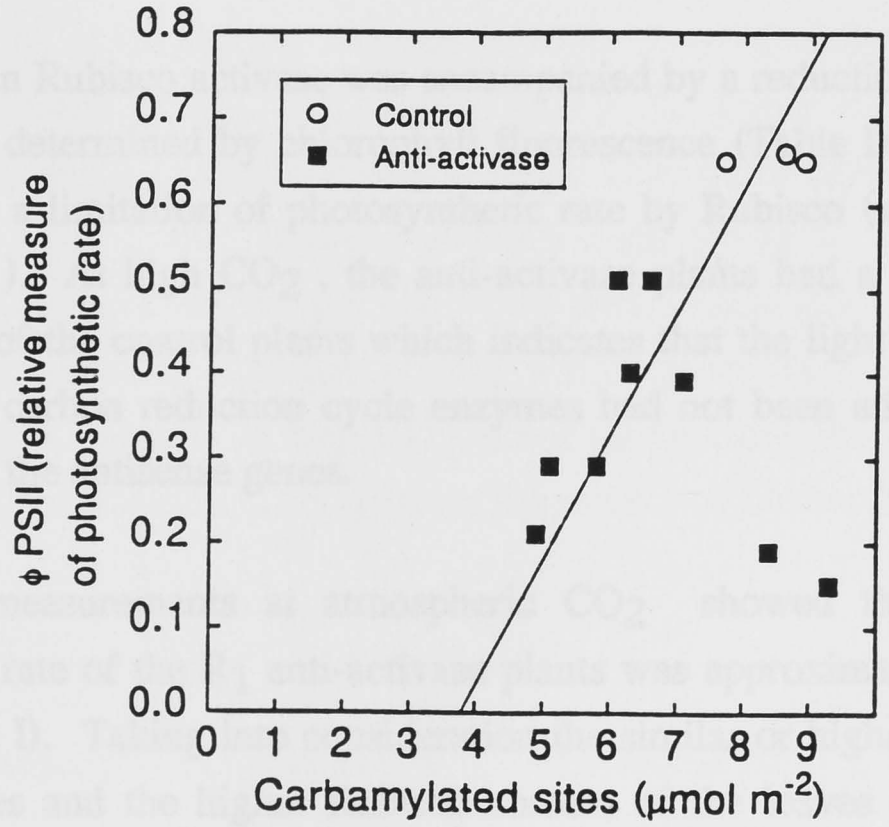

FIGURE 2.6: Relationship between Rubisco carbamylated site concentration and ϕPSII in control and anti-activase plants. Measurements and leaf samples were taken under the growth conditions, except that ϕPSII was measured at low CO_2 (0.03%), approximately 90 min after the onset of illumination following 12 h of darkness The chlorophyll fluorescence parameter, which represents the quantum efficiency of PS II, was measured on the adaxial surface and calculated according to Genty et al. (1989). Rubisco carbamylation was measured by the stoichiometric binding of [^{14}C]CABP.

2.4 DISCUSSION

2.4.1 Reduced Rubisco carbamylation and photosynthesis in anti-activase plants

Introduction of the anti-activase gene into the tobacco genome led to a reduction in Rubisco activase content. The primary transformants had a range of activase levels, varying from slight decreases to large decreases in activase content (Figure 2.3). We examined only those plants with relatively low activase levels, ie. less than 25% of wild-type levels. The Rubisco carbamylation levels of two anti-activase primary transformants, plants 52 and 50, were not very different after 90 min of illumination even though they had different activase levels. Rubisco was only 35% carbamylated in both plants compared to 75% in the controls. All subsequent experiments were carried out using the R_1 progeny of plant 52. The activase content was less than 25% of the wild-type in all of the R_1 plants. However, there may have been variation in the activase content of the R_1 plants, in the zero to 25% range, which is below the sensitivity of the immunoblot method. Under high light, the R_1 plants were found to have a mean of 34% carbamylated Rubisco after 90 min of illumination, which is similar to the anti-activase primary transformants (Table III).

The reduction in Rubisco activase was accompanied by a reduction in photosynthesis at low CO_2 as determined by chlorophyll fluorescence (Table I). These results are consistent with a limitation of photosynthetic rate by Rubisco (von Caemmerer and Farquhar, 1981). At high CO_2 , the anti-activase plants had a quantum efficiency similar to that of the control plants which indicates that the light reactions and other photosynthetic carbon reduction cycle enzymes had not been adversely affected by the presence of the antisense genes.

Fluorescence measurements at atmospheric CO_2 showed that the steady-state photosynthetic rate of the R_1 anti-activase plants was approximately half that of the controls (Table I). Taking into consideration the similar or higher intercellular CO_2 partial pressures and the higher Rubisco content of the leaves of the anti-activase plants compared to the control plants (Figure 2.5B), we conclude that diffusional limitations to CO_2 uptake or differences in Rubisco content did not contribute to the disparity in the CO_2 fixation rate. Therefore, the lower Rubisco activity in the anti-activase plants must in part be due to the lower Rubisco carbamylation levels.

High CO_2 concentrations almost completely restored photosynthetic activity in the anti-activase plants, as indicated by the quantum yield of photosystem II (Table I), and enabled the majority of R_1 antisense plants to grow (Figure 2.4). Significantly, the similarity between the carbamylation levels of Rubisco in the anti-activase plants at low and high CO_2 (Table II) indicated that the increase in photosynthetic rate was not due to an increase in Rubisco carbamylation but presumably, to an increase in catalytic rate at the few carbamylated active sites. A similar high CO_2 requirement was observed for the *rca* mutant of *A. thaliana* (Somerville et al., 1982). The lower photosynthetic rate of the *rca* mutant correlated with a decrease in Rubisco carbamylation (inferred from the ratio between intial and total activities) in the light (Somerville et al., 1982; Salvucci et al., 1986).

Our results seem inconsistent with *in vitro* studies which found that spontaneous activation proceeded faster at high CO_2 concentrations (Lorimer et al., 1976). However, these *in vitro* experiments were carried out in the absence of ligands such as RuBP and CA1P. Subsequent studies have shown that carbamylation increased with increasing CO_2 concentrations in the dark but not in the light in *T. aestivum* and *A. thaliana* (Mächler and Nösberger, 1980; Perchorowicz et al., 1981; Salvucci et al., 1986). In *Raphanus sativus* and *Chenopodium album,* carbamylation in the light was proportional to CO_2 concentration at concentrations below atmospheric but further increases in CO_2 concentration resulted in reductions in carbamylation level (von Caemmerer and Edmondson, 1986; Sage et al., 1990). These studies indicate that the relationship between Rubisco carbamylation and CO_2 concentration is more complex *in vivo* then it is *in vitro*. Rubisco carbamylation levels of tobacco leaves were insensitive to CO_2 both in the light and in the dark (Table III). The insensitivity of Rubisco carbamylation to changes in CO_2 concentration in these plants may have been the product of growth at high CO_2, since all previous studies were carried out using plants grown at ambient CO_2 (von Caemmerer and Edmondson, 1986; Sage et al., 1990).

2.4.2 High Rubisco content in the anti-activase plants

The anti-activase plants contained, on average, 1.7 times as much Rubisco as the control plants. This caused both the total soluble protein and the fraction of it partitioned to Rubisco to be greater in the anti-activase plants (Figure 2.5). This may be a long-term compensating response to the shortage of photosynthate experienced

by these plants. However, the possibility that Rubisco content may vary with the developmental status of the plant needs to be considered. The control plants grew very rapidly at high CO_2 and may have reached a later developmental stage (with lower leaf protein and Rubisco levels) than the anti-activase plants. Confidence that this is not the case is engendered by results described in Chapter 7. This raises the interesting possibility that Rubisco levels may be governed in the long term according to photosynthate supply or the balance between photosynthate supply and demand. This possibility is discussed at length in Chapter 7.

2.4.3 Another limitation to Rubisco in the absence of activase

The lower Rubisco carbamylation level of the anti-activase plants was partially offset by the increase in Rubisco content (Figure 2.5). Taking into consideration the Rubisco carbamylated site concentration and the gas exchange estimates of intercellular CO_2 partial pressure (Table II), the photosynthetic rate of the anti-activase plants after full light induction should be similar to the rate in the control plants. However, the ϕPSII ratios of the anti-activase plants were all lower than those of the controls (Figure 2.6). Therefore, there may be another limitation to RuBP carboxylase activity other than carbamylation level. Possibilities include indirect inhibition of the enzyme by high RuBP concentrations, perhaps as a consequence of high stromal pH, or a localized high resistance to CO_2 uptake within the anti-activase plant chloroplasts which have an unusually high Rubisco content. Alternatively, an inhibitor may bind to the active site of Rubisco in the absence of Rubisco activase, thereby blocking catalysis. However, we should also take into account that the ϕPSII measurements and the leaf samples for determination of Rubisco carbamylated site concentration were not taken simultaneously. Therefore, developmental or environmental changes may have contributed to the disparity between observed and expected photosynthetic rate in the anti-activase plants.

2.4.4 Conclusions

This engineering of a Rubisco activase-deficient form of tobacco provides insight into the roles of activase *in vivo*. The activase-deficient plants had a lower CO_2

assimilation rate than the control plants, which correlated with their inability to maintain Rubisco in its carbamylated form with the onset of illumination. The lower carbamylation levels in the anti-activase plants were partially offset by a higher Rubisco content. Despite this increase, the photosynthetic rate of the anti-activase plants, as indicated by ϕPSII, remained much lower than the control.

CHAPTER 3: Time-courses of Rubisco carbamylation level and CA1P release in control and anti-activase tobacco with the onset of illumination

3.1 INTRODUCTION

There are two possible ways in which *in vivo* Rubisco activity may be modulated in response to light : (i) changes in Rubisco carbamylation level, and (ii) changes in the concentration of the carboxylation-reaction-intermediate analogue, carboxyarabinitol-1-phosphate (CA1P). In this chapter, I will present and discuss the changes in Rubisco carbamylation and CA1P content in control and anti-activase tobacco plants with the onset of illumination.

Rubisco activase seems to be present in all higher plants (Salvucci et al., 1987), probably due to its critical role in the carbamylation of Rubisco. *In vitro* studies have shown that RuBP binds very tightly to the inactive site of Rubisco, and as a result the decarbamylated form of the enzyme is favoured in the presence of RuBP (Jordan and Chollet, 1983). However, the equilibrium of carbamylation, in the presence of RuBP, is altered when activase is included in the *in vitro* assay system. Activase appears to facilitate the removal of RuBP from the inactive catalytic site (Portis et al., 1986), enabling carbamylation, re-binding of RuBP and catalysis. Activase probably has a role in mediating changes in Rubisco carbamylation in response to light and CO_2 concentration, but the processes and/or metabolites involved in regulating these changes have not been identified (Chapter 1, Section 1.10).

A second level of regulatory control of Rubisco has been found in some but not all plant species. The nocturnal inhibitor, CA1P, binds very tightly to the carbamylated catalytic sites of Rubisco by virtue of its similarity to the six-carbon intermediate of the carboxylase reaction. CA1P was initially detected by comparing the maximum catalytic turnover rate (k_{cat}) of Rubisco, measured after incubation with high levels of CO_2 and Mg^{2+}, in extracts from illuminated and darkened leaves of soybean (Vu et al., 1983). The k_{cat} was much lower in the dark than in the light, indicating the accumulation of an inhibitor. CA1P binds very tightly to the carbamylated sites, and is not displaced by dilution during extraction or by RuBP in *in vitro* assays of Rubisco activity. Therefore, k_{cat} reflects the *in vivo* level of Rubisco active sites that are not complexed to inhibitors such as CA1P (Kobza and Seemann, 1988). Studies using this indirect assay and direct measurements of CA1P have shown that this compound accumulates in the leaves of some plant species in the dark and at low light intensities (Vu et al., 1984; Seemann et al., 1985; Servaites, 1990). *In vitro* studies indicate that Rubisco activase may have a role in releasing CA1P from Rubisco (Robinson and

Portis, 1988a). Therefore, depending on the CA1P content of the plant, Rubisco activase may mediate light-induced changes in Rubisco activity via modulation of carbamylation levels or by inducing CA1P release or a combination of both.

An absolute requirement for activase in facilitating and maintaining Rubisco carbamylation in higher plants was demonstrated using the activase-deficient *Arabidopsis rca* mutant (Somerville et al., 1982; Salvucci et al., 1985). However, *A.thaliana* does not contain CA1P. Therefore, it is not known if activase is essential in the removal of CA1P from the catalytic sites of Rubisco. *In vitro* studies have shown that CA1P is released from the active site and completely degraded by alkaline phosphatase in the absence of activase (Seemann et al., 1985). Analysis of the activase-deficient plants will enable us to identify the role of activase in CA1P removal *in vivo*.

3.2 MATERIALS & METHODS

3.2.1 Plant material

Self-fertilization of the primary transformants, plant 52 (pαTACT) and control (pBI121), yielded the R_1 seed which was used in these experiments.

3.2.2 Growth conditions

The R_1 seedlings were raised in a growth cabinet with a 12-h photoperiod, at 25°C (day) and 17°C (night), 0.3 to 0.5% CO_2, 60% relative humidity and 550 μmol quanta m^{-2} s^{-1}. The plants were grown in five-litre pots and analyzed approximately six to eight weeks after germination.

3.2.3 Sampling procedures

All of the plants were sampled or assayed in the growth cabinets, except those used in the gas exchange analysis. The plants were sampled by taking leaf punches which were collected into liquid nitrogen and stored at -80°C until required. For the time-course experiments, the R_1 seedlings were placed in a darkened growth cabinet at 0.3 to 0.5% CO_2 12 to 15 h before sampling. Immediately before sampling, the plants

were removed to a dark room while the growth cabinet lights were switched on. The time-zero samples were taken in the dark room and then the plants were returned to the growth cabinet when the illumination had reached 1000 μmol quanta m^{-2} s^{-1}.

3.2.4 Measurements of CO_2 assimilation rate

Methods were the same as described in Chapter 2.

3.2.5 Biochemical assays

Extraction and Rubisco content and carbamylation assays were carried out as described in Chapter 2.

The activated Rubisco catalytic rate (k_{cat}) was determined by preincubation of 25 μL of leaf extract for 10 min in the presence of 20 mM [^{14}C]$NaHCO_3$ and 20 mM $MgCl_2$. The reaction was initiated by the addition of RuBP to a final concentration of 0.5mM and terminated after 1 min by the addition of formic acid. The k_{cat} (s^{-1}) was calculated by dividing the activated Rubisco activity by the total number of catalytic sites determined by CABP binding (Chapter 2).

3.3 RESULTS

3.3.1 Photosynthesis and Rubisco carbamylation

The plants were illuminated at 1000 μmol quanta m^{-2} s^{-1} in the gas exchange system after 12 to 15 h at ambient CO_2 in the dark. An increase in the rate of carbon fixation with the onset of illumination was observed in both control and anti-activase plants (Figure 3.1A). After 30 min of illumination the assimilation rate of the anti-activase plants plateaued at a rate that was approximately half that of the control. The intercellular CO_2 partial pressure of both control and anti-activase plants increased slowly over the initial 30 min of the time-course, after which they plateaued (Figure 3.1B).

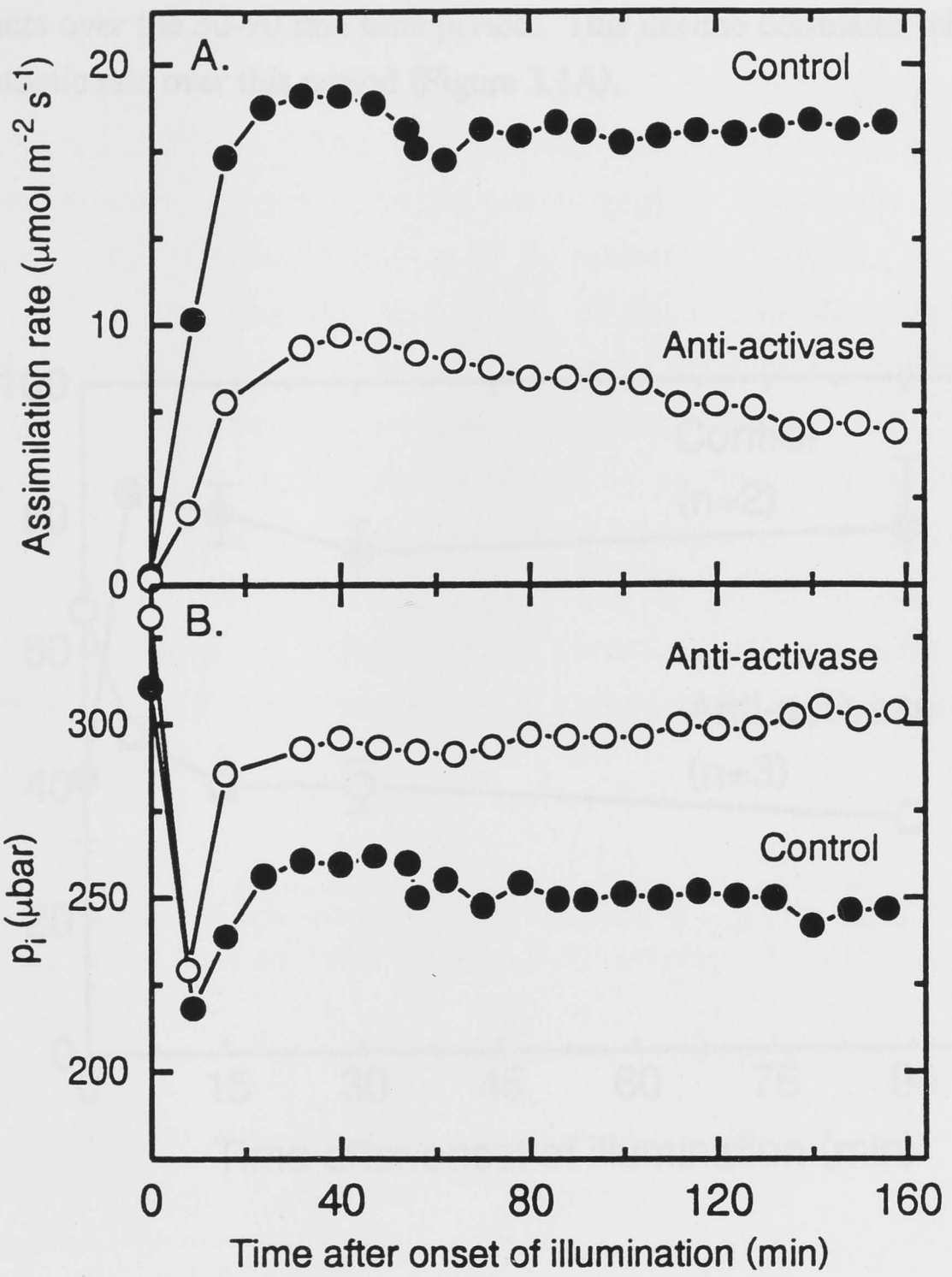

FIGURE 3.1: Time-courses of CO_2 assimilation rate and intercellular CO_2 partial pressure (p_i) after the onset of illumination for control and R_1 antisense plants. The irradiance was 1000 μmol quanta m^{-2} s^{-1}, except for the zero-time measurement which was in darkness. The leaf temperature was 25°C, the leaf to air vapour pressure difference was 11 mbar and the CO_2 partial pressure was 350 μbar.

Initial assays indicated that Rubisco carbamylation was independent of CO_2 concentration in the high-CO_2-grown tobacco plants (Chapter 2, Table III). Therefore, the time course experiments were carried out at high CO_2 . The Rubisco carbamylation level in the control plants increased with the onset of illumination,

whereas it decreased in the anti-activase plants (Figure 3.2). These changes occurred within the first 15 min of illumination, after which the Rubisco carbamylation levels reached a new equilibrium. A slow decline in carbamylation was observed in the anti-activase plants over the 30-90 min time period. This decline correlates with a decline in photosynthetic rate over this period (Figure 3.1A).

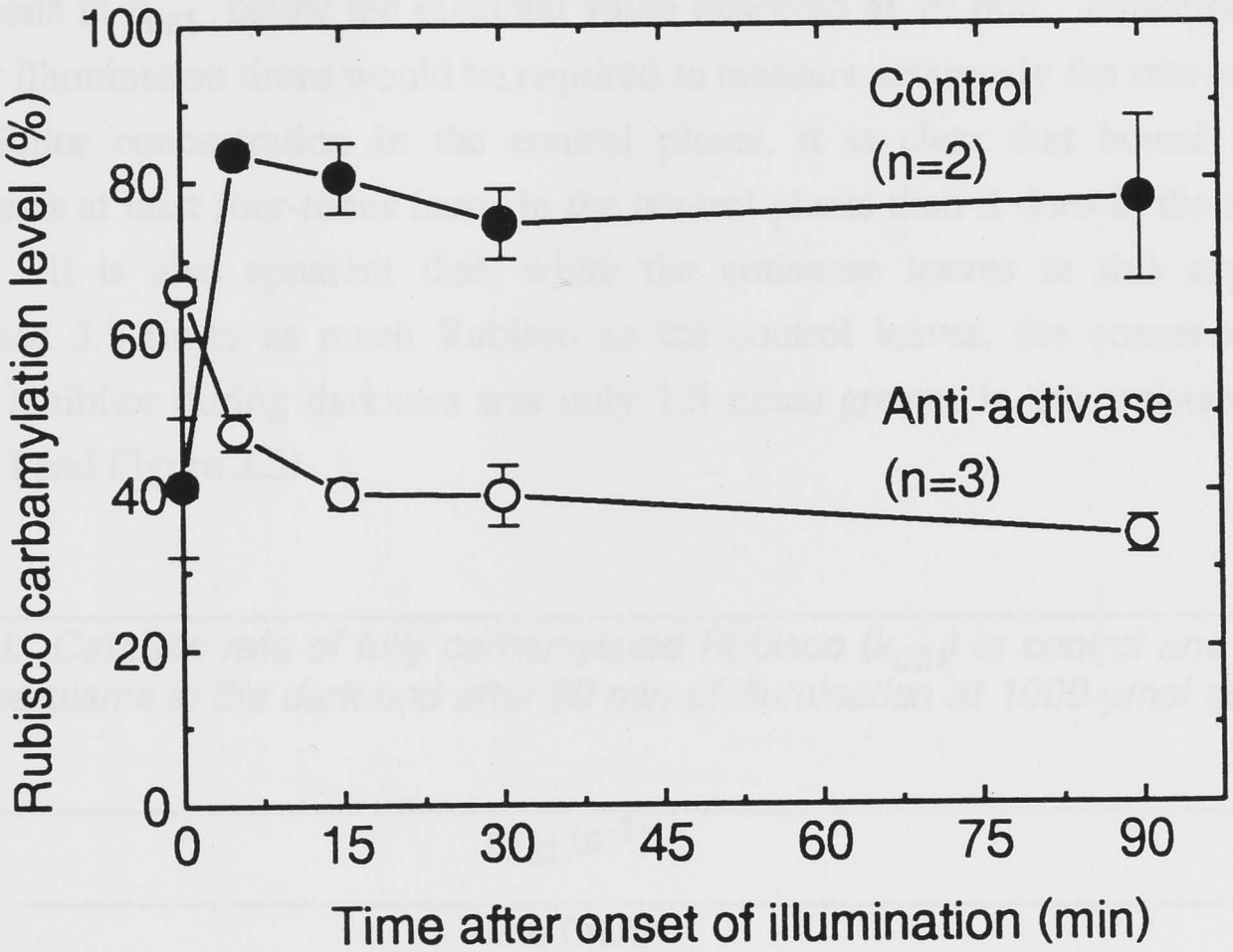

FIGURE 3.2: Time-course of Rubisco carbamylation level after the onset of illumination, following 12 h darkness in control and antisense R_1 generation plants. The irradiance was 1000 μmol quanta m^{-2} s^{-1} and the CO_2 concentration was 0.35%. Carbamylation levels were determined by CABP binding.

3.3.2 CA1P Release

The k_{cat} of Rubisco is calculated by dividing the fully activated *in vitro* activity by the total concentration of catalytic sites. Inhibitors that bind to the active site with a greater affinity than RuBP are not displaced during the *in vitro* assay, so k_{cat} reflects the *in vivo* level of Rubisco catalytic sites which are not complexed to inhibitors such

as CA1P (Kobza and Seemann, 1988). In the dark (time zero), the control plants had a lower k_{cat} than did the anti-activase plants (Table I). After 90 min of illumination, the k_{cat} had increased to 2.7 to 2.8 s^{-1} in both control and antisense plants, indicating the release of inhibitor (presumably CA1P). The kinetics of inhibitor release were followed more closely by monitoring the preincubated activity of Rubisco after the onset of illumination (Figure 3.3A). The inhibitor was released from Rubisco more slowly in the antisense plants than in the control plants. The observation is made clearer by calculating the concentration of Rubisco-bound inhibitor in the leaves following illumination, assuming that bound inhibitor was the sole cause for reductions in k_{cat} below the maximal value observed at 90 min. Although data at shorter illumination times would be required to measure accurately the rate of decline in inhibitor concentration in the control plants, it is clear that bound inhibitor disappears at least four-times faster in the control plants than it does in the antisense plants. It is also apparent that, while the antisense leaves in this experiment contained 3.5 times as much Rubisco as the control leaves, the concentration of bound inhibitor during darkness was only 1.5 times greater in the antisense leaves (Table I and Figure 3.3).

Table I: Catalytic rate of fully carbamylated Rubisco (k_{cat}) in control and R1 anti-activase plants in the dark and after 90 min of illumination at 1000 μmol quanta $m^{-2}s^{-1}$.

	k_{cat} (s^{-1})	
	Time (min)	
	0	90
Control	1.22 ± 0.26 (n=2)	2.73 ± 0.21 (n=2)
Anti-activase	2.07± 0.14 (n=3)	2.69 ± 0.28 (n=3)

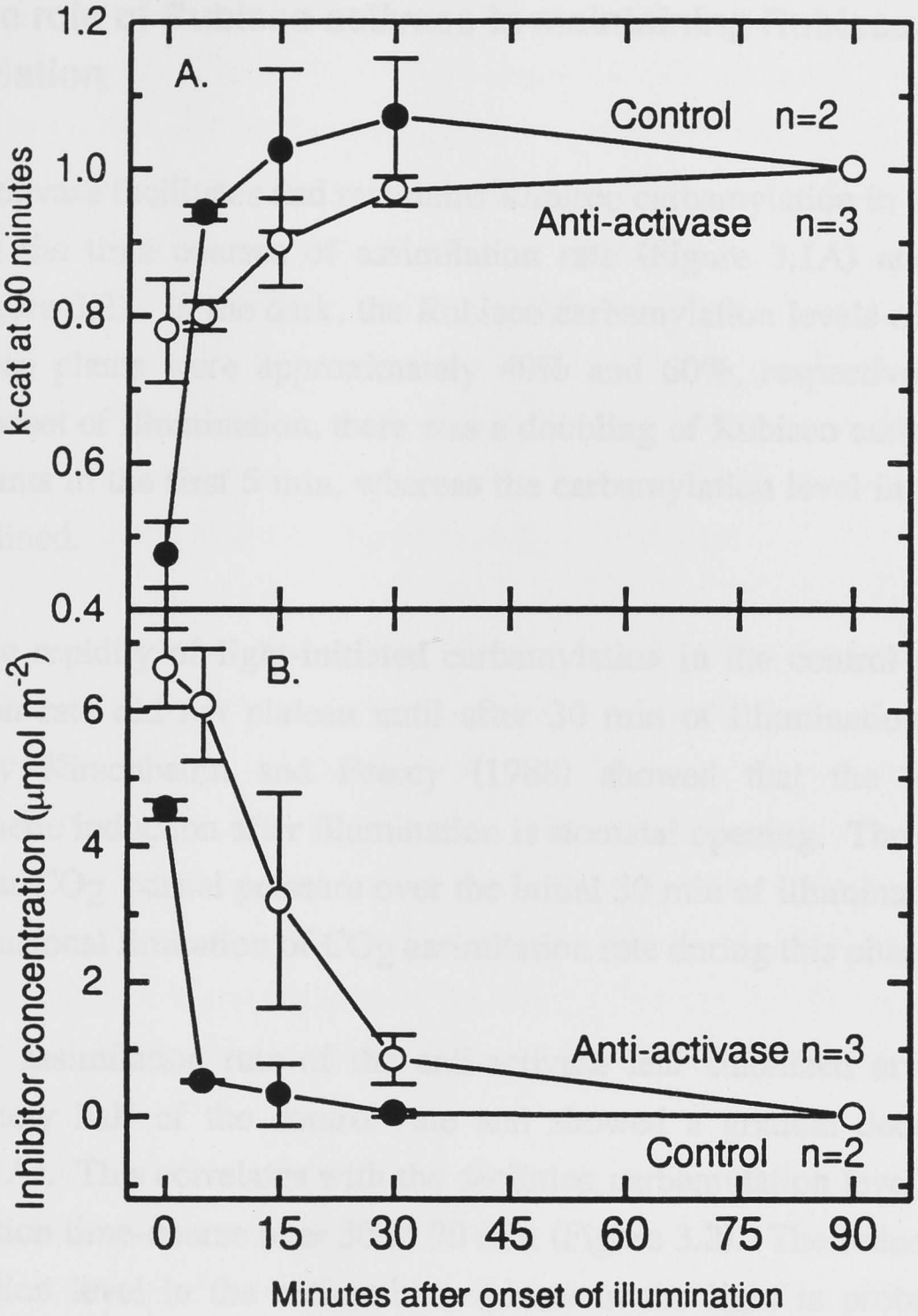

FIGURE 3.3: Release of Rubisco from CA1P inhibition with the onset of illumination. A. k_{cat} is proportional to the amount of Rubisco free from inhibitor. The k_{cat} at 90 min was 2.7 s^{-1} in both control and anti-activase leaves. In this experiment, the anti-activase leaves contained 3.5 times as much Rubisco as the control leaves. B. The concentration of inhibitor bound to Rubisco within plant extract was estimated, assuming that all reductions in k_{cat} below that observed at 90 minutes were due to presence of inhibitor. The inhibitor concentration (I) was calculated according to the following equation: $I = R\left(1 - \frac{k_{cat}^{x}}{k_{cat}^{90}}\right)$

where k_{cat}^{x} and k_{cat}^{90} are the k_{cat} values at x and 90 min, respectively, and R is the mean Rubisco concentration (μmol m^{-2}) of all leaf discs sampled over the time-course.

3.4 DISCUSSION

3.4.1 The role of Rubisco activase in maintaining Rubisco carbamylation

Rubisco activase facilitates and maintains Rubisco carbamylation in the light. This is evident in the time courses of assimilation rate (Figure 3.1A) and carbamylation levels (Figure 3.2). In the dark, the Rubisco carbamylation levels of the control and anti-activase plants were approximately 40% and 60%, respectively (Figure 3.2). With the onset of illumination, there was a doubling of Rubisco carbamylation in the control plants in the first 5 min, whereas the carbamylation level in the anti-activase plants declined.

Despite the rapidity of light-initiated carbamylation in the control plants, the CO_2 assimilation rate did not plateau until after 30 min of illumination (Figure 3.1A). Studies by Kirschbaum and Pearcy (1988) showed that the slowest step of photosynthetic induction after illumination is stomatal opening. The slow increase in intercellular CO_2 partial pressure over the initial 30 min of illumination is consistent with a diffusional limitation of CO_2 assimilation rate during this phase.

The CO_2 assimilation rate of the anti-activase leaf stabilized at a rate that was approximately half of the control rate and showed a gradual decrease over time (Figure 3.1A). This correlates with the declining carbamylation level observed in the carbamylation time-course over 30 to 90 min (Figure 3.2). The reduction in Rubisco carbamylation level in the anti-activase plants in the light is probably due to the accumulation of RuBP. RuBP binds more tightly to the inactive catalytic site than it does to the carbamylated site of Rubisco, thereby sequestering Rubisco in the inactive form in the absence of activase. The production of RuBP in the light would promote decarbamylation of Rubisco. In both the *A. thaliana rca* mutant and tobacco anti-activase plants, there was a recovery in Rubisco carbamylation in the dark to levels equal to or greater than those observed in the control leaves. This recovery in Rubisco carbamylation was accompanied by depletion of the RuBP pool in the *rca* mutant of *A. thaliana* (Salvucci et al., 1986).

3.4.2 Release of CA1P

The inhibitor CA1P bound to approximately half of the active sites of tobacco Rubisco in the dark (Table I). The release of this inhibitor from Rubisco was compared in control and anti-activase plants by determining the k_{cat} of Rubisco in leaves in the dark and at different times following the onset of illumination (Figure 3.3A). The fraction of Rubisco active sites sequestered by CA1P in the dark was greater in the control than in the antisense plants as shown by the k_{cat} values, despite a 50% larger bound-CA1P concentration in the antisense plants (Figure 3.3B). This was because, in this experiment, the antisense leaves contained 3.5 times as much Rubisco as the control leaves. Therefore, the ratio of CA1P to active sites was lower in the antisense leaves and, consequently, k_{cat} was higher.

The dark-to-light increase in k_{cat} that accompanies CA1P release occurred to similar extents in antisense and control plants, indicating that the light-initiated removal of CA1P proceeded despite low activase concentrations in the antisense plants. This result is consistent with *in vitro* studies carried out by Seemann et al. (1985) which showed that CA1P was released from the active site and completely degraded by alkaline phosphatase in the absence of activase. The displaced CA1P is degraded by a CA1P phosphohydrolase located in the chloroplast stroma (Seemann et al. 1990). The degradation of the displaced CA1P would further enhance dissociation.

Although on illumination, the k_{cat} of Rubisco in the antisense plants eventually attained the same level as in the control plants, it did so more slowly (Figure 3.3A). Calculations based on the assumption that all reductions in k_{cat} below the maximal value observed at 90 minutes were due to CA1P bound to Rubisco, showed that CA1P was released at least four-times faster in the control plants than in the antisense plants (Figure 3.3B). These results indicate a role for activase in accelerating CA1P release.

3.4.3 Inhibition of Rubisco in the anti-activase plants

The analysis of the anti-activase plants in the previous chapter indicated that these plants had photosynthetic rates that were less then expected based on measures of Rubisco carbamylated site concentration. The complete recovery in extractable k_{cat} in

the anti-activase plants in the light indicates the absence of tight binding inhibitors. Therefore, if an inhibitor is responsible for the lower k_{cat} then its affinity for the catalytic site must be low enough to allow its release during extraction.

3.4.4 Conclusions

Rubisco decarbamylates in the light in the absence of Rubisco activase, perhaps due to RuBP binding tightly to Rubisco's decarbamylated sites. The low Rubisco carbamylation level in the activase-deficient plants correlated with a low CO_2 assimilation rate compared to the controls. CA1P was still released from Rubisco's active sites when the anti-activase plants were illuminated. Therefore, CA1P binding did not contribute to the difference in photosynthetic rate between control and anti-activase plants after light induction. However, the rate of CA1P release with the onset of illumination was much slower in the anti-activase plants than in the controls.

CHAPTER 4: A quantitative immunoblot method for determining the activase content of plant extracts

4.1 INTRODUCTION

A method for determining the activase content of plant extracts is required for the complete analysis of activase-deficient tobacco plants. Activity assays are often used to measure an enzyme's concentration *in vivo*. Rubisco activase has two assayable activities: (i) it facilitates the release of sugar phosphates from the catalytic site of Rubisco, enabling carbamylation (Portis, 1992); and (ii) it has an ATPase activity (Robinson and Portis, 1989b). ATP hydrolysis by Rubisco activase is not closely linked to the Rubisco activation activity; it will occur in the presence and absence of active or inactive Rubisco (Robinson and Portis, 1989b).

Unfortunately, the ATPase and sugar-phosphate-removal activities of Rubisco activase cannot be used as a measure of activase content in plant extract. The sugar phosphate removal activity of Rubisco activase is measured *in vitro* by monitoring the increased activity of purified Rubisco, added to the assay mixture in the inactive form with RuBP bound (ER) (Salvucci et al., 1985). Lan et al. (1992) used this method to assay light-dependent changes in activase activity in leaves. They added plant extract to the assay mixture instead of purified activase, and they started the assay by addition of ER. Unfortunately, there is a high background of endogenous Rubisco activity in the plant extract in this assay. Consequently, the background to signal ratio is high, especially when assaying low concentrations of activase, and this limits the sensitivity of the assay. ATPase activity can also not be used as an indication of activase activity. Plant extracts also contain several types of ATPases other than Rubisco activase. Therefore, the ATPase activity of a plant extract may not reflect its activase content.

Activase is localised in the chloroplasts *in vivo* (Salvucci et al., 1985) , and it is present at very high concentrations in this organelle (approximately 10 mg/mL, Chapter 1, Section 1.9.2). Partial purification of Rubisco activase from Rubisco and other ATPases in the plant extract would enable the use of the *in vitro* activity assays outlined in the previous paragraph. However, these assays also have other limitations. Extraction and partial purification of the activase would break the chloroplast membranes and dilute the activase. *In vitro* experiments have shown that the specific activities of activase, both in Rubisco carbamylation and ATPase assays, are dependent on its concentration in solution. Salvucci (1992) used polyethylene glycol to increase the effective concentration of activase in solution *in vitro*. Under these conditions, both the Rubisco carbamylation and ATPase activities of activase increased. Therefore, activase activity is not a linear function of the amount of

activase added to an assay. This means that the range of activase concentrations in the anti-activase plants would probably be difficult to detect using an *in vitro* activity assay.

An immunological assay for activase has been developed as a response to these problems. There are many different types of quantitative immunological assays that offer high specificity to the target protein and high sensitvity. Some of the techniques trialled were enzyme linked immunosorbent assay (ELISA), sandwich ELISA and rocket immunoelectrophoresis (RIE). These methods were not appropriate for varying reasons, ranging from the type of primary antibody used, to the high soluble protein content of the plant extract. These methods and their restrictions will be discussed in more detail later.

A new, sensitive method for the quantitation of activase was developed using immunoblotting. Western or immunoblotting combines the resolution of gel electrophoresis with the specificity and sensitivity of immunochemical detection. This method used enhanced chemiluminescence (ECL) detection, due to its high sensitivity and low background. The activase bands on the films were quantified using densitometry.

4.2 MATERIALS AND METHODS

4.2.1 Isolation and purification of proteins

4.2.1.1 Glutathione *S*-transferase-spinach activase fusion protein (GST-activase)

The spinach *rca* cDNA, encoding only the mature 45 kD polypeptide without the transit peptide, was cloned previously by Hudson et al. (1992a). The *Nde*I (filled)-*Eco*RI insert from pSACT$_c$ (Hudson et al., 1992a) was subcloned into the *Sma*I and *Eco*RI sites of pGST-2T (AMRAD - Melbourne, Australia). This plasmid directed the synthesis of a fusion polypeptide in *E.coli* composed of spinach activase fused by its amino terminus to the carboxyl terminus of the *Schistosoma japonicum* glutathione *S*-transferase. The fusion protein was purified from other *E.coli* proteins on a glutathione-agarose column as described by Smith and Johnson (1981). This method was used to produce very pure activase suitable for use in rabbit immunisation.

4.2.1.2 Activase

Activase was purified from spinach as described by Robinson et al. (1988), and from tobacco using the method of Wang et al. (1992).

4.2.1.3 Protein quantification

Protein concentrations were measured using the Pierce Coomassie detection kit, with BSA as a standard.

4.2.2 Antibody production and manipulation

4.2.2.1 Immunisation

Antibodies were raised in rabbits. Freund's complete adjuvant was used for the primary injections and all subsequent injections were carried out using Freund's incomplete adjuvant. GST-activase antiserum was obtained from a rabbit injected once a month for 4 months prior to bleeding. Each injection contained 0.5 mg of GST-activase in 1 mL of adjuvant. Subsequent booster shots were given approximately one week prior to bleeding. They contained the same amount of antigen as injected during immunisation.

Tobacco activase antiserum was obtained after injection once a month for 3 months prior to bleeding. Each injection contained 0.45 mg of tobacco activase in 1mL of adjuvant. The final injection was delivered approximately one week before bleeding. Spinach activase was not used to raise polyclonal antibodies.

4.2.2.2 Affinity purification of antibodies

Polyclonal antibodies to GST-activase had to be purified for use in the sandwich ELISA detection system for tobacco activase antigen (Section 4.2.4.4). Two mg of pure tobacco activase antigen was bound to 1 mL of Pierce Reacti-Gel (6x), (1,1'-Carbonyldimidazole-activated, cross-linked 6% agarose) in 0.1M boric acid - NaOH [pH 8.5], containing 0.9% NaCl, for 42 h at 4°C, and subsequently washed by

decantation with 2M Tris-HCl [pH 8.0] to block the remaining reactive sites. The Reacti-gel was then packed in a column. One bed-volume of antiserum was applied to the column at room temperature and the flow was stopped for 5 min to allow the polyclonal antibodies to bind. The unbound antibodies and other serum proteins were removed by washing with 40 bed-volumes of 20 mM Tris-HCl [pH 8.0], 0.5M NaCl (Tris-buffered saline, TBS) and the bound antibodies eluted by passing 20 bed-volumes of 100 mM glycine - HCl [pH 2.5] through the column. The eluate was immediately neutralised by addition to 2 bed-volumes of 1M Tris - HCl [pH 8.0].

4.2.2.3 Biotinylation of antibodies

Two different forms of polyclonal anti-GST activase antibody were required for the sandwich ELISA assay. The first batch was affinity-purified as outlined in the previous paragraph, and the second batch was labelled with biotin, using the method described by Weir (1976).

4.2.3 Antibody analysis

4.2.3.1 Immunoblots

Immunoblots were carried out immediately after collecting the antiserum to ensure that there were activase-specific antibodies present. Purifed GST-activase, tobacco activase and spinach activase were subjected to SDS-gel electrophoresis using the Pharmacia Phastsystem. Wet electroblotting methods and alkaline phosphatase development were used. For more details about these methods see Section 4.2.4.5.

4.2.3.2 Enzyme-linked immunosorbent assay (ELISA)

The antibody titres of the polyclonal antisera were determined using an ELISA assay (Figure 4.1). The wells of PVC, Dynatech Immulon 2 plates were coated with: (i) 50μL of a 20μg mL^{-1} purified antigen preparation when comparing anti- GST-activase and anti-tobacco activase, or (ii) 50μL of a 2μg mL^{-1} GST-activase preparation when comparing the different batches of anti- GST-activase sera. The purified antigen was diluted using 20mM Tris-HCl, 0.5M NaCl [pH 8.0] (TBS). After

incubation overnight at 4°C, the wells were emptied and the plates washed 3 x with TBS plus 0.05% Tween (TTBS). The wash and all subsequent steps were carried out at room temperature. Polyclonal rabbit antisera directed against tobacco activase or GST-activase were serially diluted with 1%BSA/TTBS and added to the wells coated with the corresponding antigen. The plate was left to incubate for 2 h, after which the unbound antibody was removed by washing 3 x with TTBS. Goat anti-rabbit IgG conjugated to alkaline phosphatase (Bio-Rad) was diluted 1:3000 with 1%BSA/TTBS and 50 μL added to the wells, followed by incubation at room temperature for 2 h. The plates were washed 3 x with TTBS and the wells incubated for 5-10 min with 100 μL of *p*-nitrophenylphosphate in diethanolamine buffer [pH 9.5] (Bio-Rad substrate kit). The reaction was stopped by adding 100 μL of 0.4M NaOH. The absorbance at 405 nm was read using a Titertek Multiskan Plus Mark 11 spectrophotometer.

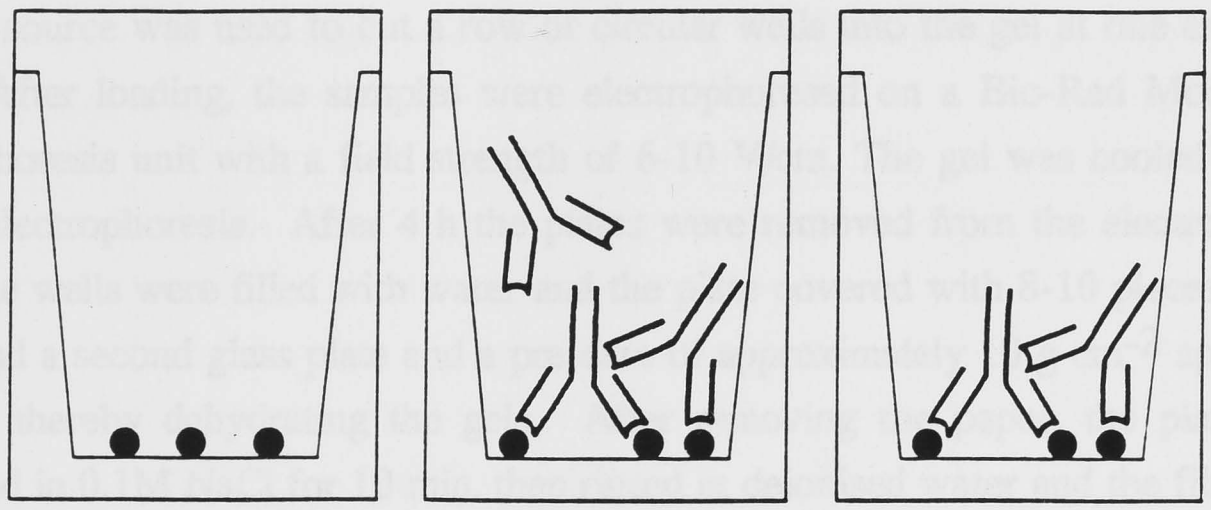

FIGURE 4.1: Standard ELISA. This assay was used for determining antibody titre. (reproduced from Harlow and Lane, 1988).

4.2.4 Activase analysis

4.2.4.1 Tobacco leaf extract

Leaf punches (2 cm^2) from air-grown (0.03% CO_2) plants were extracted in 0.5 mL of buffer (50 mM bis-Tris propane [pH 7.0], 10 mM $MgCl_2$, 1 mM sodium EDTA, 10 mM DTT, 1.5% polyvinylpolypyrrolidone, 1 mM phenyl methyl sulphonyl fluoride), and leaf punches (2 cm^2) from high-CO_2-grown (0.3-0.5%) plants were extracted in 1 mL. Mercaptoethanol and SDS were added to the extract to 4% [v/v] and 2% [w/v] respectively, before boiling for 10 min.

4.2.4.2 Tobacco activase standards

Purified tobacco activase standards were prepared with a diluent of 0.3 mg mL^{-1} BSA in TBS, unless otherwise specified. The inclusion of high concentrations of BSA in the diluent prevented significant losses of the very low concentrations of activase (0-60 $\mu g\ mL^{-1}$) due to non-specific binding to pipette tips and microfuge tubes.

4.2.4.3 Rocket immunoelectrophoresis (RIE)

Glass plates (100 x 100 mm) were covered with 15 mL of 1% [w/v] agarose containing 2% [v/v] unpurified GST-activase antiserum. A gel puncher attached to a vacuum source was used to cut a row of circular wells into the gel at one end of the plate. After loading, the samples were electrophoresed on a Bio-Rad Model 1415 electrophoresis unit with a field strength of 6-10 V/cm. The gel was cooled to 13°C during electrophoresis. After 4 h the plates were removed from the electrophoresis cell. The wells were filled with water and the plate covered with 8-10 pieces of filter paper and a second glass plate and a pressure of approximately 10 g cm^{-2} applied for 10 min, thereby dehydrating the gels. After removing the paper, the plates were immersed in 0.1M NaCl for 10 min, then rinsed in deionised water and the filter paper - pressure treatment repeated. The gels were dried in a 70°C oven and then stained in 0.25% [w/v] Coomassie brilliant blue R-250, 50% [v/v] methanol and 10% [v/v] acetic acid for 2-3 min, followed by 3 x 10 min washes in a destaining solution of 5% [v/v] methanol and 7.5% [v/v] acetic acid.

4.2.4.4 Standard and sandwich ELISAs

Standard ELISAs (Figure 4.1), similar to those outlined in Section 4.2.3.2, were carried out using PVC (Dynatech Immulon 2) or nitrocellulose-bottomed (Amersham) plates. In these assays the tobacco activase standards were not diluted with the BSA solution, the purified activase was bound to the wells in a solution of TBS. The activase in the tobacco extract was bound to the plates by adding undiluted extract to the wells. All other aspects of these assays were identical to the ELISA procedure outlined in Section 4.2.3.2.

Sandwich ELISAs (Figure 4.2) were carried out using PVC-bottomed plates. Affinity-purified GST-activase antibodies were bound to the plates overnight at 4°C in a carbonate buffer [pH 9.5] (1.6 gm Na_2CO_3 and 2.9 gm $NaHCO_3$ in 1L of distilled water). The carbonate buffer promotes binding of the F_c' fragment of the antibody to the plate, thereby presenting the F_{ab}' arms for antigen binding. After washing the plates 3x with TTBS, the purified tobacco activase standards and tobacco extract were added to the wells and incubated at room temperature for 2 h. After washing, biotinylated GST-activase antiserum diluted in 1% BSA / TTBS was added to the wells and incubated for 2 h. The plates were washed again, after which avidin conjugated to alkaline phosphatase was diluted 1:12,000 in 1%BSA/TTBS and added to the wells and incubated for 2 h. The plates were washed 3x and the wells incubated for 5-10 min with 100 µL of *p*-nitrophenylphosphate in diethanolamine buffer [pH 9.5] (Bio-Rad substrate kit). The reaction was stopped by adding 100 µL of 0.4M NaOH. The absorbance at 405 nm was read using a Titertek Multiskan Plus Mark 11 spectrophotometer.

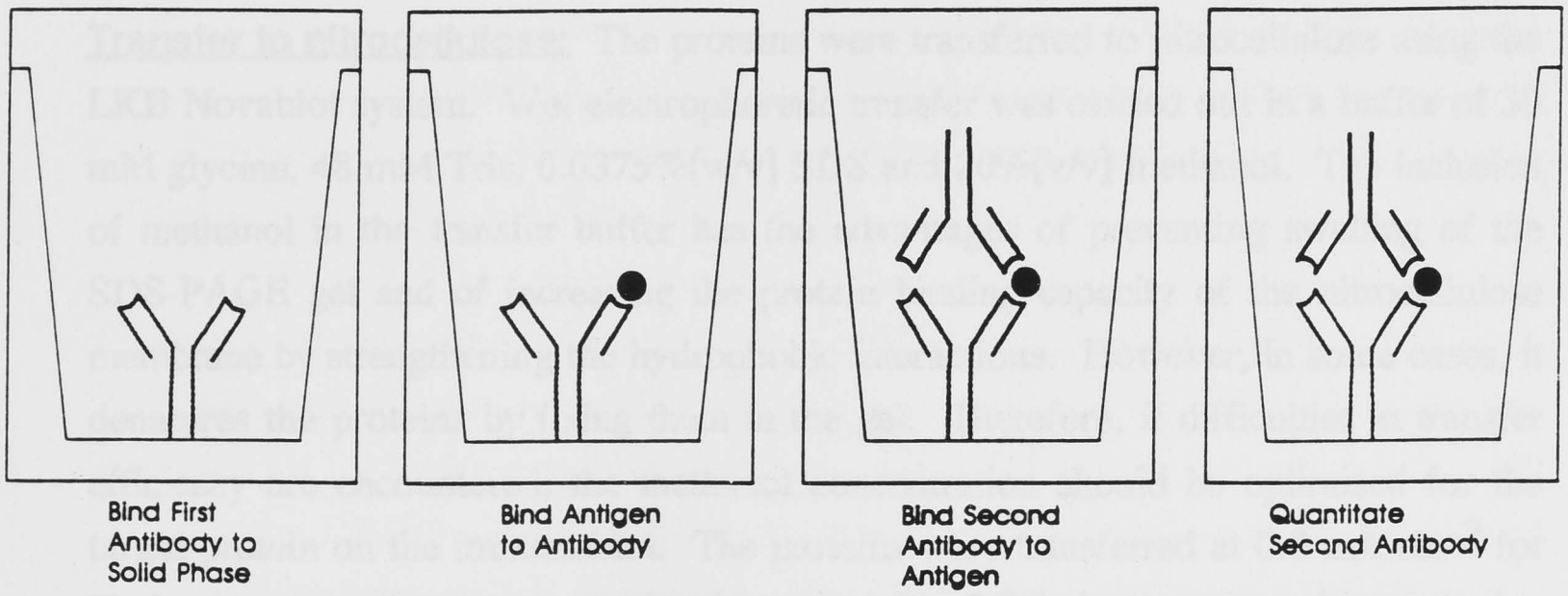

FIGURE 4.2: Sandwich ELISA (reproduced from Harlow and Lane, 1988)

4.2.4.5 Immunoblots

Electrophoresis of samples. Prior to electrophoresis all samples were boiled for 10 min in a buffer containing 2%[w/v] SDS, 4%[v/v] mercaptoethanol, 5%[v/v] glycerol, 60 mM Tris-HCl [pH 6.8] and 0.01 %[w/v] bromophenol blue. Two different electrophoresis systems were used, either Phastgel or Midget gel.

(i) When using the fully automated Pharmacia Phastsystem the samples were separated on 0.45mm 12.5% homogenous polyacrylamide Phastgels. Phastgel SDS buffer strips, containing 0.2M tricine, 0.2M Tris [pH 8.1], 0.55%[w/v] SDS, were used to run the gels. Phastgel separation method #2 was used, as described in the Phastsystem Owners Manual. Each gel contained 6 wells. The samples (4 μL) were loaded manually onto the applicator and, once the separation programme commenced, the applicator dropped automatically to the top of the Phastgels.

(ii) Larger volumes of sample (15μL) were separated at 12-25 mA (90-180V) for 1.5 - 2h, using 1mm Novex 16% homogenous polyacrylamide gels and a modified Bio-Rad Midget gel rig. The proteins were separated using an electrophoresis buffer of 25 mM Tris, 250 mM glycine [pH 8.3] and 0.1%[w/v] SDS. This system was used exclusively for the quantitative immunoblots. The running temperature was maintained at 25°C by passing tap water through the middle of the gel rig.

Transfer to nitrocellulose: The proteins were transferred to nitrocellulose using the LKB Novablot system. Wet electrophoretic transfer was carried out in a buffer of 39 mM glycine, 48 mM Tris, 0.0375%[w/v] SDS and 20%[v/v] methanol. The inclusion of methanol in the transfer buffer has the advantages of preventing swelling of the SDS-PAGE gel and of increasing the protein binding capacity of the nitrocellulose membrane by strengthening the hydrophobic interactions. However, in some cases, it denatures the proteins by fixing them in the gel. Therefore, if difficulties in transfer efficiency are encountered, the methanol concentration should be optimised for the target protein on the immunoblot. The proteins were transferred at 0.8 mA cm^{-2} for 1h in the case of non-quantitative blots and for 2.5 h in the case of quantitative immunoblots.

Blocking: Blocking of the nitrocellulose membrane with high concentrations of proteins prevents non-specific binding of antibodies. Blocking conditions were dependent on the subsequent detection system. Those blots that were to be developed using alkaline phosphatase detection were blocked with 3% BSA in 20 mM Tris-HCl [pH 8.0], 0.5 M NaCl (Tris buffered saline, TBS), overnight at 4°C. When using the enhanced chemiluminescence (ECL) development system the blots were blocked with 10% milk powder in TBS for 2 h at room temperature on a rocking platform and overnight at 4°C. BSA and milk powder can be used interchangeably for blocking.

However, higher concentrations of blocking protein have to be used when using the ECL detection system than when using alkaline phosphatase detection. This minimises background when using the very sensitive ECL detection system. Milk powder was used when blocking at high protein concentrations because it was inexpensive and readily available.

Detection systems: All steps were carried out at room temperature on a rocking platform.

Alkaline phosphatase development. The blots were washed with TTBS after blocking, followed by a 1h incubation with the anti- GST-activase serum. The serum was diluted 1:500 in 1% BSA / TTBS. The blot was then given 3 x 30 sec washes in TTBS and probed with biotinylated goat anti-rabbit IgG (Amersham), which had been diluted 1:500 in 1% BSA / TTBS. Following incubation for 1 h, the blot was washed 3 x with TTBS and probed with streptavidin - alkaline phosphatase (Bio-Rad), diluted 1:500 in 1%BSA / TTBS. After 1 h incubation, the blot was washed 3 x with TBS and the activase bands visualised by incubation with the substrates 5-bromo-4-chloro-3-indoyl phosphate and nitroblue tetrazolium (substrate kit from Bio-Rad). The reaction was stopped by washing the blot in water.

Enhanced chemiluminescence detection. Following blocking and between each incubation, the blot was washed 1 x 15 min, and 2 x 5 min, in TTBS. The blot was incubated for 1.5 h with the primary antibody, anti- GST-activase, diluted 1:250 in 5% milk powder / TTBS. After washing, the blot was probed with goat anti-rabbit IgG conjugated to horse radish peroxidase (Amersham) for 1 h, diluted 6/10,000 in 5% milk powder / TTBS, and then washed in TTBS. The nitrocellulose was blotted dry using filter paper and incubated with the Amersham ECL reagents for 1 min. Detection reagent 1 decays to hydrogen peroxide, the substrate for peroxidase (the peroxidase was conjugated to the secondary antibody, goat anti-rabbit IgG in the quantitative immunoblots). Reduction of hydrogen peroxide by the enzyme is coupled to the light producing reaction by detection reagent 2 (Figure 4.3). This contains luminol, which on oxidation produces blue light. The light output is increased and prolonged by the presence of an enhancer so that it can be detected on a blue light sensitive film. Excess reagent was removed from the nitrocellulose by blotting on filter paper and the immunoblots exposed to Amersham Hyper-film for 15 sec.

After development, the Hyper-film was scanned using a Quick Scan Jr. densitometer from Helena laboratories. The gain dial on the densitometer was set at 3 (range 1-10) for all scans. The electronic integrator attached to the densitometer was used to measure the area under the activase peaks.

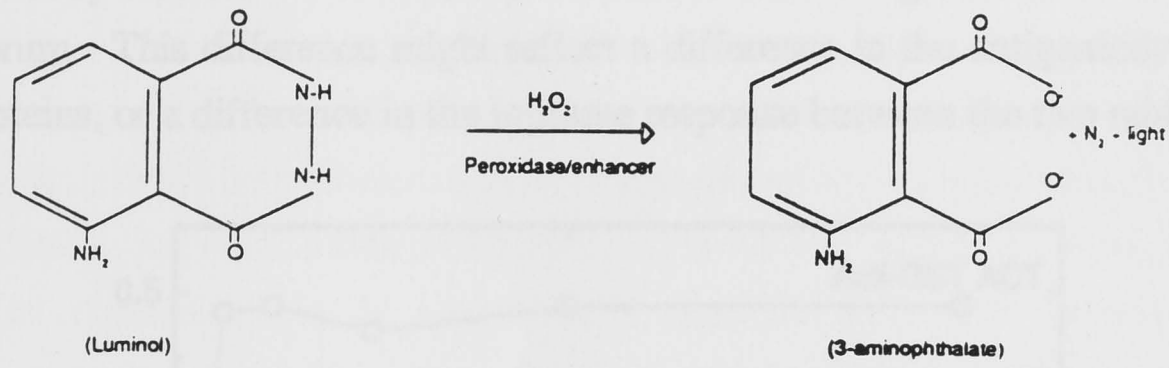

FIGURE 4.3: The enhanced chemiluminescence (ECL) reaction (Amersham)

Internal standards: 15 ng of GST-activase was added as an internal standard to all samples before application to the gel. This protein has a molecular mass of 70 kD, whereas tobacco activase is approximately 40 kD. Therefore, two separate, clear bands were evident in those lanes of the immunoblot that contained both tobacco activase and GST-activase. Inaccuracies in sample loading and variations in the efficiency of transfer from gel to nitrocellulose were normalised by measuring the ratio between the areas of the two peaks.

4.2.4.6 Dot blots

Some samples were applied directly to nitrocellulose and blocked / probed as outlined for the immunoblots.

4.3 RESULTS

4.3.1. Collection of primary antibody

The immunogens used to raise possible primary antibodies were tobacco activase and the spinach activase glutathione *S*-transferase fusion protein (GST-activase). The antibody titres of the respective antisera were determined using an ELISA (Figure

4.1). The optimal antibody concentration occurs at the point where the maximum absorbance is obtained for the least amount of antiserum added. The optimal concentration of the GST-activase antiserum was 2.5 - 5 x 10^{-4} compared to 4 x 10^{-3} or higher for the tobacco activase antiserum (Figure 4.4). This result indicates that the antibody titre in the GST-activase serum is 8-16 x higher than in the tobacco activase serum. This difference might reflect a difference in the antigenicity between the two proteins, or a difference in the immune response between the two rabbits.

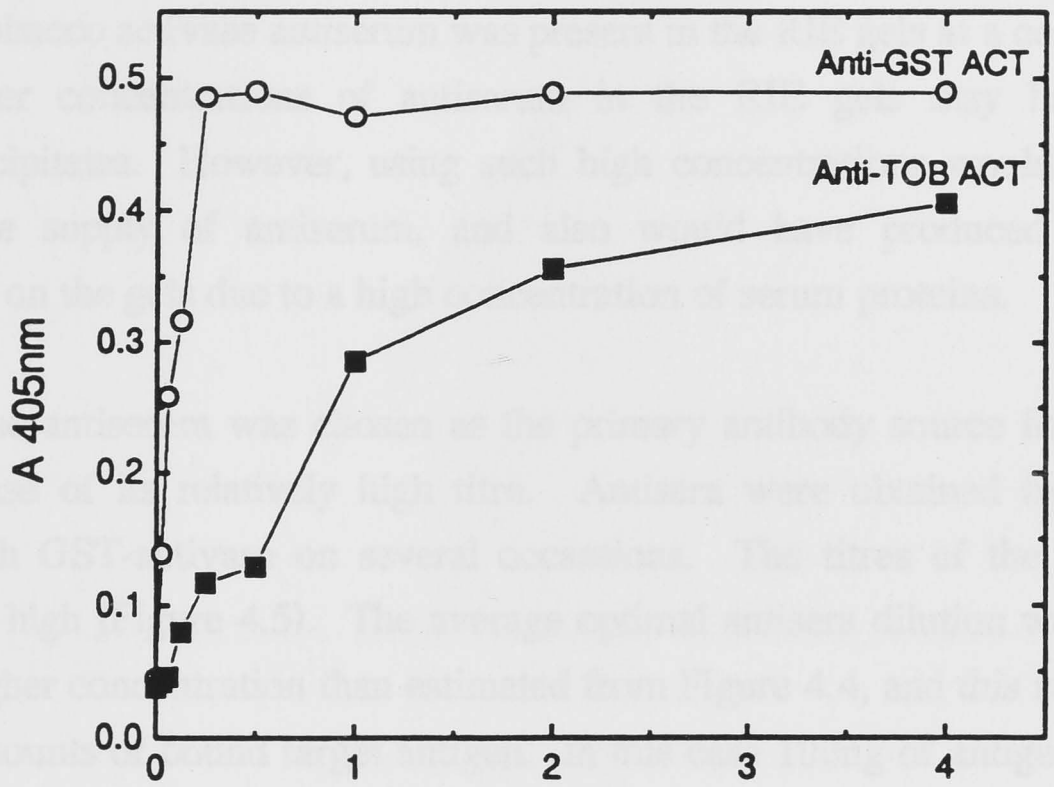

FIGURE 4.4: The effect of antisera dilution on absorbance in an antibody capture-ELISA assay. 1000 ng of antigen (either tobacco activase (TOB ACT) or GST-activase) was used to coat each well (max. binding is 100 ng per well), followed by incubation with antisera (either anti-TOB ACT or anti-GST-activase) for 1h. The plate was washed and the wells incubated with secondary antibody, goat anti-rabbit alkaline phosphatase for 1h, followed by another wash. The phosphatase substrate, *p*-nitrophenylphosphate, was added to the wells and the reaction terminated after 10 min. by addition of NaOH. The absorbance of each well was then determined at 405nm.

4.3.2 Immunoprecipitation

The low titre of the tobacco activase antiserum precluded its use in rocket immuoelectrophoresis (RIE). RIE is a quantitative technique that uses immunoprecipitation and electrophoresis. Antigen solutions, either tobacco activase standard or tobacco extract, were loaded into circular wells at one end of an antibody-containing gel, after which the proteins in the antigen solution were propelled though the gel by an electric field. As the antigens migrate away from the wells they become

more dilute. The 'Rocket-shaped' precipitin lines form when the antigen concentration is equivalent to the antigen binding site concentration of the antibodies in the gel. The length of the 'rockets' is proportional to antigen concentration. RIE with GST-activase antigen and antiserum produced rocket-shaped precipitates whereas RIE gels with tobacco activase antigen and antiserum did not (data not shown). RIE requires relatively high concentration of antibody. If the antibody concentration is low, the 'rockets' are very long and difficult to visualize. The relatively low titre of the antiserum is probably why rockets could not be observed on the tobacco activase RIE gels. The tobacco activase antiserum was present in the RIE gels at a concentration of 3%. Higher concentrations of antiserum in the RIE gels may have produced immunoprecipitates. However, using such high concentrations would have quickly depleted the supply of antiserum, and also would have produced a very dark background on the gels due to a high concentration of serum proteins.

GST-activase antiserum was chosen as the primary antibody source for the activase assay because of its relatively high titre. Antisera were obtained from the rabbit injected with GST-activase on several occassions. The titres of the antisera were consistently high (Figure 4.5). The average optimal antisera dilution was 2.5×10^{-3}. This is a higher concentration than estimated from Figure 4.4, and this is probably due to lower amounts of bound target antigen. In this case 100ng of antigen was used to coat each well, and in the previous experiment 1000ng of antigen was used (Figure 4.4). Although the nominal binding capacity is 100 ng per well, larger quantities of antigen are required to ensure maximal binding (100ng) (Harlow and Lane, 1988).

Immunoprecipitates did not form between tobacco activase antigen and GST-activase antiserum in RIE gels (data not shown). Therefore, an alternative system for quantifying tobacco activase had to be developed.

4.3.3 Specificity of the primary antibody

On a immunoblot, the GST-activase antiserum cross-reacted with GST-activase, spinach activase and tobacco activase (Figure 4.6). The gel depicted in Figure 4.6A is a duplicate of the gel from which the immunoblot in Figure 4.6B was derived. 18 μg of GST-activase was loaded onto the Phastgel (Figure 4.6A) and the intensity of the GST-activase band on the immunoblot was accordingly high. The amount of spinach activase (4 μg) loaded onto the gel was relatively low (Figure 4.6A) but a clear band was observed on the immunoblot (Figure 4.6B). The amount of tobacco activase (8

μg) loaded onto the gel was approximately twice the amount of spinach activase loaded (Figure 4.6A). However, the intensity of the tobacco activase band on the immunoblot was only about half that of the spinach activase band.

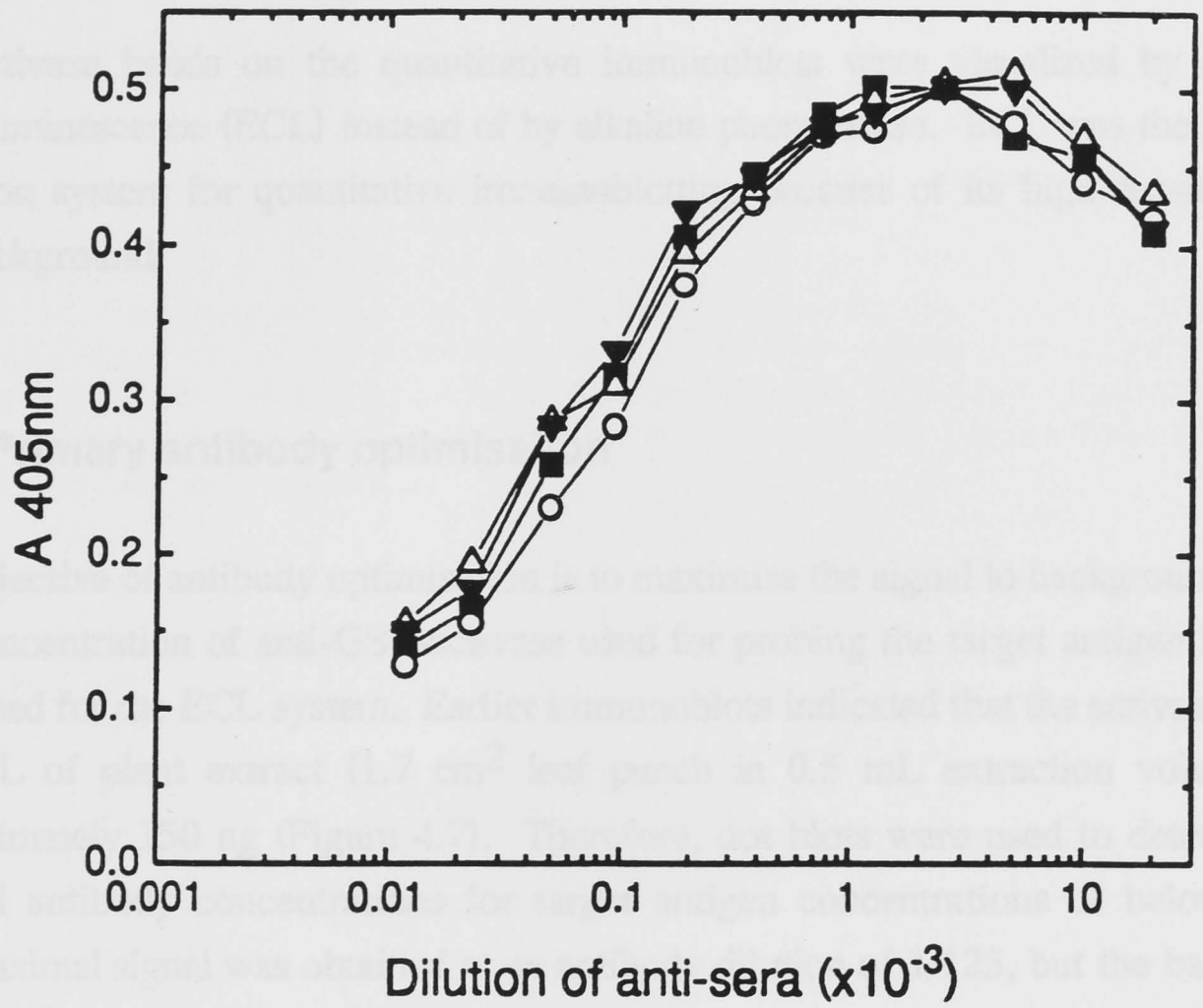

FIGURE 4.5: A comparison of antibody titre in different batches of GST-activase antisera using an antibody capture-ELISA assay. 100 ng of GST-activase was used to coat each well, followed by incubation with anti-GST-activase for 1 h. The plate was washed and the wells incubated with secondary antibody, goat anti-rabbit alkaline phosphatase for 1 h, followed by another wash. The phosphatase substrate, *p*-nitrophenylphosphate, was added to the wells and the reaction terminated after 10 min by addition of NaOH. The absorbance of each well was then determined.

4.3.4 Semi-quantitative immunoblots

A comparison of purified tobacco activase standards on a Phastgel immunoblot was used to assess if immunoblots were quantitative. Visual comparison of the different standards indicates that band intensity is approximately proportional to the amount of tobacco activase loaded (Figure 4.7). The wild-type band is of a similar intensity to the 150 ng purified tobacco activase standard, taking into account the extraction volume (1.7 cm^2 leaf punch in 0.5 mL) and amount of extract loaded (2 μL) we can

estimate that the activase concentration in the wild-type plant was approximately 220 mg m^{-2}.

4.3.5 Quantitative immunoblots

The activase bands on the quantitative immunoblots were visualized by enhanced chemiluminescence (ECL) instead of by alkaline phosphatase. ECL was the preferred detection system for quantitative immunoblotting because of its high sensitivity and low background.

4.3.6 Primary antibody optimisation

The objective of antibody optimisation is to maximise the signal to background ratio. The concentration of anti-GST-activase used for probing the target antigen had to be optimised for the ECL system. Earlier immunoblots indicated that the activase content in 2 μL of plant extract (1.7 cm^2 leaf punch in 0.5 mL extraction volume) was approximately 150 ng (Figure 4.7). Therefore, dot blots were used to determine the optimal antibody concentrations for target antigen concentrations of below 50 ng. The maximal signal was obtained at an antibody dilution of 1/125, but the background was very high. Therefore, a dilution of 1/250 was used.

4.3.7 Comparison of Phastsystem and Midget gel rig

Samples must be accurately loaded onto the SDS-PAGE gel in order for the immunoblot to be quantitative. The application of samples to the SDS-PAGE gel in the Phastsytem is automated. Unfortunately, the automated application system did not always apply equal volumes of sample to each of the lanes. This was apparent simply by comparing the volume of sample remaining on the different lanes of the applicator after loading. Consequently, another electrophoresis apparatus had to be used. The Bio-Rad Midget gel rig was chosen. A series of tobacco activase standards separated on the Midget gel rig are shown in Figure 4.8. Another benefit of this system is that the wells can hold 15 μL. This means that relatively large volumes of activase-deficient plant extract can be loaded, thereby increasing the sensitivity of the assay.

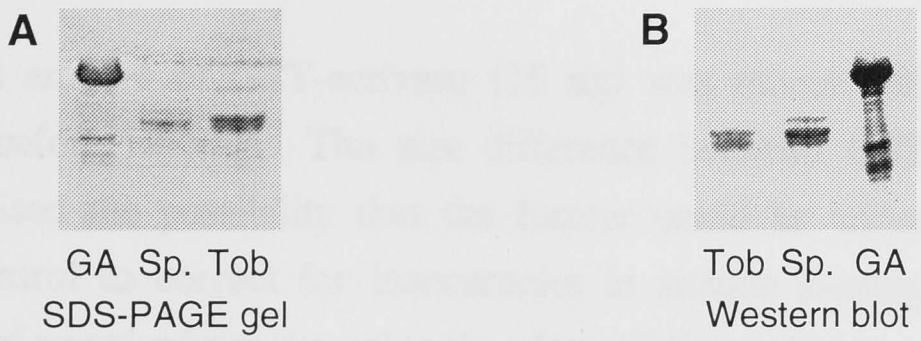

Figure 4.6: A comparison of an immunoblot probed with anti-GST-activase serum, and an SDS-PAGE gel containing identical concentrations of GST-activase, spinach activase and tobacco activase. Two phastgels were loaded with identical amounts of GST-activase (18μg), spinach activase (4μg) and tobacco activase (8μg). One of the phastgels was stained with Coomassie blue (A), and the proteins in the other gel were transferred to nitrocellulose for immunoblotting (B). The primary antibody was anti-GST-activase, and its binding was detected using goat anti-rabbit alkaline phosphatase and the insoluble substrates, 5-bromo-4-chloro-3-indoyl phosphate and nitroblue tetrazolium.

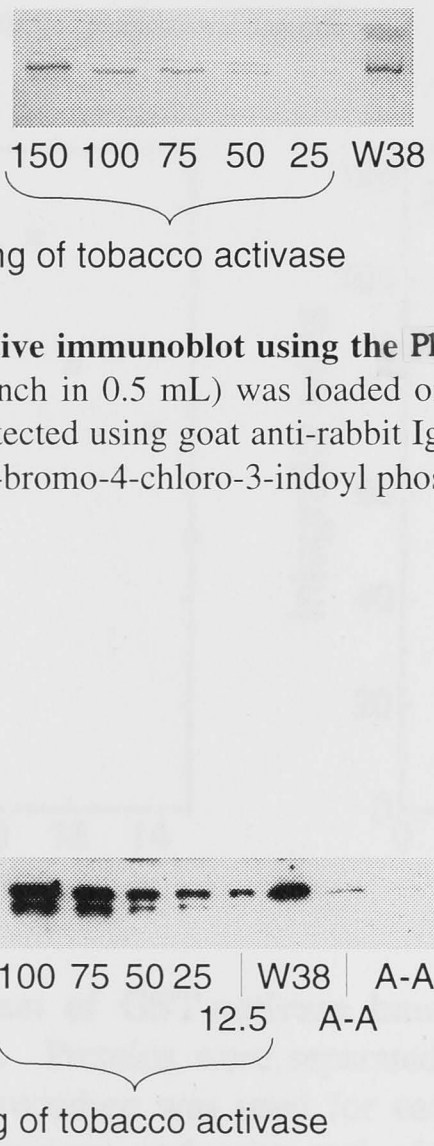

Figure 4.7: A semi-quantitative immunoblot using the Phastgel system. Approximately 2 μL of W38 extract (1.7 cm^2 leaf punch in 0.5 mL) was loaded onto the gel. The binding of anti-GST-activase to the antigen was detected using goat anti-rabbit Ig G conjugated to alkaline phosphatase and the insoluble substrates, 5-bromo-4-chloro-3-indoyl phosphate and nitroblue tetrazolium.

Figure 4.8: Tobacco activase standards and tobacco extract on an ECL immunoblot. Samples were separated using Novex Precast gels (16% SDS, homogenous). Tobacco leaves (0.5 cm^2) were extracted in 0.5 mL. 2.5 μL of wild-type extract or 10μL of anti-activase was loaded per lane. The primary and secondary antibodies were anti-GST-activase and goat anti-rabbit Ig G conjugated to horse radish peroxidase, respectively.

4.3.8 Internal control

A constant amount of GST-activase (15 ng) was mixed with the tobacco activase standards before loading. The size difference between GST-activase and tobacco activase raised the possibility that the former could be added to all samples as an internal control to correct for inaccuracies in sample loading and variations in the efficiency of transfer from the gel to the nitrocellulose. A comparison of the density of internal control bands on two different gels can be seen in Figure 4.9. Tap water was passaged through the internal chamber of the gel rig. This prevented the 'smiling' effect which was apparent in some of the early gels (Figure 4.9A). Nevertheless, the outer lanes on each side of the gels yielded bands that were less dense, and often wider, than the bands in the middle of the gel (Figure 4.9B). Therefore, when carrying out quantitative immunoblots, all samples loaded into the outer wells were replicated in the middle wells of the same blot or on subsequent blots. The internal standards were used when developing the quantitative immunoblot method. However, because the intensities of the internal standard bands showed little variation, internal standardisation was subsequently discontinued.

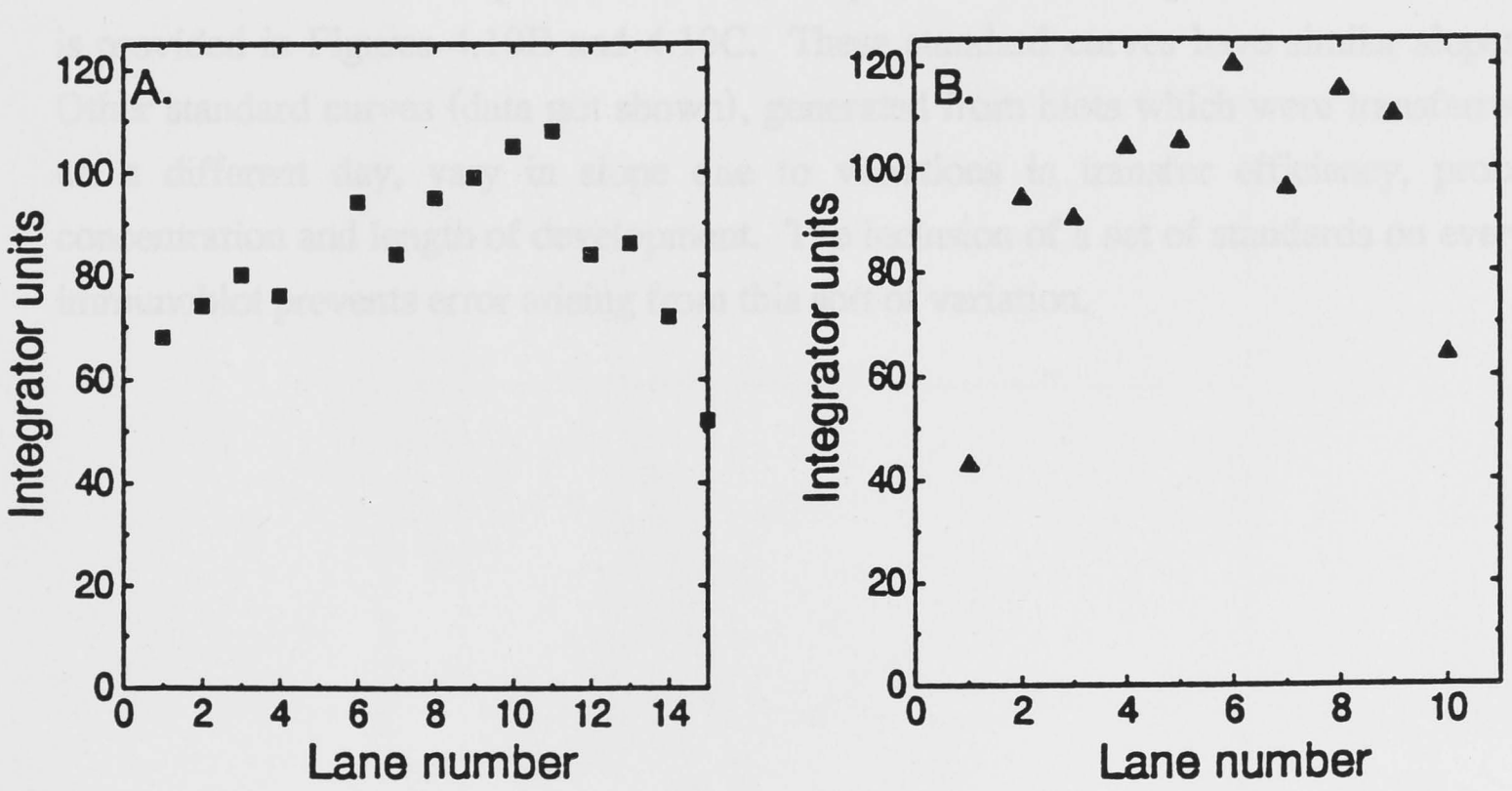

FIGURE 4.9: A comparison of GST-activase band density across the lanes of two different ECL immunoblots. Proteins were separated on Novex precast gels. The same electroblotting and probing procedure was used for each gel. The primary and secondary antibodies were anti- GST-activase and goat anti-rabbit IgG conjugated to horse radish peroxidase, respectively. The samples loaded onto blot A were separated at 25mA (125-180V) for 1.5-2h, cooling was not used. The samples loaded onto blot B. were separated at 12-20mA (90-125V) for 3h, during which time the gel was cooled by passing tap water through the internal chamber of the gel rig.

4.3.9 Standard curves

Standard curves were generated using purified tobacco activase. Unlike tobacco leaf extracts, which yielded only a single band, the purified preparation generated two bands on the ECL immunoblot (Figure 4.8). The gene encoding tobacco activase does not contain an alternative mRNA splicing site. Therefore, there is only one type of tobacco activase polypeptide (Chapter 1, Section 1.8). Partial degradation of the 42 kD tobacco activase polypeptide during purification was probably the cause of the double banding. These bands did not resolve into separate peaks when scanned on the densitometer and for the purpose of integration they were treated as a single peak. The accuracy of the Quick Scan Jr. densitometer was checked by comparison with an LKB laser densitometer. The standard curves produced from the different densitometers were identical, and the optical density of the 100 ng standard was approximately 1. Therefore, the assay was restricted to a range of 0 - 100 ng.

The standard curve in Figure 4.10 indicated that the activase assay was most sensitive in the 0 - 100 ng range. A comparison of two standard curves generated from immunoblots that were separated, transferred, probed and developed, at the same time is provided in Figures 4.10B and 4.10C. These standard curves have similar slopes. Other standard curves (data not shown), generated from blots which were transferred on a different day, vary in slope due to variations in transfer efficiency, probe concentration and length of development. The inclusion of a set of standards on every immunoblot prevents error arising from this sort of variation.

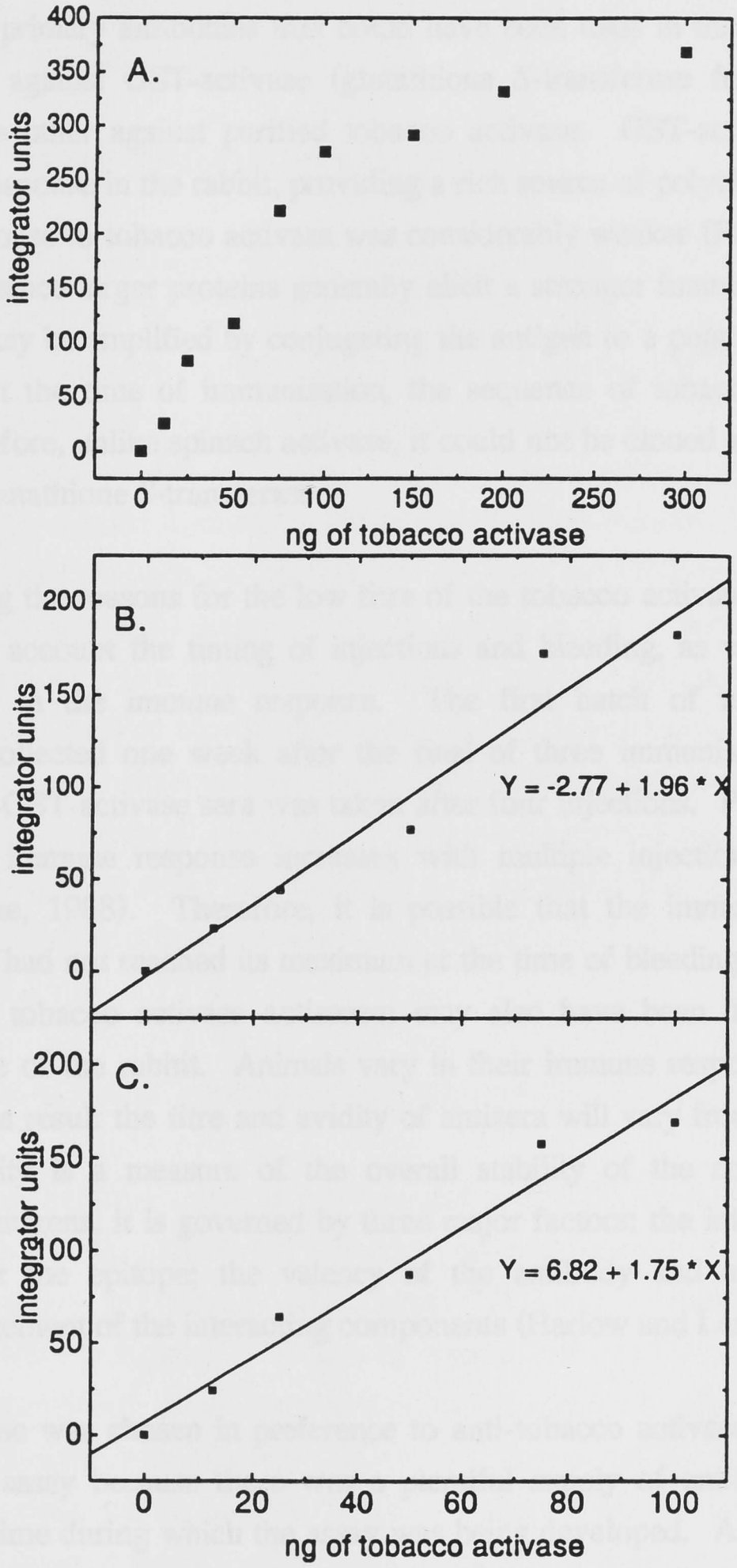

FIGURE 4.10: A comparison of standard curves for the tobacco activase assay, generated from ECL immunoblots. ECL immunoblots were scanned on a Quick Scan Jr. densitometer and the peak area was quantified simultaneously on a built-in integrator.

4.4 DISCUSSION

4.4.1 Use of anti-GST-activase as the primary antibody

There were two primary antibodies that could have been used in the activase assay. One was raised against GST-activase (glutathione *S*-transferase fused to spinach activase) and the other against purified tobacco activase. GST-activase elicited a strong immune response in the rabbit, providing a rich source of polyclonal antibodies, whereas the response to tobacco activase was considerably weaker (Figure 4.4). This is not surprising since larger proteins generally elicit a stronger immune response. A weak response may be amplified by conjugating the antigen to a peptide (Harlow and Lane, 1988). At the time of immunisation, the sequence of tobacco activase was unknown. Therefore, unlike spinach activase, it could not be cloned and expressed in *E.coli* fused to glutathione *S*-transferase.

When considering the reasons for the low titre of the tobacco activase antiserum, we should take into account the timing of injections and bleeding, as well as rabbit to rabbit variability in the immune response. The first batch of tobacco activase antiserum was collected one week after the final of three immunisation injections, whereas the anti-GST-activase sera was taken after four injections. Past studies have shown that the immune response increases with multiple injections (reviewed in Harlow and Lane, 1988). Therefore, it is possible that the immune response to tobacco activase had not reached its maximum at the time of bleeding. However, the low titre of the tobacco activase antiserum may also have been due to the poor immune response of the rabbit. Animals vary in their immune response to different antigens, and as a result the titre and avidity of antisera will vary from one animal to the next. Avidity is a measure of the overall stability of the complex between antibodies and antigens, it is governed by three major factors: the intrinsic affinity of the antibody for the epitope; the valency of the antibody and antigen; and the geometric arrangement of the interacting components (Harlow and Lane, 1988).

Anti-GST-activase was chosen in preference to anti-tobacco activase as the primary antibody in the assay because there was a plentiful supply of antibody-rich serum available at the time during which the assay was being developed. A benefit of using the GST-activase antiserum was its specificity. The GST-activase immunogen was purified from *E.coli*, by virtue of its affinity for immobilised glutathione, and as a

result, the antiserum produced did not cross-react with tobacco proteins other than activase.

4.4.2 Choosing an appropriate immunological technique (The rationale behind using quantitative immunoblots)

4.4.2.1 Rocket immunoelectrophoresis (RIE)

RIE depends on the formation of an immunoprecipitate between antigens and antibodies (for description of RIE see Section 4.3.2). Antigen-antibody complexes only precipitate if a three-dimensional lattice is formed (Roitt, 1980). This requires multivalent interactions between the antibodies and their target. The absence of an immunoprecipitate between anti-GST-activase and tobacco activase indicates that the antiserum does not contain antibodies which have a high valency for the different antigenic determinants on tobacco activase. This means the GST-activase antiserum has a low avidity for the target antigen. The low avidity of the tobacco activase / anti-GST-activase interaction is a side-effect of using a primary antibody that has been raised against a similar rather than identical antigen. An immunoprecipitate may have formed between tobacco activase and antibodies raised against the fusion protein, tobacco activase glutathione *S*-transferase. However, as mentioned previously, the tobacco activase sequence could not be cloned and expressed in *E.coli* at the time of immunisation. Therefore, this option was not available.

4.4.2.2 Enzyme-linked immunosorbent assays (ELISAs)

The cross-reaction between tobacco activase and anti-GST-activase in titre assays indicated that an ELISA system for detecting activase content could be applied. Antibody capture assays (Figure 4.1) using PVC and nitrocellulose-bottomed microtitre plates were investigated. This assay system involves binding the antigen to a solid support, after which the primary antibodies are added. In this case, polyclonal antiserum was the source of primary antibodies. Polyclonal antiserum contains a mixture of antibodies, which bind to different epitopes on the antigen. This is advantageous because it amplifies the amount of target antigen available for the secondary antibody. The secondary antibody specifically binds to the primary antibody and it is conjugated to an enzyme which can be detected colourimetrically. A

quantitative ELISA assay for purified tobacco activase was successfully developed for the PVC plates. However, the assay was not quantitative for tobacco activase in extracts due to the relatively low binding capacity of the PVC wells (approximately 100 ng protein per well). Semi-quantitative immunoblots (Figure 4.7) and purification studies (Robinson et al., 1988) indicate that activase accounts for approximately 2% of soluble protein. This means that the maximum amount of tobacco activase that can be bound to PVC wells when coating them with unpurified extract is approximately 2 ng. This minute amount of target antigen cannot be measured reliably.

The limited binding capacity of the ELISA plate wells was partially overcome by using nitrocellulose-bottomed plates. Nitrocellulose binds approximately 1000 times more protein per surface area than does PVC. All the proteins within a sample of extract appeared to be bound using the nitrocellulose plates. However, when the activase content of the tobacco extract was assayed using this method, it was much lower than expected based on semi-quantitative immunoblots (Figure 4.7). Therefore, it seems that the ELISA method under-estimates the activase content of plant extracts. Subsequent dot-blot assays of activase content confirmed the observations using the nitrocellulose plates. A smaller signal was observed when samples of tobacco extract were dotted onto nitrocellulose and probed using anti-GST-activase, than when the same volume of sample was electrophoresed before immunoblotting. Perhaps the many other proteins in the plant extract that bind to the nitrocellulose interfere with the binding of the GST-activase antibodies to tobacco activase. Regardless of the reason, another technique for quantitating activase was required.

4.4.2.3 Sandwich ELISA

A two-antibody sandwich ELISA (Figure 4.2) was also trialled. This technique involves the binding of the primary antibody to the bottom of the ELISA plates, after which the unpurified extract is added to the wells and the antigen within the extract is bound and detected in an enzyme-linked assay. This system is ideal for the quantitation of an antigen within an unpurified extract, because the first antibody binding acts as a purification step. However, a very pure and concentrated solution of primary antibody is required for the initial binding to the ELISA plate. The GST-activase antibody was from polyclonal serum and, as a result, it had to be purified before use in this assay. The method chosen was immunoaffinity purification. In this procedure pure antigen is bound covalently to a solid support. The antibodies within

the polyclonal pool that are specific for the antigen are allowed to bind. The unbound antibodies are removed by washing, and the specific antibodies are eluted. Very stringent conditions (pH 2.5) had to be used when eluting in order to get a high yield of antibodies from the column. This very low pH disrupts the acid-sensitive interactions between the antibody and antigen. However, it also broke the covalent bond between the GST-activase antigen and the solid support, and this resulted in the primary antibodies being contaminated with GST-activase protein. Consequently, the background to signal ratio in the sandwich ELISA assay was too high.

4.4.2.4 Immunoblotting

After testing many different techniques, it became apparent that the only reliable method available for assaying activase levels was immunoblotting. A rough estimate of the *in vivo* activase concentration was obtained using the semi-quantitative Pharmacia Phastgels (Figure 4.5) and this technique was successfully used to compare the relative activase content of the anti-activase primary transformants (Chapter 2, Figure 2.3). Immunoblots have several advantages when assaying an extract that is high in soluble protein, and when working with antibodies that have a low avidity for their target antigen. Electrophoresis of the tobacco leaf extracts acts as a purification step which separates the target antigen from the other proteins, making it easily accessible to the GST-activase antibodies. Furthermore, the high local concentration of antigens on the membrane provides a better chance for the antibodies to bind through both F_{ab} arms (Figure 4.11), thereby increasing the avidity of the interaction. The antigen density also favours the retention of low-affinity antibodies on the membrane by increasing the frequency with which antibodies leaving the membrane bind to adjacent sites (Harlow and Lane, 1988).

Immunoblots are not usually used to measure antigen concentration. However, the development of enhanced chemiluminescence (ECL) detection systems has enabled densitometry to be used in the quantification of immunoblot band density. ECL detection is very sensitive; amounts of activase as low as 5 ng could be visualised on most immunoblots (data not shown). It was vital that the immunoblot development technique was very sensitive, since it had to detect very low concentrations of activase in the anti-activase plants. A restriction of this method of quantitation is that the volume of extract that can be loaded onto the Novex gels is limited. The maximum volume of extract loaded into the wells was 10 μL (together with 5 μL of SDS-dye).

This small volume can be compensated to some extent by extracting the leaf discs in very small volumes of buffer. However, high-CO_2-grown leaf discs must be extracted in at least 0.5 mL per cm^2, otherwise it is difficult to extract all of the protein efficiently. Another limitation of this method is that it is very time-consuming. It takes at least 2 complete days to collect the leaves, carry out extractions, prepare purified activase standards, separate the proteins on SDS-PAGE, transfer to nitrocellulose, probe with antibodies, conduct the ECL procedures and, finally, to carry out densitometry. Also, the assay is only linear in the 0-100 ng range. This means that all samples of extract loaded onto the gel must contain activase within this range, otherwise the assay may be inaccurate. The long lag period between beginning and finishing the immunoblot assay means that overloading of extract, such that the activase content exceeds 100 ng, is not detected until at least 2 days after beginning the assay. In these cases the assay must be repeated and the activase content of these plants is not known for at least another 2 days. These limitations mean that this method cannot be used as a screening procedure, such as when trying to detect the severity of antisense supression in primary transformants or a segregating population.

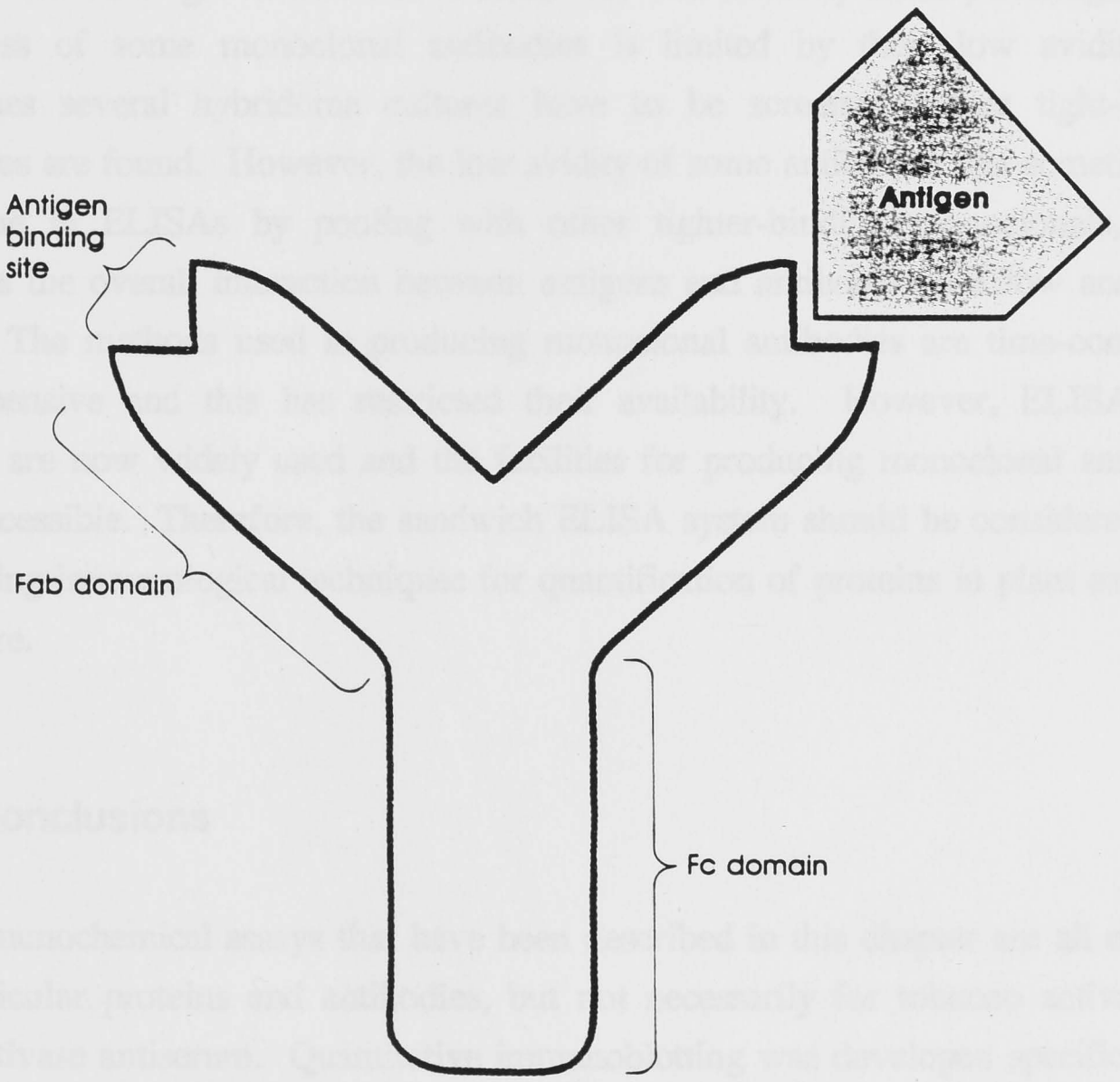

FIGURE 4.11: Schematic drawing of a typical antibody molecule (reproduced from Harlow and Lane, 1988).

An ELISA assay system is not labour-intensive and it would enable large numbers of samples to be assayed in a relatively short period of time. However, as I mentioned in the previous section, sandwich ELISA systems must be used when assaying crude extract, and this requires very pure antibodies. In future, when developing assay systems for proteins in crude extract, perhaps monoclonal antibodies could be used for binding to the ELISA plate. Monoclonal antibodies are obtained from *in vitro* cultures of hybridomas, which are immortal somatic cell hybrids that secrete antibodies (Roitt, 1980). The hybridomas are produced by the fusion of myeloma cells with antibody-secreting cells from immunized animals. Each hybridoma culture produces monoclonal antibodies which are specific for only one epitope on the antigen. At least two monoclonal antibodies are required for a sandwich ELISA; one for binding to the plate and another, specific for a different epitope, for use in the enzyme-linked assay. Alternatively, one monoclonal antibody can be bound to the plate and polyclonal antisera or pooled monoclonal antibodies can be used in the enzyme-linked assay. The use of polyclonal sera or pooled monoclonals has the benefit of amplifying the signal in the assay since several antibodies will bind to different epitopes on each antigen, whereas when a single monoclonal is used, only one antibody binds per antigen. The usefulness of some monoclonal antibodies is limited by their low avidity, and sometimes several hybridoma cultures have to be screened before tight-binding antibodies are found. However, the low avidity of some antibodies can sometimes be overcome in ELISAs by pooling with other tighter-binding monoclonals, which stabilizes the overall interaction between antigens and antibodies (Harlow and Lane, 1988). The methods used in producing monoclonal antibodies are time-consuming and expensive and this has restricted their availability. However, ELISA assay systems are now widely used and the facilities for producing monoclonal antibodies more accessible. Therefore, the sandwich ELISA system should be considered when developing immunological techniques for quantification of proteins in plant extract in the future.

4.4.3 Conclusions

The immunochemical assays that have been described in this chapter are all effective for particular proteins and antibodies, but not necessarily for tobacco activase and GST-activase antiserum. Quantitative immunoblotting was developed specifically for the measurement of tobacco activase with the anti-GST-activase antibody. This assay system could easily be used to quantify other proteins. The only requirement is for an

antibody that will recognise the target antigen. This antibody does not have to be purified and it does not need a high avidity for the target antigen. While this method could easily be adapted for measuring other proteins, it is time-consuming and labour intensive, and this restricts the number of samples that can be processed. Therefore, other immunological techniques should be considered if large numbers of samples have to be processed. Despite its limitations, the quantitative immunoblot is a useful method. The sensitivity of this assay makes it useful in the analysis of activase-deficient tobacco plants. Its reliability in measuring activase protein in unfractionated extracts is unprecedented and it has enabled much of the work presented in subsequent chapters of this thesis.

CHAPTER 5: The effect of activase-deficiency on photosynthesis in air-grown tobacco

5.1 INTRODUCTION

The initial analysis of the anti-activase plants confirmed the critical role of activase in maintaining the carbamylation of Rubisco (Chapter 2). However, these experiments (Chapter 2 and 3) raised many questions about the effect of activase-deficiency on photosynthetic rate and Rubisco content. A more detailed analysis of the R_1 progeny of anti-activase plant #52 will be discussed in subsequent chapters in order to provide some answers to these questions.

The development of a quantitative assay for activase protein (Chapter 4) enables us to determine the minimum ratio between activase and Rubisco that will support wild-type levels of photosynthesis and Rubisco carbamylation in the anti-activase plants. Consequently, we may be able to draw some conclusions about the way in which Rubisco and activase interact. Studies carried out by Wang et al. (1992) suggest that an intimate protein-protein interaction between Rubisco and Rubisco activase must be involved in the release of inhibitors from Rubisco's catalytic sites (Chapter 1, Section 1.9.3). However, the nature of this interaction has not been clarified. Activase's promotion of Rubisco carbamylation may require molar concentrations of activase equivalent to those of Rubisco. If this is the case, activase may remain bound to Rubisco in the light, like a ligand or missing subunit. As a ligand, activase binding to Rubisco, in concert with ATP hydrolysis may somehow maintain Rubisco in a confirmation that reduces the affinity of its inactive sites for RuBP, thereby altering the carbamylation equilibria. On the other hand, if the amount of activase necessary to maintain Rubisco's carbamylation is very much less than the molar equivalent of Rubisco, then a catalytic role for activase might be suggested.

Earlier experiments indicated that the photosynthetic rates of the anti-activase plants were less then expected based on assays of Rubisco carbamylated site concentration and intercellular CO_2 partial pressure (Chapter 2). However, photosynthetic rates and Rubisco carbamylation levels were not measured simultaneously in these plants. This raises the possibility that the discrepancy between observed and expected rates was the product of environmental or developmental changes. In this chapter, I will present measurements of photosynthesis and Rubisco carbamylation and content that were obtained simultaneously. The data presented in this chapter were obtained by the analysis of plants grown in air (0.03% CO_2). High CO_2 concentrations were essential for the successful passage of anti-activase primary transformant plantlets from tissue

culture into soil (Chapter 2), and high CO_2 was used in subsequent experiments to ensure survival of all anti-activase progeny (Chapters 2 and 3). However, it was not known if all the R_1 progeny of primary transformant #52 required high CO_2 concentrations for growth. Therefore, these plants were germinated and raised at atmospheric CO_2.

Anti-SSU plants, with reduced Rubisco content, were included in this study as an additional control. The phenotype and segregation ratio of the anti-SSU R_1 progeny have been described previously (Hudson et al., 1992b). In this chapter, the observed and expected photosynthetic rates of the anti-SSU plants will be compared to those of the anti-activase plants.

5.2 MATERIALS & METHODS

5.2.1 Plant material and growth conditions

The plant material was the R_1 progeny of *Nicotiana tabacum* transformed with either pαTACT (anti-activase), pαSSU (anti small subunit) or pBI121 (control). The anti-activase and anti-SSU seeds were obtained from primary transformants #52 (2 T-DNA inserts) and S4 (1 T-DNA insert) respectively. The anti-activase plants were produced as described in Chapter 2 and the production of the anti-SSU plants is described in Hudson et al., (1992b).

Plants were germinated and grown in an air-conditioned glasshouse at ambient CO_2 during a Canberran winter (typical midday irradiance, 600 μmol quanta $m^{-2}s^{-1}$). The seed was germinated in pots containing sterilized garden soil. The seedlings were transferred to small tubes (7.5cm diameter, 15cm height) approximately 4 weeks after germination and, 8 weeks after germination, the plants were transferred to 5-L pots. A complete nutrient solution containing 12mM nitrate was applied three times a week (Hewitt & Smith, 1975).

5.2.2 Sampling procedures

Leaf discs of 0.5 cm^2 were taken in the glasshouse, 7 weeks after germination, for initial determination of activase content. Nine weeks after germination, gas exchange measurements were made on selected plants. The gas exchange chamber was fitted with a freeze clamp apparatus (Badger et al., 1984) and, after gas exchange

measurements, leaves were rapidly freeze clamped *in situ* for the determination of Rubisco carbamylation and metabolite levels. The Chl fluorescence of all plants was measured in the laboratory at 10.5 weeks after germination on the uppermost, fully expanded leaves and, 3 weeks later, further leaf discs were taken in the glasshouse, from the uppermost fully expanded leaves, for determination of Rubisco content.

5.2.3 Leaf gas exchange and freeze-clamping of leaves

Leaf gas exchange measurements were made in an open gas exchange system, as described by Brugnoli et al. (1988). However, the system was fitted with a clamp-on chamber that contained a freeze-clamp apparatus (Badger et al., 1984), modified by Leegood and von Caemmerer (1988). The leaf chamber covered an area of 9.6 cm^2. Measurements were made at an irradiance of 1500 μmol quanta $m^{-2}s^{-1}$, 350 μbar CO_2, leaf temperature of 25°C and a leaf to air vapour pressure difference of 10 mbar. After gas exchange measurements, leaves were rapidly freeze clamped *in situ*. The freeze-clamp had been modified to yield a frozen leaf disc divided into two halves, each of 2.7 cm^2. One half was used for measurements of Rubisco content, carbamylation level and activity as well as soluble protein and activase content. The other half was used for assays of RuBP and PGA.

Chl fluorescence was measured with a fluorimeter (Pam 101; Waltz, Effeltrich, Germany) in the laboratory in air, at 600 μmol quanta $m^{-2}s^{-1}$ and 22°C, after the plants had been exposed to approximately 6 h of daylight. The ϕ PSII was calculated according to the method of Genty et al. (1989).

5.2.4 Quantitative immunoblot

Tobacco activase standard was purified using the method of Wang et al. (1992) and was diluted with 0.3 mg mL^{-1} BSA in TBS buffer. Leaf punches (0.5cm^2) were extracted at 0°C in 0.25 mL of 50mM Hepes-KOH [pH 7.1], 5mM $MgCl_2$, 1mM sodium EDTA, 10mM DTT and 1mM PMSF. Mercaptoethanol and SDS were added to the extract to 4% [v/v] and 2% [w/v], respectively, before boiling for 10 min. The extract was centrifuged and a sample of the supernatant was separated on a 1mm thick, Novex 16% homogenous polyacrylamide gel using a modified Bio-Rad Midget gel rig. Tobacco activase standards were included on every gel. The proteins were electroblotted to nitrocellulose and blocked with 10% milk powder in 20mM Tris-HCl [pH 8.5], 0.5M NaCl (Tris-buffered saline, TBS) at 4°C overnight. The blot was

probed with the following antibodies in 5% milk powder, 0.05% Tween in Tris-buffered saline (TTBS): (a) primary antibody, anti-GSH *S*-transferase/spinach activase fusion protein (Chapter 4, Section 4.2.1.1), and (b) secondary antibody, goat anti-rabbit immunoglobulin conjugated to horseradish peroxidase (Bio-Rad). The activase bands were visualized by incubating the blot with Amersham ECL detection reagents for 1 min and exposing it to Amersham Hyper-film for 15 s. The density of the activase bands was quantified using the integrator on a Quick Scan Jr. densitometer from Helena laboratories. The gain dial on the densitometer was set at 3 (range 1-10) for all scans.

5.2.5 Rubisco and soluble protein assays

Leaf punches ($2.7cm^2$) were extracted in 2.7 mL of 50mM Hepes-KOH [pH 7.1], 1mM sodium EDTA, 10mM DTT and 1mM PMSF, on ice. Rubisco carbamylation was measured immediately (within 10-15 s) using the method described in Chapter 2. Then the initial Rubisco activity and total activity after full carbamylation *in vitro* were determined using a spectrophotometric assay system linked to NADH consumption.

The initial Rubisco activity was determined by adding 50 μL of extract to a 2 mL assay mixture of 125 mM EPPS-NaOH [pH 7.8], 25mM $MgCl_2$, 10 mM $NaHCO_3$, 170 μM NADH, 1 mM ATP, 5 mM phosphocreatine, 200 μM RuBP and coupling enzymes (creatine phosphokinase (Sigma C3755, 15U), carbonic anhydrase (Boehringer 103 195, 185U), 3 phosphoglycerate kinase (Boehringer 108 448, 55U), glyceraldehyde 3 PDH (Boehringer 105 694, 25U) and TIM / glycerol-3-phosphate dehydrogenase (Boehringer 737 259, 77U / 24U)) at 25°C, the A_{340} was monitored for 1 min and the Rubisco activity was calculated assuming that 4 molecules of NADH were oxidized per RuBP consumed. At the same time, 50 μL of the extract was incubated in the assay solution (with saturating CO_2 and Mg^{2+}), minus RuBP, at 25°C for 10 min. After which the fully carbamylated Rubisco activity was determined using the same system as for the initial Rubisco activity, except that the assay was started by adding RuBP.

The Rubisco content was measured as described in Chapter 2 and the soluble protein was determined using the Pierce Coomassie detection kit, with BSA as a standard.

5.2.6 RuBP & PGA assays

The leaf punches (2.7 cm^2) used for determining RuBP and PGA pool size were extracted in 500 μL of 1M perchloric acid on ice and neutralised with 60 μL of 5M K_2CO_3. The particulate matter in the sample was pelleted by spinning in a microfuge for 5 min and the supernatant was decanted to another microfuge tube containing approximately 10 mg of charcoal. After vortexing, the tube was centrifuged and the supernatant collected. 180 μL of the extract was used in a spectrophotometric enzyme-linked assay system similar to that used for determining initial and total Rubisco activity. The 2 mL assay mixture containing 125 mM Hepes / NaOH [pH 7.8], 25 mM $MgCl_2$, 10 mM $NaHCO_3$, 170 μM NADH and 180 μL of extract, 1 mM ATP and 5 mM phosphocreatine was incubated at 25°C and the A_{340} monitored prior to the addition of 20 μL of coupling enzymes (see Section 5.2.5 for description of coupling enzymes and their concentrations) and the reaction followed on the spectrophotometer until the absorbance had stabilized. 50 μg of purified *R. rubrum* Rubisco was added and the A_{340} followed again until the absorbance stabilized. The first decrease in absorbance is proportional to PGA content (2 NADH molecules oxidized per PGA molecule) and the second decrease is proportional to RuBP (4 NADH molecules oxidized per RuBP molecule).

5.3 RESULTS

5.3.1 Phenotype of R_1 antisense plants

The R_1 control and anti-activase plants were grown in a glasshouse at atmospheric CO_2. Under these conditions there was a large variation in the size of the anti-activase plants (Figure 5.1A). The parent of the anti-activase plants (primary transformant #52) contained two T-DNA inserts (Chapter 2, Figure 2.3). Therefore we expect the progeny to contain 0-4 inserts. If we assume that growth is negatively correlated to insert number, and that each of the two T-DNA inserts in the genome of the #52 parent were of equal potency, then we might expect there to be five size classes in the R_1 progeny; corresponding to plants with 0, 1, 2, 3 and 4 T-DNA inserts, respectively. A relationship like this, between plant size and antisense dose, has been observed previously in transgenic plants, in the air-grown anti-SSU R_1 progeny of S4 (John Evans - personal communication). However, the anti-activase R_1

progeny segregated into six size classes (rather than 5), and there was considerable variation in plant size within some of these groups. The large number of size groups could be explained by the parent #52 containing 2 T-DNA inserts of different potency. Past studies have shown that the position of T-DNA insertion in the genome will influence the expression of the antisense gene (Grierson, 1993). There are 9 different genotypes within the anti-activase R_1 progeny: 1 wild-type revertant, 2 single-insert, 3 double-insert, 2 triple-insert and 1 quadruple insert. This means that a difference in the potency of the two T-DNA inserts in parent #52, due to a positional effect, could have produced R_1 progeny which segregated into a maximum of 9 different size classes. If this was the case, some of the differences between the size classes may have been too subtle to detect. Consequently, only six size classes were apparent.

With the self-fertilizing parent having two inserts, we can expect 6.25% of progeny to be wild-type segregants, and 25% of progeny to be single insert plants. About 7.5% of plants grew as quickly as the control plants (gp 6), and these plants were identified as putative wild-type segregants (Figure 5.1A). If the single insert plants are growing slightly slower than the wild-type segregants, then they are probably the next largest plants (gp 5) (Figure 5.1A). Gp 5 contained only 15% of the total population of anti-activase plants. We expect 25% of the progeny to contain single-inserts. Therefore, some of the anti-activase single-insert plants are probably located in gps. 4 and 6. The putative single-insert plants in gp 5 had a wide range of assimilation rates (Figure 5.1B). Some of the heterogeneity in the putative single-insert plants may be due to differences in the potency of the T-DNA inserts, as a result of the positional effects I discussed in the previous paragraph. However, if this phenomenon accounted for all the variation in this group we might expect to see two discrete populations of single-insert plants; instead we saw a continuum of assimilation rates and activase contents across the group. Analysis of the putative wild-type segregants in Figure 5.1 showed that these plants were reduced in activase content (Figure 5.2A). Therefore, no wild-type segregants were positively identified. This is surprising since we expected 6.25% of the progeny to be wild-type segregants. The heterogeneity in the putative-single-insert progeny and the difficulty in identifying a wild-type segregant might be explained if the anti-activase parent #52 containined more than two T-DNA inserts. However, this seems unlikely since the number of T-DNA inserts in the parent #52 was assayed by inverse PCR, and the presence of two T-DNA inserts confirmed by kanamycin resistance studies on the R_1 progeny (Chapter 2). It is possible that the correct percentage of wild-type segregants may have been observed if a greater number of R_1 progeny were screened.

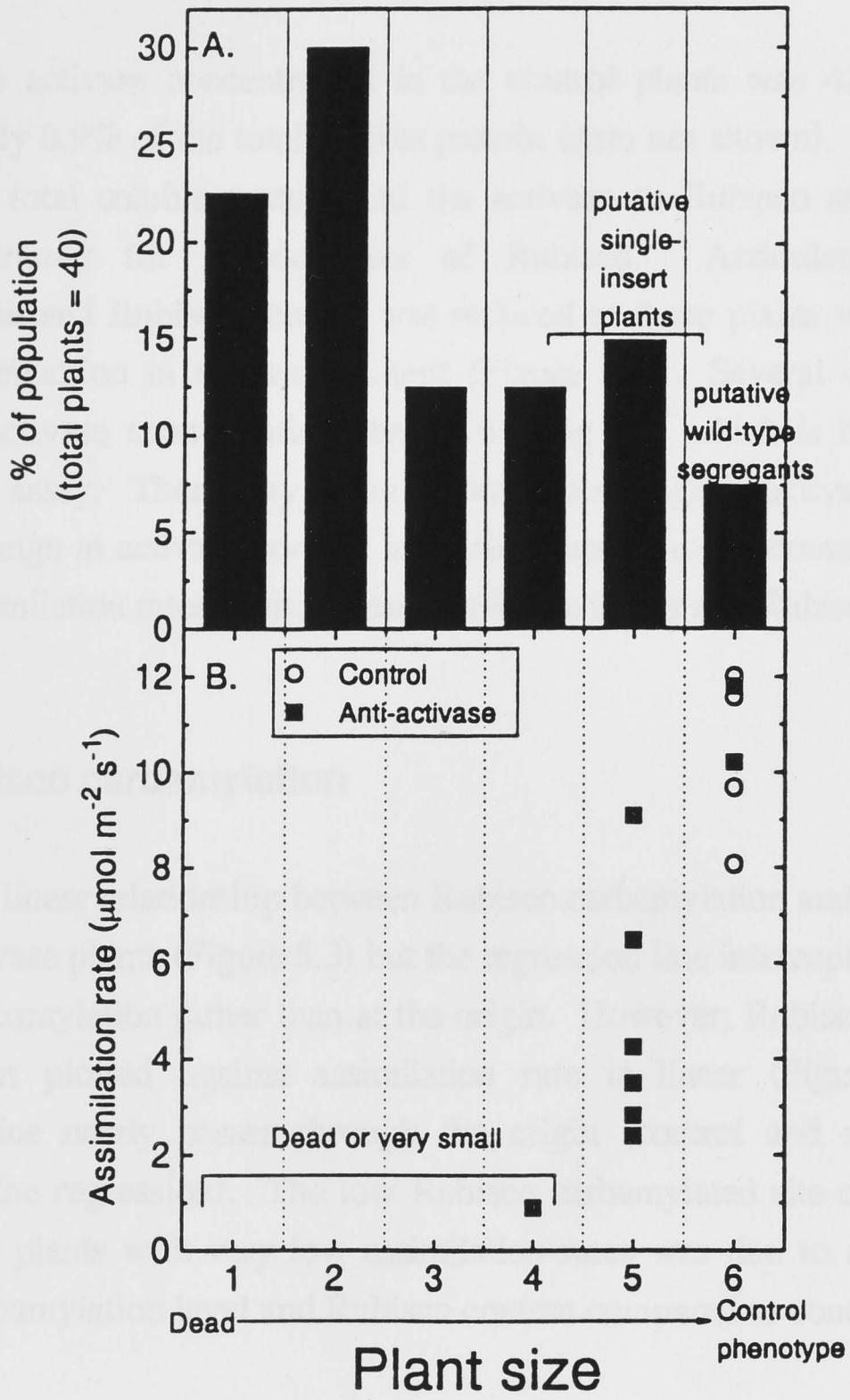

FIGURE 5.1: Variation in growth and assimilation rate of low-CO_2-grown anti-activase plants. The control and anti-activase plants are the self-progeny of a pBI121 transformant and pαTACT transformant 52, respectively. The plants were classified into 6 groups depending on size: 1. Died immediately after germination; 2. Alive, but had not developed beyond germination; 3. Two cotyledons + 1-2 unexpanded leaves; 4. Two cotyledons + 3-5 expanding leaves; 5. Early rosette stage (a cluster of expanding and fully expanded leaves). Rosettes varied in diameter; 6. Late rosette stage (just prior to stem elongation), wild-type phenotype. Control plants were germinated under exactly the same conditions as the anti-activase plants. The control plants germinated and grew evenly. **A. Distribution in plant size. B. Variation in assimilation rate in control and anti-activase plants.** The gas exchange measurements were made at an irradiance of 1500 μmol quanta $m^{-2}s^{-1}$, the leaf temperature was 25°C, the leaf to air vapour pressure difference was 11 mbar, and the CO_2 partial pressure was 350 μbar. Gas exchange measurements on anti-activase plants were restricted to those from groups 6,5, and one plant from group 4. This was because virtually all plants from groups 1, 2, 3 and 4 were too small for analysis.

5.3.2 Quantitation of tobacco activase

The average activase concentration in the control plants was 42 mg m^{-2} , this is approximately 0.9% of the total soluble protein (data not shown). Rubisco accounted for 31% of total soluble protein and the activase to Rubisco stoichiometry was 1 activase tetramer for 10 octamers of Rubisco. Assimilation rate, Rubisco carbamylation and Rubisco content was reduced in those plants which had a greater than 95% reduction in activase content (Figure 5.2). Several of the anti-activase plants had activase concentrations below 0.5 mg m^{-2} which is below the detection limit for the assay. There may be an undetectable range in activase content in these plants. A range in activase content in these plants would account for their observed range in assimilation rates, Rubisco carbamylation levels and Rubisco content.

5.3.3 Rubisco carbamylation

There was a linear relationship between Rubisco carbamylation and assimilation rate in the anti-activase plants (Figure 5.3) but the regression line intercepts the x-axis at 21% Rubisco carbamylation rather than at the origin. However, Rubisco carbamylated site concentration plotted against assimilation rate is linear (Figure 5.4A) and the regression line nearly passes through the origin (control and anti-activase points included in the regression). The low Rubisco carbamylated site concentration in the anti-activase plants with very low assimilation rates was due to a reduction in both Rubisco carbamylation level and Rubisco content compared to controls (Figure 5.2C).

The leaves of anti-SSU plants had Rubisco carbamylated site concentrations similar to the worst-affected anti-activase plants assayed (Figure 5.4A). The low Rubisco carbamylated site concentration in the anti-SSU plants was entirely due to a reduction in Rubisco content relative to controls (data not shown). Despite a similarity in Rubisco carbamylated site concentration between the anti-SSU and the worst-affected anti-activase plants, two out of three of the anti-SSU plants had considerably higher assimilation rates.

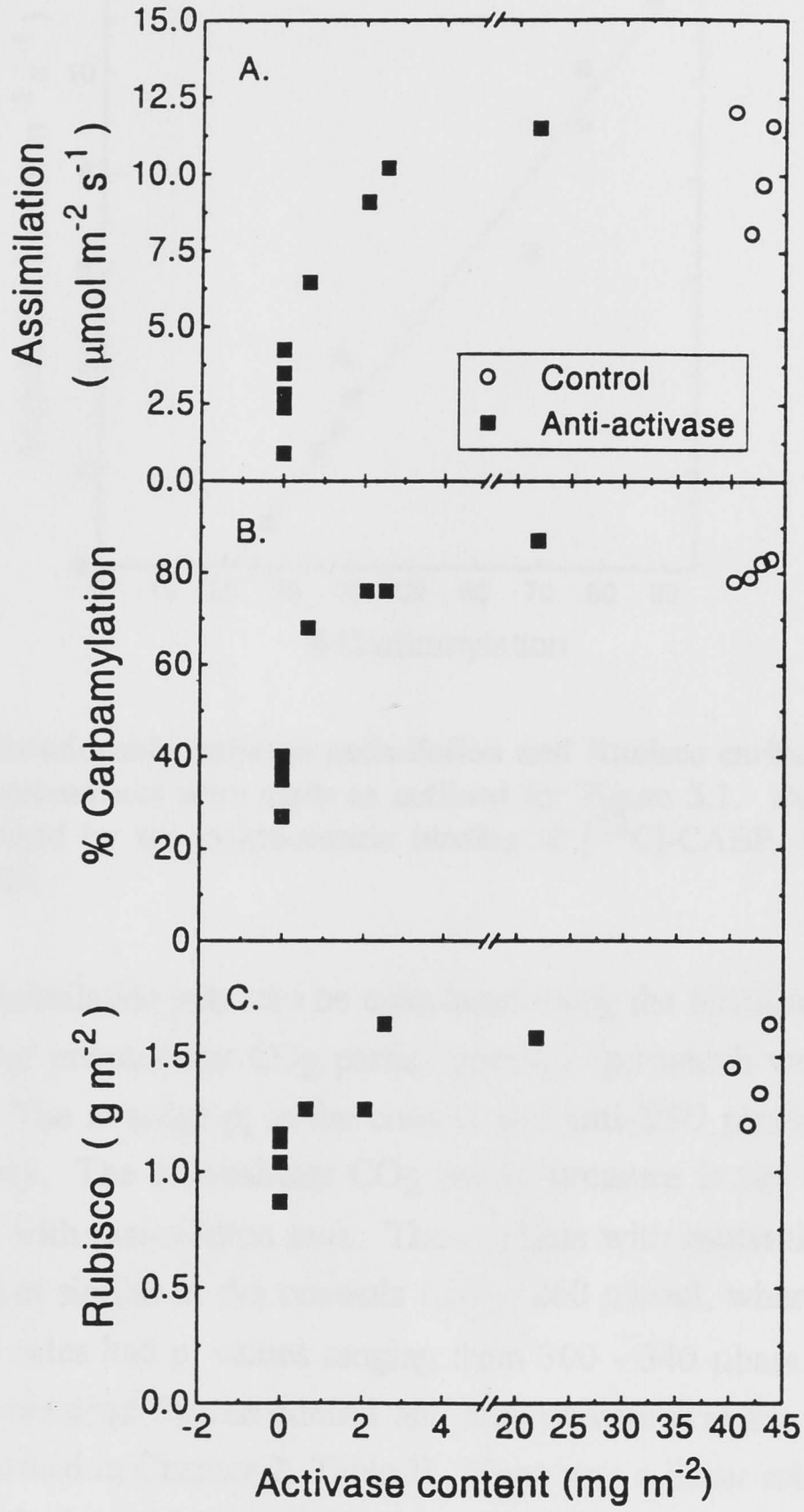

FIGURE 5.2: Assimilation rate and Rubisco carbamylation and content at varioius activase concentrations. All measurements and leaf samples were taken at least 2 h after the onset of illumination. Activase content was measured by quantitative ECL immunoblot. The detection limit of the activase assay was 0.5 mg m^{-2}. Those plants with activase levels below this are plotted as having zero activase content. The gas exchange measurements were made at an irradiance of 1500 µmol quanta $m^{-2}s^{-1}$, the leaf temperature was 25°C, the leaf to air vapour pressure difference was 11 mbar, and the CO_2 partial pressure was 350 µbar. Both Rubisco carbamylation and content were determined by the stoichiometric binding of [^{14}C]-CABP.

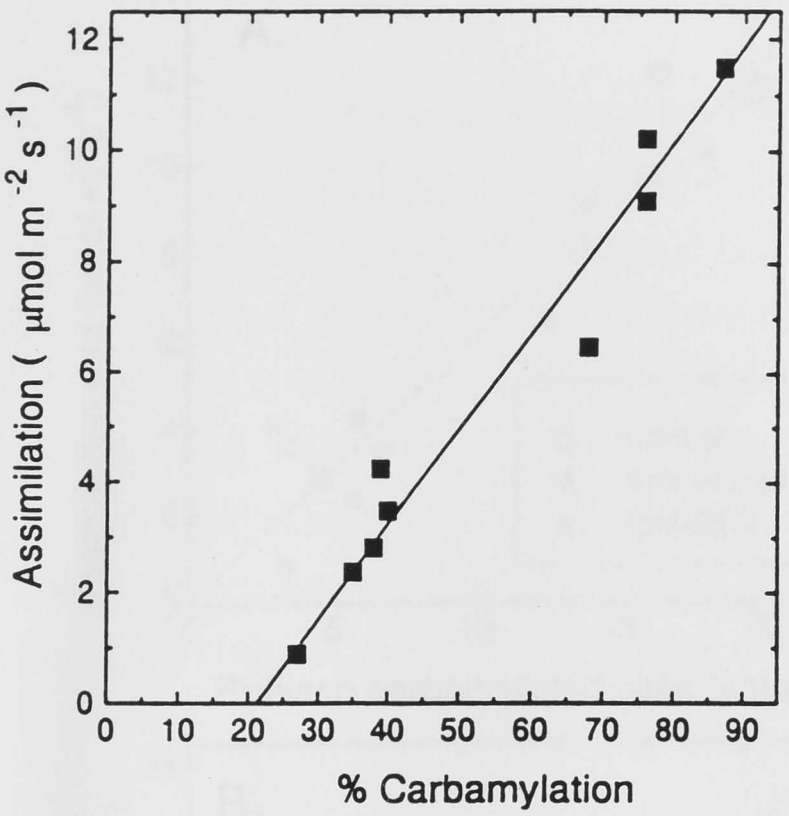

FIGURE 5.3: Relationship between assimilation and Rubisco carbamylation level. The gas exchange measurements were made as outlined for Figure 5.1. Rubisco carbamylation level was determined by the stoichiometric binding of [^{14}C]-CABP. (Data replotted from Figure 5.2A and B).

The expected assimilation rate can be calculated using the Rubisco carbamylated site concentration and intercellular CO_2 partial pressure (p_i)(which was measured during gas exchange). The average p_i in the control and anti-SSU plants was 242 and 292 µbars respectively. The intercellular CO_2 partial pressure in the anti-activase plants varied inversely with assimilation rate. Those plants with relatively high assimilation rates had p_i values similar to the controls (240 - 260 µbars), whereas the plants with low assimilation rates had p_i values ranging from 300 - 340 µbars. These values are similar to those obtained for the control and anti-activase primary transformants and R_1 progeny described in Chapter 2, Table II. There was a linear relationship between the expected and observed assimilation rates but the regression line did not pass through the origin (Figure 5.4B, dashed regression line, control and anti-activase points only). The expected assimilation rates were an over-estimate of the observed assimilation rates in both control and anti-activase plants. Anti-SSU plants were included in this experiment as an additional control. These plants had observed assimilation rates that were similar to their expected rates (Figure 5.4B). Consequently, the regression line for the control and anti-SSU points nearly passed through the origin (Figure 5.4B, dotted line).

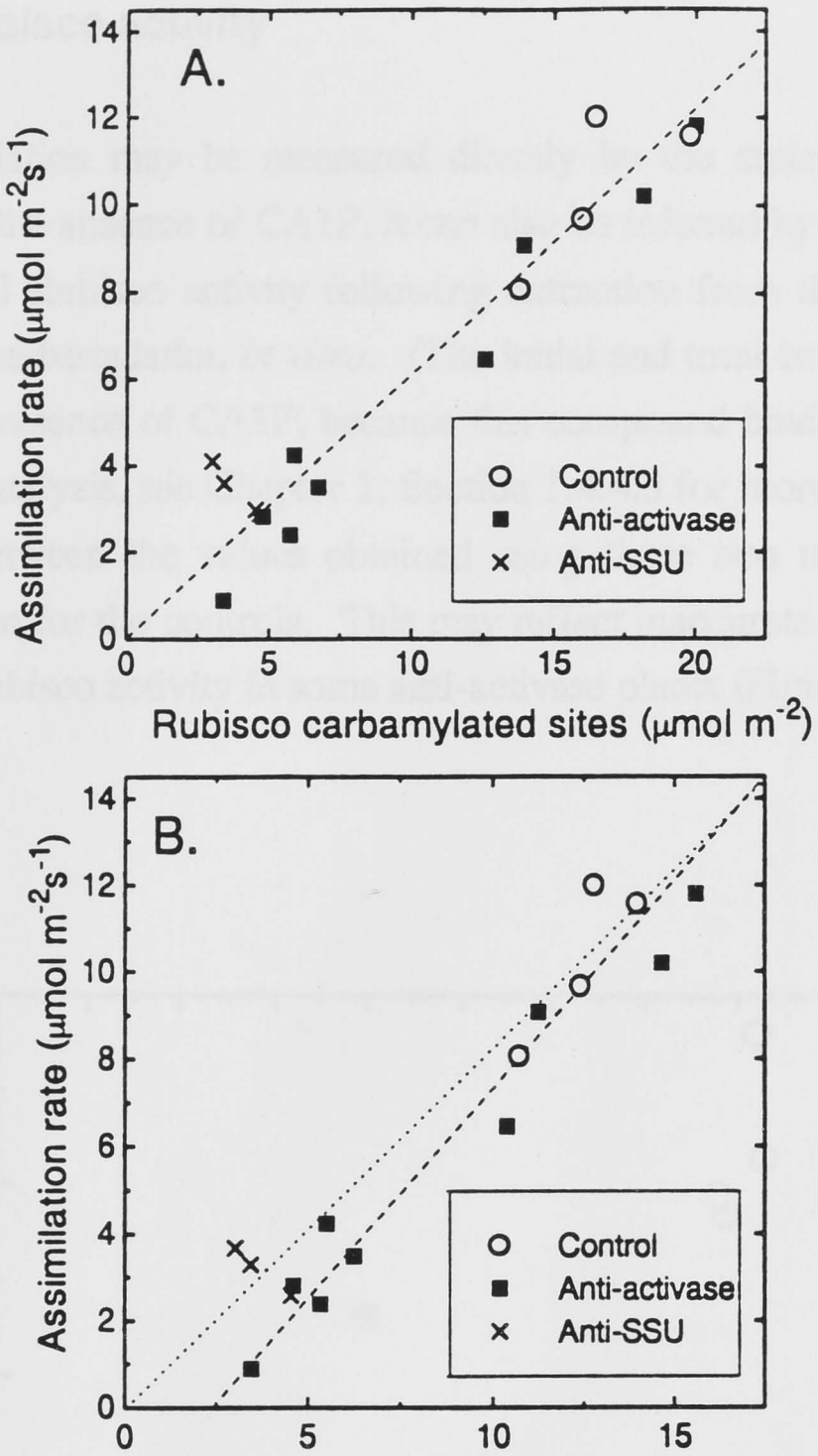

FIGURE 5.4: Relationship of observed assimilation rate to Rubisco carbamylated site concentration and expected assimilation rate. The data in Figure 5.4A is replotted from Figure 5.2. The regression line in Figure 5.4A includes control and anti-activase points. In Figure 5.4B, the dashed regression line is for both control and anti-activase points; whereas, the dotted regression lines includes control and anti-SSU points. The gas exchange measurements were made as described in the figure legend for 5.1. Rubisco carbamylated site concentration was determined by the stoichiometric binding of [^{14}C]-CABP. The expected assimilation rate, A, was calculated using the following equation:

$$A = \frac{(p_i - \Gamma_*)\ V_{c_{max}}}{p_i + K_c\,(1 + 0 / K_o)}$$

$V_{c_{max}} = k_{cat}$ x carbamylated Rubisco sites

k_{cat} (*in vivo*) = 3.6

Γ_* = 37 μbar

$K_c\,(1 + O / K_o)$ = 730 μbar

Values for k_{cat} , Γ_*, and $K_c\,(1 + O / K_o)$, were obtained from von Caemmerer et al. (in press), and gas exchange measurements of p_i were used.

5.3.4 Initial Rubisco activity

Rubisco carbamylation may be measured directly by the stoichiometric binding of [^{14}C]-CABP. In the absence of CA1P, it can also be inferred by determining the ratio between the initial Rubisco activity following extraction from the leaf and the 'total' activity after full carbamylation *in vitro*. (The initial and total activities will be underestimated in the presence of CA1P, because this compound binds tightly to Rubisco's sites and blocks catalysis, see Chapter 1, Section 1.4.4.3 for more details). There was more variation between the values obtained using these two methods for the anti-activase plants than for the controls. This may reflect inaccurate measurements of the very low initial Rubisco activity in some anti-activase plants (Figure 5.5).

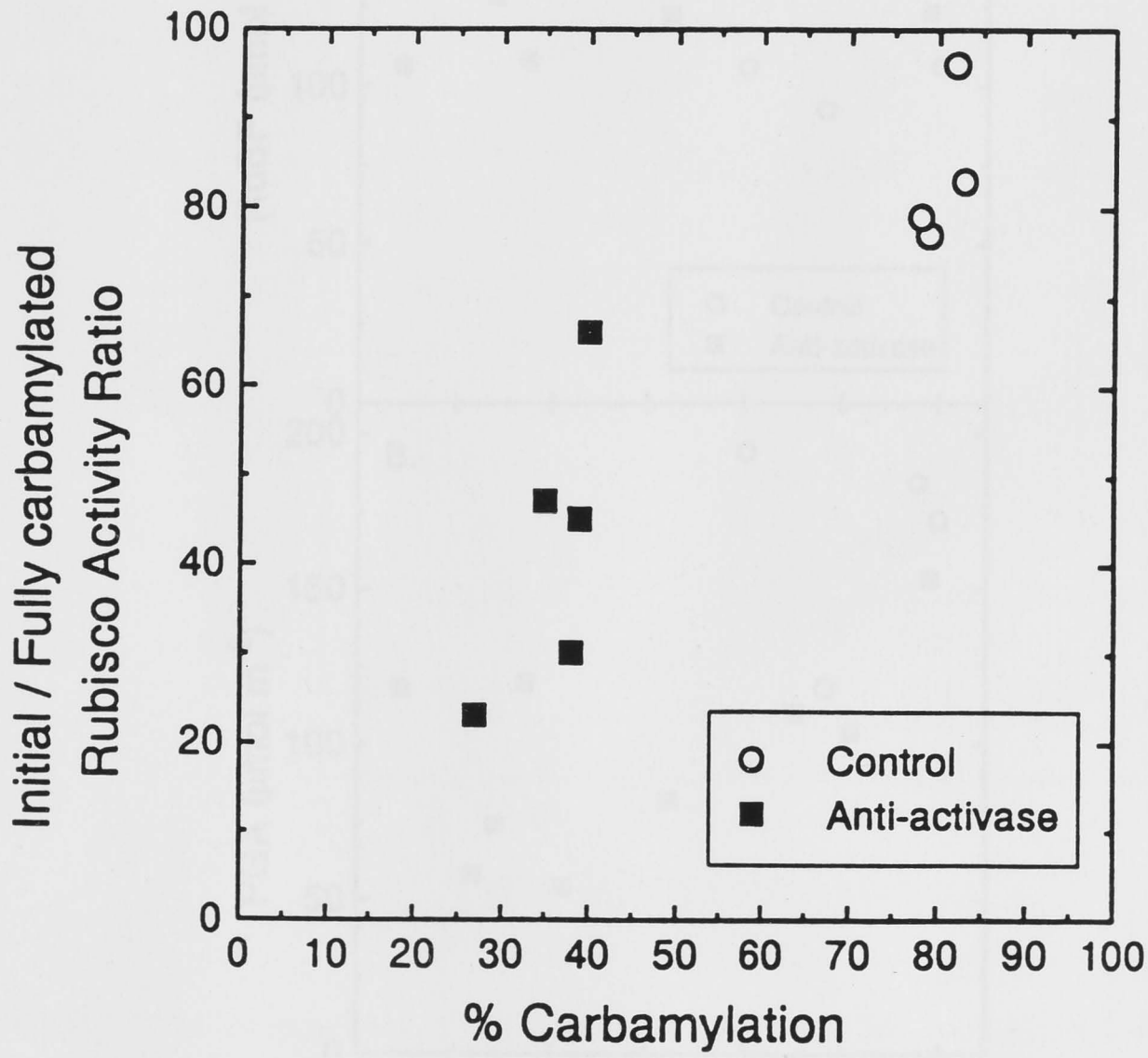

FIGURE 5.5: A comparison of two different methods used for determining Rubisco carbamylation level. Rubisco carbamylation was measured by the stoichiometric binding of [^{14}C]-CABP and the initial / fully carbamylated Rubisco activity ratio was measured using the spectrophotometric assay.

5.3.5 RuBP / PGA

The RuBP concentrations in the control and anti-activase leaves were very similar (Figure 5.6A), whereas the PGA concentrations were more variable (Figure 5.6B). The lowest PGA concentrations were observed in the anti-activase plants with the lowest assimilation rates, and the highest PGA concentrations were observed in the control plants which had relatively high assimilation rates. The average RuBP / PGA ratio in the controls was 0.76 ± 0.07, compared to 1.96 ± 0.33 in the anti-activase plants.

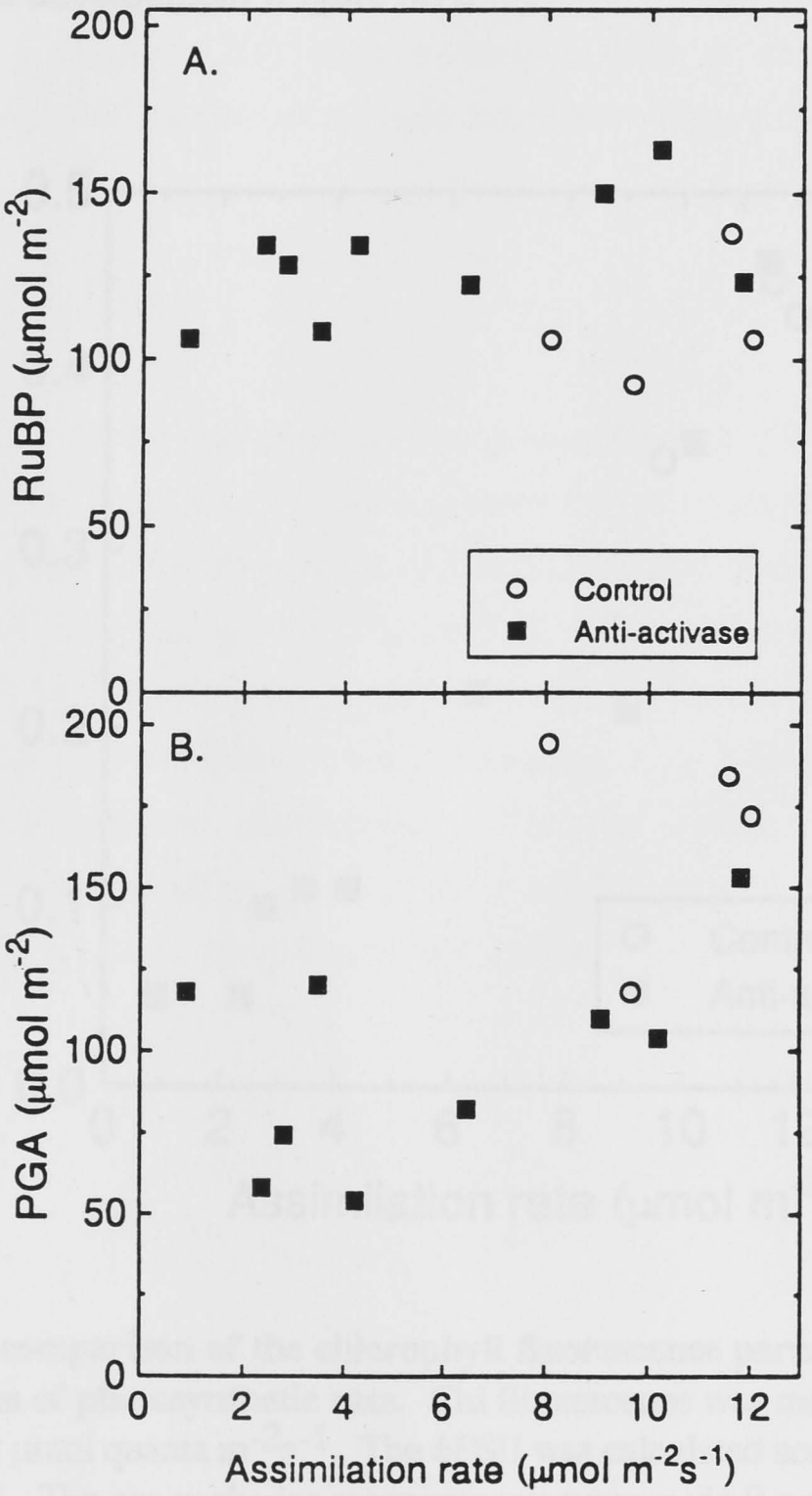

FIGURE 5.6: A comparison of the RuBP and PGA concentration in control and anti-activase plants. RuBP and PGA were assayed using an enzyme-linked spectrophotometric assay.

5.3.6 CO_2 assimilation rate

CO_2 assimilation rate was measured 9 weeks after germination using gas exchange; and 10.5 weeks after germination, chlorophyll fluorescence was measured to obtain an indication of photosynthetic rate. The Chl fluorescence parameter, ϕPSII, measures the quantum efficiency of PSII. ϕPSII reflects the activity of the light reactions and the consumption of their products. Therefore, it provides a quick and useful estimate of light reaction activity and, by inference, photosynthetic rate. The estimates of assimilation rate obtained using these different methods correlated well even though they were measured under different light intensities, using different methods and at different stages of development (Figure 5.7).

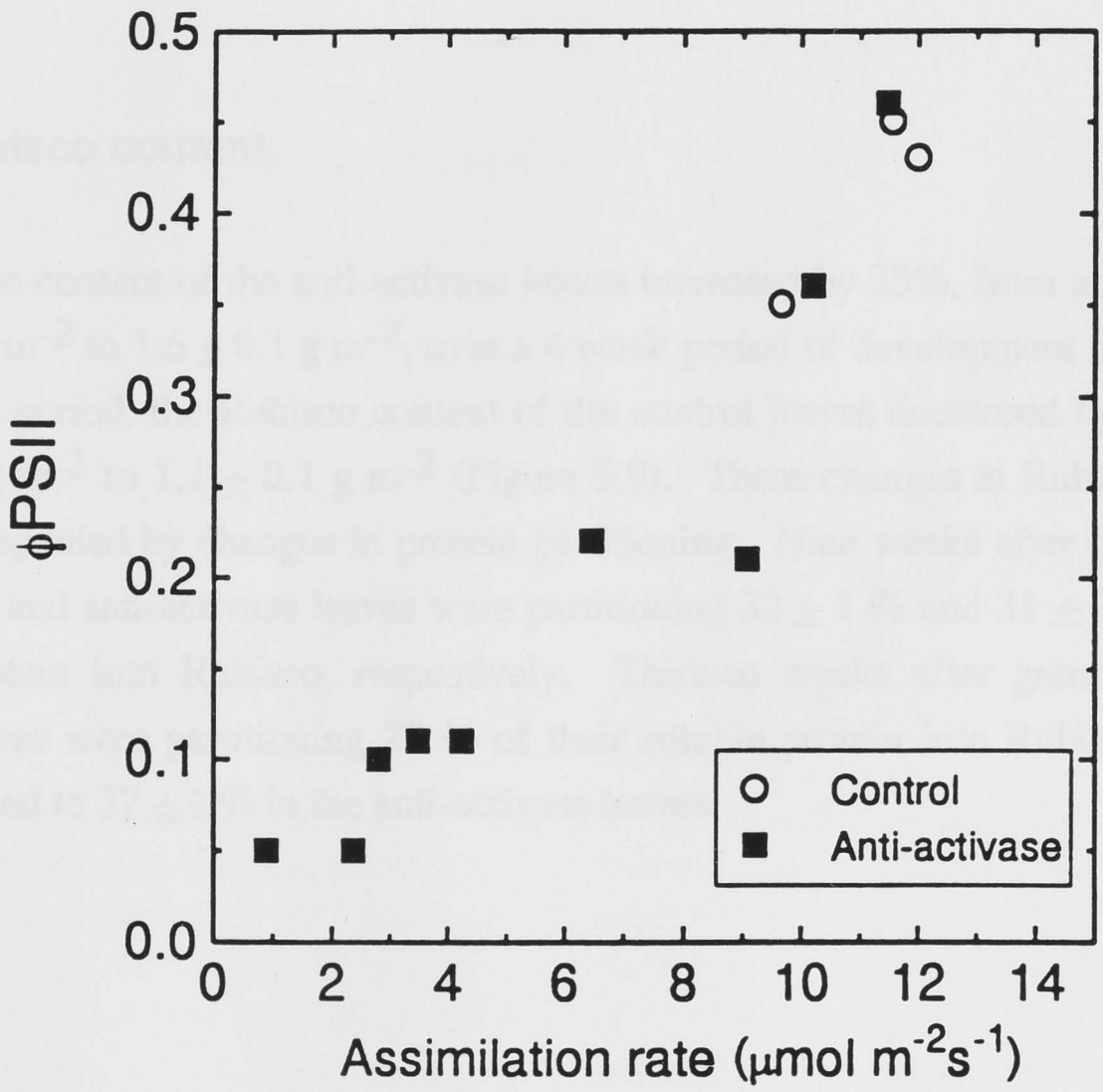

FIGURE 5.7: A comparison of the chlorophyll fluorescence parameter (ϕPSII), and gas exchange measures of photosynthetic rate. Chl fluorescence was measured 10.5 weeks after germination at 600 μmol quanta $m^{-2}s^{-1}$. The ϕPSII was calculated according to the method of Genty et al. (1989). The gas exchange measurements were made 9 weeks after germination at an irradiance of 1500 μmol quanta $m^{-2}s^{-1}$, as described in Figure 5.1.

Gas exchange analysis of two anti-activase plants with non-detectable levels of activase, and Rubisco carbamylation levels of 40% indicated that, at atmospheric CO_2 their CO2 assimilation rates were Rubisco-limited over a wide range of light intensities. The rate of RuBP carboxylation becomes faster with increases in CO_2 concentration. This means that, under conditions where photosynthetic rate is Rubisco-limited, the photosynthetic rate of intact plants will increase with rises in CO_2 concentration. However, the rate of photosynthesis will begin to plateau when the plant becomes light-limited. Under these conditions the photosynthetic rate will continue to increase slightly due to a diversion of energy from oxygenation to carboxylation. The control plants became light-limited at increasingly higher CO_2 concentrations as the light intensity was increased (Figure 5.8A). However, the assimilation rate / internal CO_2 concentration curves of the anti-activase plants followed Rubisco-limited kinetics at all light intensities (Figure 5.8B).

5.3.7 Rubisco content

The Rubisco content of the anti-activase leaves increased by 33%, from an average of 1.2 ± 0.1 g m^{-2} to 1.6 ± 0.1 g m^{-2}, over a 4 week period of development (Figure 5.9). During this period, the Rubisco content of the control leaves decreased by 21% from 1.4 ± 0.1 g m^{-2} to 1.1 ± 0.1 g m^{-2} (Figure 5.9). These changes in Rubisco content were accompanied by changes in protein partitioning. Nine weeks after germination, the control and anti-activase leaves were partitioning 32 ± 1 % and 31 ± 2 % of their soluble protein into Rubisco, respectively. Thirteen weeks after germination, the control leaves were partitioning 29 % of their soluble protein into Rubisco, but this had increased to 37 ± 1 % in the anti-activase leaves.

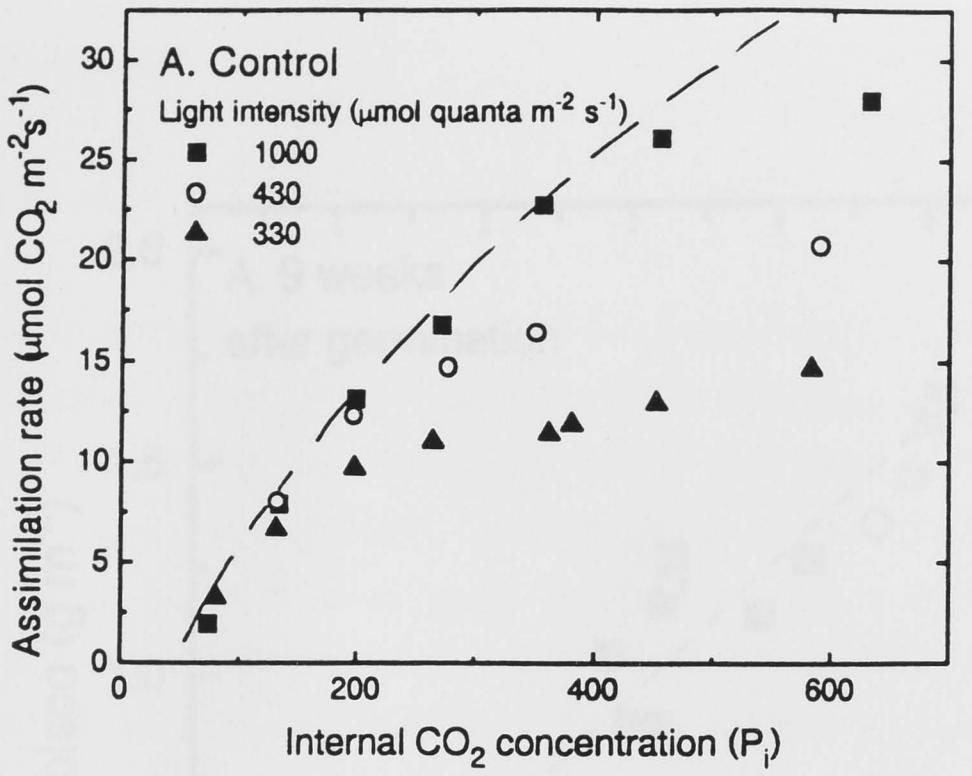

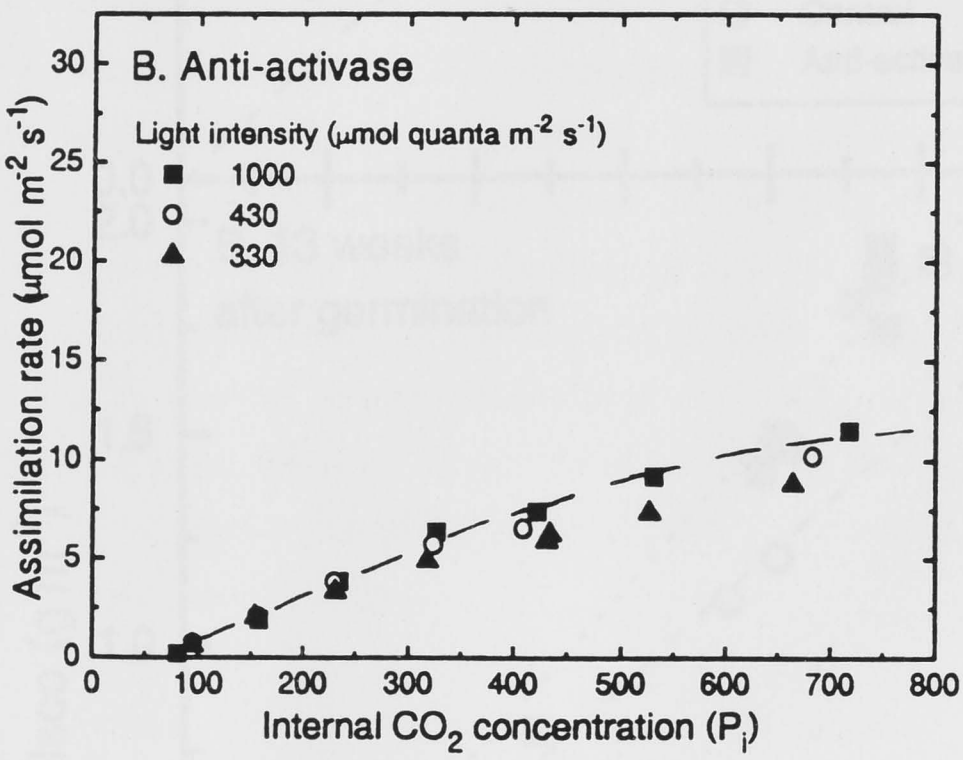

FIGURE 5.8: Relationship between photosynthetic rate and internal CO_2 concentration in a control and anti-activase plant. A. Assimilation rate vs. internal CO_2 concentration (P_i) in a control plant with 80% Rubisco carbamylation at 1500 μmol quanta $m^{-2}s^{-1}$. B. Assimilation rate vs. internal CO_2 concentration (P_i) in an anti-activase plant with 40% Rubisco carbamylation at 1500 μmol quanta $m^{-2}s^{-1}$. Gas exchange was carried out 9 weeks after germination, as described in Figure legend 5.1. The theoretical Rubisco-limited photosynthetic rate, A, is shown as a dotted line. It was calculated using the following equation:

$$A = \frac{(p_i - \Gamma_*)\ V_{c_{max}}}{p_i + K_c\,(1 + 0 / K_o)} - R_d$$

$V_{c_{max}} = 83$ (controls) or 25 (anti-activase plants)
$\Gamma_* = 37$ μbar
$K_c\,(1 + O / K_o) = 730$ μbar
$R_d = 1$ μmol CO_2 $m^{-2}s^{-1}$

Values for k_{cat} , Γ_*, and $K_c\,(1 + O / K_o)$, were obtained from von Caemmerer et al. (in press), and gas exchange measurements of p_i were used.

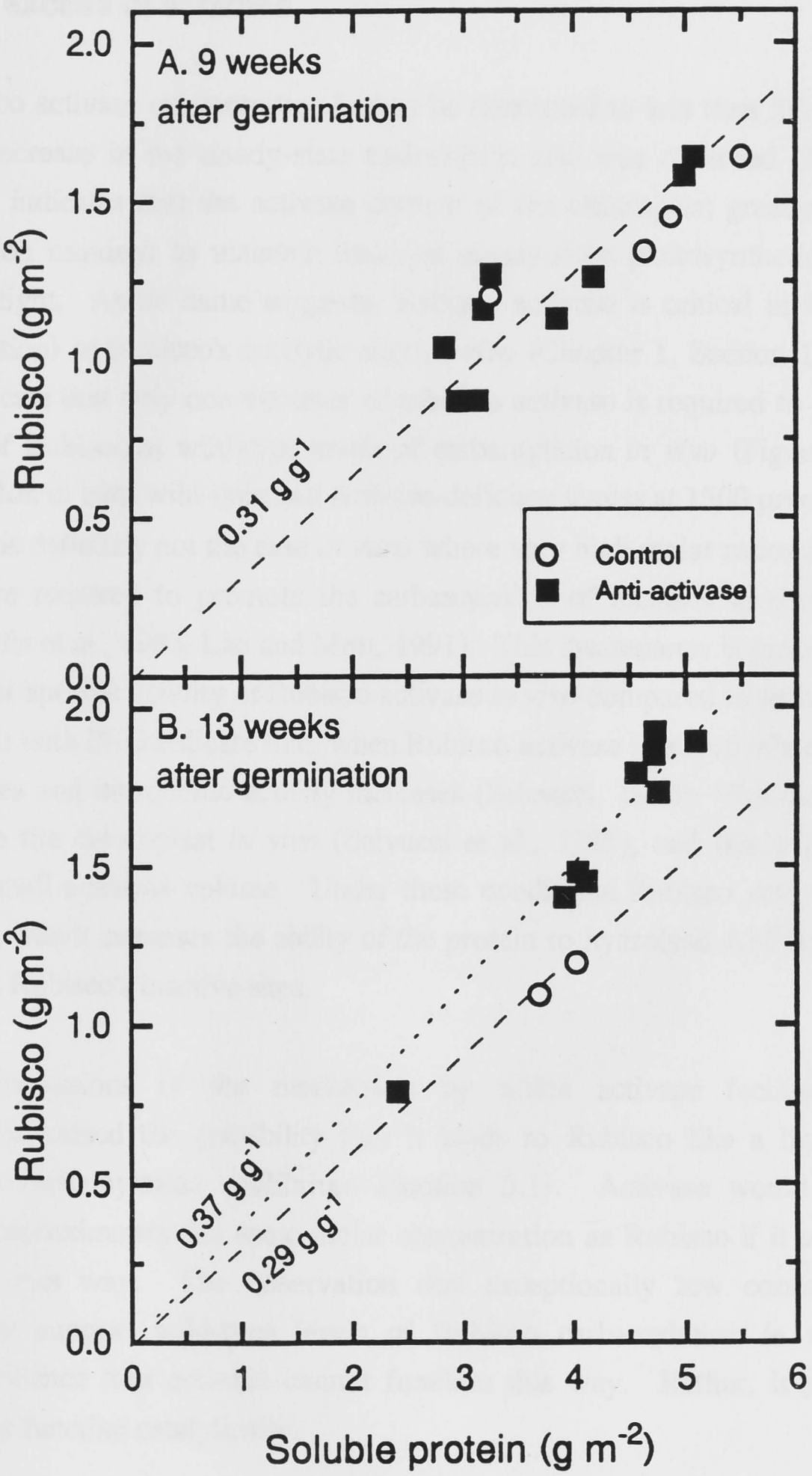

FIGURE 5.9: A comparison of protein partitioning into Rubisco in control and anti-activase plants at different developmental stages. Rubisco content was determined by the stoichiometric binding of [^{14}C]-CABP, and protein content was determined using a Coomasssie Blue dye-binding assay.

5.4 DISCUSSION

5.4.1 An excess of activase

The Rubisco activase concentration had to be decreased to less than 5% of wild-type before a decrease in the steady-state assimilation rate was observed (Figure 5.2A). This result indicates that the activase content of the chloroplast greatly exceeds the concentration required to maintain maximal steady-state photosynthetic rates under saturating light. As its name suggests, Rubisco activase is critical in the activation (carbamylation) of Rubisco's catalytic sites *in vivo* (Chapter 1, Section 1.6.2). These results indicate that only one tetramer of tobacco activase is required to maintain 200 octamers of Rubisco at wild-type levels of carbamylation *in vivo* (Figure 5.2B, 80% carbamylation in both wild-type and activase-deficient leaves at 1500 μmol quanta m^{-2} s^{-1}). This is definitely not the case *in vitro* where very high molar ratios of activase to Rubisco are required to promote the carbamylation of Rubisco in the presence of RuBP (Portis et al., 1986; Lan and Mott, 1991). This discrepancy is probably due to a much higher specific activity of Rubisco activase *in vivo* compared to *in vitro*. *In vitro* experiments with PEG indicate that, when Rubisco activase is effectively concentrated, it aggregates and its specific activity increases (Salvucci, 1992). Rubisco activase is localised to the chloroplast *in vivo* (Salvucci et al., 1985), and this organelle has a relatively small aqueous volume. Under these conditions Rubisco activase probably aggregates, which increases the ability of the protein to hydrolyse ATP and to release RuBP from Rubisco's inactive sites.

Previous discussions of the mechanism by which activase facilitates Rubisco carbamylation raised the possibility that it binds to Rubisco like a ligand, thereby altering the carbamylation equlibrium (Section 5.1). Activase would have to be present at approximately the same molar concentration as Rubisco if it was bound to Rubisco in this way. The observation that exceptionally low concentrations of activase can support wild-type levels of Rubisco carbamylation *in vivo* provide concrete evidence that activase cannot function this way. Rather, it suggests that activase may function catalytically.

In vitro experiments indicate that activase has no effect on the equilibrium of Rubisco carbamylation in the absence of RuBP (Chapter 1, Section 1.6.2). These observations are consistent with the theory that activase simply acts as a catalyst of sugar phosphate removal. RuBP binds very tightly to Rubisco's inactive sites *in vitro*, thereby blocking

carbamylation. However, in the presence of activase, RuBP is quickly released and carbamylation occurs (Portis, 1990). Also, RuBP has a stimulatory effect on Rubisco carbamylation in the presence of activase (Portis et al., 1986). *In vitro* experiments indicate that increases in RuBP concentration stimulate increases in Rubisco carbamylation level when activase is included in the assay mixture (Portis et al., 1986). Therefore, in the presence of activase, RuBP seems to change from being a negative effector of carbamylation to being a positive effector (Chapter 1, Section 1.4.4.1). This result indicates that activase probably influences the equilibrium of the carbamylation reaction by altering the affinity of Rubisco's inactive sites for RuBP. Past studies have shown that a reduction in the affinity of RuBP for Rubisco's inactive sites would enable this compound to act as a positive effector of Rubisco carbamylation, and would account for the high levels of Rubisco carbamylation *in vivo* (von Caemmerer and Edmondson, 1986).

The affinity of Rubisco's inactive sites, [E], for RuBP, [R], could be altered either by an increase in the rate at which RuBP is released or a decrease in the rate at which RuBP is bound (Figure 5.10). Past studies indicate that activase is able to increase the rate at which RuBP bound to Rubisco's inactive sites is released (Portis, 1990). It is also possible that activase influences the rate at which RuBP binds to Rubisco's inactive sites, but it is very difficult to measure this rate. If activase only affects the affinity of the sites by increasing the rate at which RuBP is released, then it follows that RuBP could immediately re-bind and again block carbamylation. However, recent *in vitro* studies indicate that RuBP binds very slowly to the inactive site of Rubisco (Wang and Portis, 1992). Therefore, an increase in the rate of release from [ER] is all that would be necessary to promote a dynamic equilibrium in favour of carbamylation. Ultimately, all that is necessary is that activase can bind to [ER] and release [R] faster than [R] binds to [E]. If activase alters the dynamic equilibrium simply by removing RuBP from Rubisco's inactive sites, then it must bind to Rubisco and release RuBP quickly. Since, one tetramer of activase is sufficient to maintain 200 octamers of Rubisco at wild-type levels of Rubisco carbamylation (Figure 5.2), this means that this tetramer of activase would have to interact with 200 octamers of Rubisco in less time then it takes [R] to bind tightly to [E].

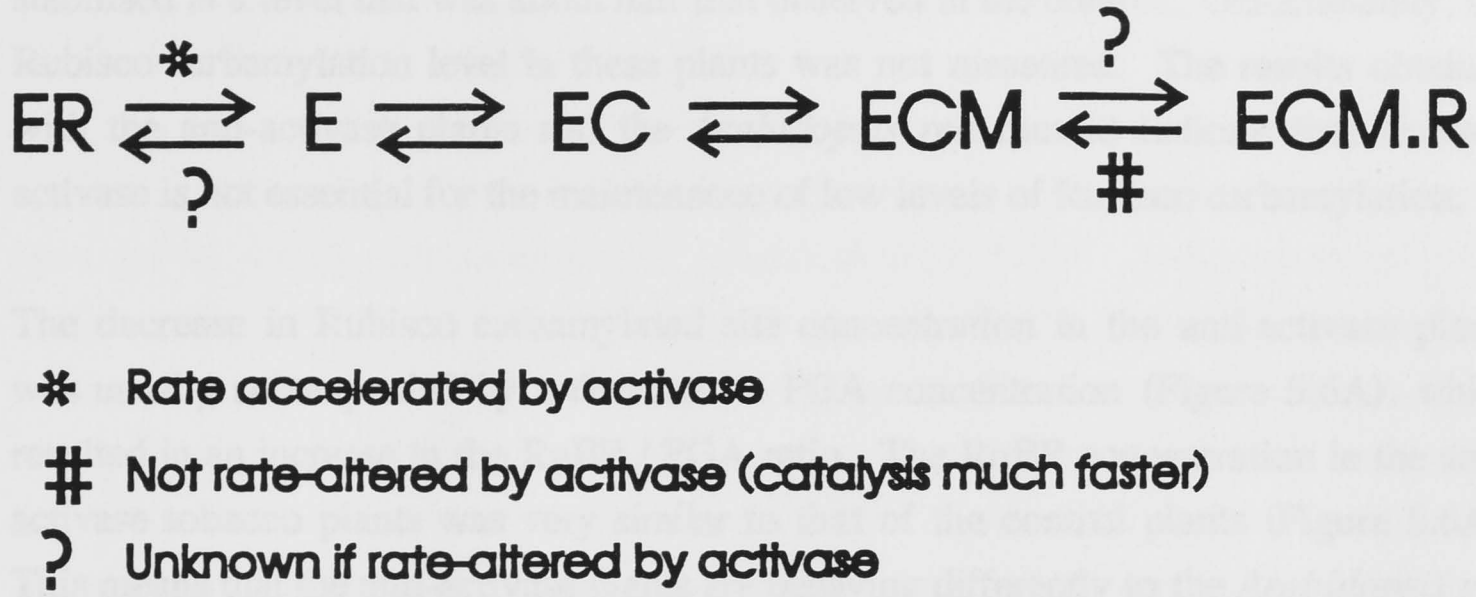

FIGURE 5.10: Possible effect of activase on Rubisco carbamylation equilibrium

5.4.2 Activase-deficiency impairs photosynthesis and reduces carbamylation

The reduction of Rubisco activase content to less than 8% of wild-type affected assimilation rate due to a decline in Rubisco carbamylated site concentration (Figure 5.2). Those anti-activase plants with less than 5% of wild-type activase content had a range of Rubisco carbamylation levels. This range probably correlates with a range in activase content, between 0 - 5 % of wild-type concentration. This is a tentative conclusion because we do not know the exact activase concentration in those anti-activase plants which contained less than 0.5 mg m^{-2}, since this was the detection limit of the activase assay.

There was a strong relationship between Rubisco carbamylation level and assimilation rate in the anti-activase plants (Figure 5.3). However, Rubisco carbamylation level did not drop below 25% of total sites even in the worst-affected anti-activase plants measured. The relationship between Rubisco carbamylation level and assimilation rate was linear and the regression line intercepted the x-axis at approximately 20% Rubisco carbamylation (Figure 5.3). This result indicates that Rubisco carbamylation would not drop below 20%, even in the plants with no activase. This result is consistent with the data obtained from the *Arabidopsis rca* mutant, which was completely deficient in activase. A time-course of initial activity of Rubisco in intact leaves was generated from control and mutant *Arabidopsis* plants after the onset of illumination (Somerville et al., 1982). This time-course showed that the initial activity of Rubisco in the mutant

stabilised at a level that was about half that observed in the control. Unfortunately, the Rubisco carbamylation level in these plants was not measured. The results obtained with the anti-activase plants and the *Arabidopsis rca* mutant indicate that Rubisco activase is not essential for the maintenance of low levels of Rubisco carbamylation.

The decrease in Rubisco carbamylated site concentration in the anti-activase plants was usually accompanied by a decrease in PGA concentration (Figure 5.6A), which resulted in an increase in the RuBP / PGA ratio. The RuBP concentration in the anti-activase tobacco plants was very similar to that of the control plants (Figure 5.6A). This means that the anti-activase plants are behaving differently to the *Arabidopsis rca* mutant, which accumulated four to eight-times the RuBP concentration of wild-type *Arabidopsis* plants (Somerville et al., 1982; Salvucci et al., 1986). The accumulation of high concentrations of RuBP in the leaves of the Arabidopsis *rca* mutant might have indicated that the inability to modulate Rubisco carbamylation, due to activase-deficiency, leads to disruptions in the RuBP / PGA ratio. This result is consistent with Mott et al.'s (1984) theory that changes in Rubisco carbamylation may occur in order to match the rate of RuBP consumption with the capacity for RuBP regeneration, thereby maintaining a stable RuBP / PGA ratio (Chapter 1, Section 1.4.2). However, our results with the anti-activase plants indicate that changes in Rubisco carbamylation level are not essential for the maintenance of stable RuBP pools. The RuBP concentrations in the anti-activase and control leaves were similar, despite a lower Rubisco carbamylation level (ie. a lower capacity for RuBP consumption) in the anti-activase leaves.

One of our aims in this study was to see how activase-deficiency affected the photosynthetic response to light and CO_2 concentration. We carried out gas exchange analysis on two transgenic plants with non-detectable levels of activase and Rubisco carbamylation levels of 40%. We observed that the photosynthetic rates of the activase-deficient plants were always limited by Rubisco activity, even at very low light intensities (Figure 5.8B). Earlier results indicated that the low assimilation rate of these plants at high light was due to a reduction in Rubisco carbamylation level and Rubisco content (Figure 5.2). It is likely that these factors also limit assimilation rate at low light. In future experiments, it may be interesting to analyse anti-activase plants with higher activase concentrations. These plants may be limited by Rubisco carbamylation level at high light, but not at low light. Future analysis of these plants may provide insight into the factors regulating Rubisco carbamylation level in response to changes in light intensity.

5.4.3 Photosynthetic rate is proportional to Rubisco carbamylated site concentration in air - grown plants

The Rubisco carbamylation levels of all control and anti-activase plants were assayed from leaves which were sampled at saturating light (1500 μmol quanta $m^{-2}s^{-1}$). Under these conditions, the plants with non-detectable activase had Rubisco carbamylation levels of about 40%, which was about half that observed in the controls. At the developmental stage these measurements were taken, the anti-activase plants had a lower Rubisco content than the controls (Figure 5.2C). The reduction in carbamylation level and Rubisco content in these plants correlated with low photosynthetic rates, which were less than 25% of those observed in the controls (Figure 5.2A). Estimates of Rubisco carbamylated site concentration in each plant were used this to calculate their expected assimilation rate (Figure 5.4B). The expected assimilation rates of both the control and anti-activase plants were generally higher than the observed rates. Dark respiration (R_d) was not measured in these plants. Therefore, this parameter was not included in the equation used to calculate the expected assimilation rate (Figure legend 5.4). This probably accounts for the expected assimilation rate being slightly higher than the observed rates. It is interesting to note that the regression line describing the relationship between observed and expected photosynthetic rate in the control and anti-activase leaves did not pass through the origin (dashed line, Figure 5.4B), whereas the regression line for control and anti-SSU plants did (dotted line, Figure 5.4B). This may indicate a greater disparity between observed and expected assimilation rate in the anti-activase plants than in control and anti-SSU plants, but this is difficult to resolve. A small difference in observed and expected assimilation rate, such as this, could not be detected reliably without taking into consideration dark respiration and the CO_2 transfer conductance (from the intercellular space to inside the chloroplast) in the equation used for calculating expected assimilation rate (see figure legend 5.4). A greater disparity between the observed and expected photosynthetic rates of the anti-activase plants was apparent in the data in Chapter 2. However, the observed and expected photosynthetic rates were not assayed simultaneously. Therefore, environmental or developmental changes could have contributed to the large difference in observed and expected photosynthetic rate in these plants.

5.4.4 Conclusions

Activase is present in control leaves at a much greater concentration than is required to maintain maximal levels of Rubisco carbamylation under steady-state conditions. Our studies have shown that a twenty-fold decrease in activase content is required before a reduction in Rubisco carbamylation occurs. It is not known why the wild-type plants contain such high concentrations of activase. Their high levels of activase may be beneficial under non-steady-state conditions. Future experiments with the anti-activase plants will be able to investigate this possibility.

CHAPTER 6: The effect of activase deficiency on photosynthesis in tobacco grown in a CO_2-enriched atmosphere

6.1 INTRODUCTION

The initial analysis of the anti-activase plants was carried out at high CO_2, to ensure survival of all anti-activase primary transformants and R_1 progeny of plant #52 (Chapters 2 and 3). However, analysis of high-CO_2-grown plants is complicated by the physiological repercussions of high CO_2, namely high starch content, rapid growth and senescence. Therefore, in Chapter 5, the anti-activase plants were grown and analysed in air. The lower rate of plant growth enabled an extensive analysis of the anti-activase plants to be carried out. However, not all of the anti-activase progeny survived when grown in air. The data reported in the subsequent two chapters were obtained by analysing high-CO_2-grown plants. Therefore, all the R_1 progeny of plant #52, even those unable to grow in air with activase levels presumably below the detection limit of the quantitative immunoblot assay, are represented in the data.

In this chapter, I will compare the analyses of high CO_2 (0.3%) and air (0.03% CO_2) grown plants. The differences in Rubisco carbamylation level, Rubisco content and RuBP / PGA pool size in plants grown in air and high CO_2, and also the disparity in observed and expected photosynthetic rate in the anti-activase plants will be discussed. The R_1 progeny of an anti-SSU primary transformant (S7) have been included in these analyses as an additional control. The anti-SSU plants have reduced Rubisco content due to the insertion of an antisense gene directed against the Rubisco small subunit (Hudson et al., 1992b). The segregating anti-activase and anti-SSU R_1 populations will be compared and contrasted in this chapter.

6.2 MATERIALS & METHODS

6.2.1 Plant material and growth conditions

The plant material was the R_1 progeny of *Nicotiana tabacum* transformed with either pαTACT (anti-activase), pαSSU (anti-small subunit of Rubisco) or pBI121 (control). The anti-activase and anti-SSU seed was obtained from primary transformants #52 (2 T-DNA inserts) and S7 (1 T-DNA insert), respectively. The anti-activase plants were produced as described in Chapter 2, and the anti-SSU plants were produced by Hudson et al. (1992b). The R_1 seedlings were germinated and raised in a growth cabinet with a 12-h photoperiod at 25°C (day) and 17°C (night), 0.3% CO_2 and an

irradiance of 600 μmol quanta $m^{-2}s^{-1}$. Seedlings were transferred into tubes (diameter 7.5 cm, height 15 cm), containing sterilized garden soil approximately 18 days after germination. Ten days later, they were transferred to 5-L pots. A complete nutrient solution containing 12mM nitrate was applied three times a week to all seedlings throughout development (Hewitt and Smith, 1975).

6.2.2 Sampling procedures

The chlorophyll fluorescence of the uppermost, fully expanded leaves of all plants was measured 24 days after germination. Guided by these measurements, a subset of plants were selected for determination of Rubisco content and carbamylation, soluble protein content and RuBP and PGA pool sizes. The uppermost, expanded leaves of all these plants were sampled under the growth conditions, except that the CO_2 concentration was lowered to 0.03%, 28 days after germination. The CO_2 concentration was raised again to 0.3% immediately after sampling . Leaf punches (0.5 cm^2) for determining activase concentration were collected after 1-2 h of illumination and a 1.8 cm^2 leaf disc were taken after 3-5 h in the light for determination of Rubisco carbamylation, and Rubisco and soluble protein content. Immediately after the Rubisco carbamylation leaf punch was taken, a hand-held freeze-clamp device was used to obtain a 6.16 cm^2 leaf disc from each plant for determination of RuBP and PGA pool sizes.

6.2.3 Measurements of CO_2 assimilation rate

Gas exchange measurements were made 30 - 33 days after germination. Plants were taken from the growth cabinets and placed in the gas exchange system with 350 μbar CO_2 and 1000 μmol quanta m^{-2} s^{-1}, the leaf temperature was 25°C and the vapour pressure difference was 10 mbar. The measurements were made in an open gas-exchange system, as described by Brugnoli et al. (1988) with modifications as outlined by Hudson et al. (1992b).

Chl fluorescence was measured under the growth conditions, except that the CO_2 concentration was lowered to atmospheric at least 12 h before measurements were taken. The CO_2 concentration was lowered so that the range of photosynthetic rates in the anti-activase plants would be amplified. Chl fluorescence was measured using a fluorimeter (Pam 101; Waltz, Effeltrich, Germany). Measurements were taken 24 and

34 days after germination. The ϕPSII was calculated according to the method of Genty et al. (1989).

6.2.4 Activase content

The immunoblot blot procedure was identical to the method described in Chapter 5, except that the leaf discs (1.5 cm^2) were extracted in 1.5 mL.

6.2.5 Biochemical assays

Rubisco content, carbamylation and soluble protein were assayed using the methods described in Chapter 2 with modifications described in Chapter 5.

RuBP and PGA were measured using the method described in Chapter 5 except that the leaf discs (6.16 cm^2) were extracted in 500 μL.

6.3 RESULTS

6.3.1 Phenotype of the R_1 antisense plants

The anti-activase and anti-SSU R_1 plants were screened using the chlorophyll fluorescence parameter, ϕPSII. ϕPSII measures the quantum efficiency of PSII. Under constant irradiance and, CO_2 and O_2 concentrations, ϕPSII will provide a quick and convenient measure of relative photosynthetic rate within a group of plants. The control plants had ϕPSII measurements within the 0.6 - 0.65 range (data not shown). Approximately 50% of the anti-activase plants were in the 0.5 - 0.7 range and the remainder of the progeny were distributed fairly evenly between 0 - 0.5 (Figure 6.1A). The distribution in ϕPSII in the anti-SSU progeny correlated with the expected segregation for progeny of a single insert primary transformant. We expected 25% of the progeny to be wild-type segregants (0.6 - 0.7), 50% to be hemizygous (1 T-DNA) (0.4 - 0.6) and 25% to be homozygous (2 T-DNAs) (0.2 - 0.4) (Figure 6.1B). The anti-SSU R_1 progeny grown at high CO_2 had the same range and distribution of ϕPSII (Figure 6.1B) as had been observed when the same R_1 progeny were grown in air (John Evans - personal communication). However, there was a difference in the range and distribution of ϕPSII and assimilation rate in the anti-activase R_1 progeny grown at high CO_2 (Figure 6.1A) and air (Figure 5.1), respectively. The self-fertilising parent of the anti-activase R_1 progeny contained two T-DNA inserts. Therefore we expect 6.25% of the progeny to be wild-type revertants, and 25% to be hemizygous single-insert plants. We tentatively identified the R_1 progeny with the highest ϕPSIIs as wild-type revertants (6.5% of total population, Figure 6.1A), and the plants with the next highest ϕPSIIs as single-insert hemizygous plants (26% of total population, Figure 6.1A). The putative single-insert plants grown at high CO_2 all had high ϕPSII ratios similar to the controls (Figure 6.1A). However, the putative single-insert plants grown in air had a variety of assimilation rates, ranging from 3 -9 μmol CO_2 $m^{-2}s^{-1}$ (Figure 5.1, average assimilation rate in air-grown controls was 10 μmol CO_2 $m^{-2}s^{-1}$).

The control, anti-activase and anti-SSU plants appeared to grow at similar rates (stem elongation commenced in all plants over a 3-4 day period). The healthiest anti-activase and anti-SSU plants were the same size as the control plants. There was some variation in plant size within both the anti-activase and anti-SSU populations. However, discrete size groups were not apparent. Some of the anti-activase progeny with very low ϕPSII ratios developed veinal chlorosis approximately 24 days after germination. The older leaves of these plants wilted badly after short exposures (30 min) to atmospheric CO_2.

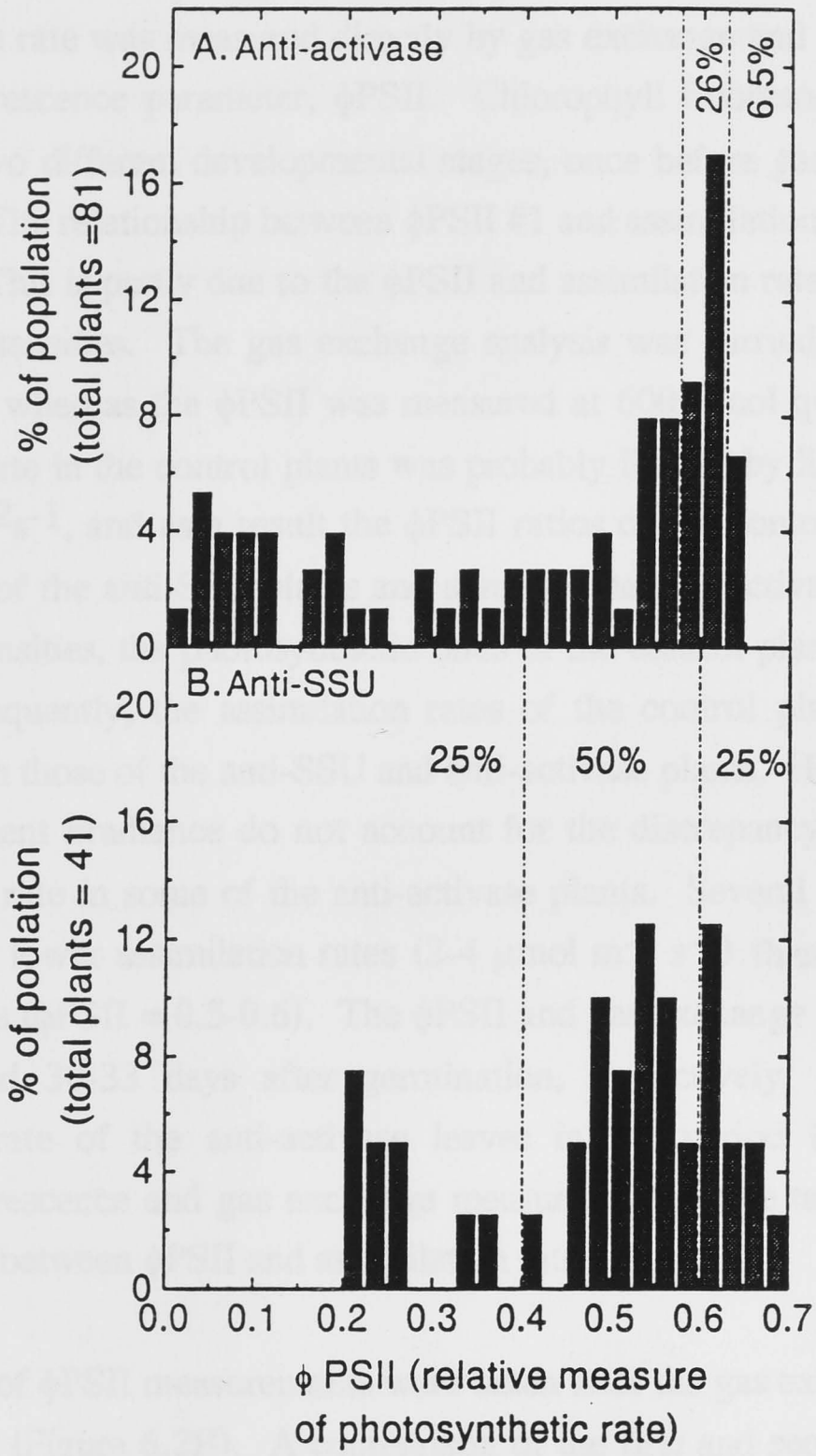

FIGURE 6.1: Variation in ϕPSII in anti-activase and anti-SSU R_1 progeny. Anti-activase and anti-SSU plants were both grown at high CO_2 (0.3%). A relative measure of photosynthetic rate was obtained by calculating the chlorophyll fluorescence parameter, ϕPSII. Chlorophyll fluorescence measurements were taken on the adaxial surface and ϕPSII was calculated according to the method of Genty et al. (1989). The light intensity was 600 μmol quanta $m^{-2}s^{-1}$ and the CO_2 concentration was 0.03%. The ϕ PSII of the control plants ranged from 0.6 - 0.65. **A. The anti-activase plants** are the self-progeny of pαTACT transformant 52. Inverse PCR has shown that transformant 52 contained two T-DNA inserts. Therefore, we expect approximately 6.25% of the progeny to be revertants, and approximately 25% of the progeny to be single-insert hemizygous plants. **B. Anti-SSU plants** are the self-progeny of pαSSU transformant S7. S7 contains one T-DNA insert. Therefore, we expect approximately 25% of the progeny to be revertants, 50% to be hemizygous plants, and 25% to be homozygous plants.

6.3.2 Measurements of CO_2 assimilation rate

CO_2 assimilation rate was measured directly by gas exchange and indirectly using the chlorophyll fluorescence parameter, ϕPSII. Chlorophyll fluorescence measurements were taken at two different developmental stages, once before gas exchange analysis and once after. The relationship between ϕPSII #1 and assimilation rate was not linear (Figure 6.2A). This is partly due to the ϕPSII and assimilation rate being measured at different light intensities. The gas exchange analysis was carried out at 1000 μmol quanta m^{-2} s^{-1}, whereas the ϕPSII was measured at 600 μmol quanta $m^{-2}s^{-1}$. The photosynthetic rate in the control plants was probably limited by light intensity at 600 μmol quanta $m^{-2}s^{-1}$, and as a result the ϕPSII ratios of the control plants were very similar to those of the anti-SSU plants and some of the anti-activase plants; whereas, at high light intensities, the photosynthetic rates of the control plants were not limited by light. Consequently, the assimilation rates of the control plants were generally much higher then those of the anti-SSU and anti-activase plants. However, differences in the measurement irradiance do not account for the discrepancy between ϕPSII #1 and assimilation rate in some of the anti-activase plants. Several of the anti-activase plants had much lower assimilation rates (2-4 μmol m^{-2} s^{-1}) than expected based on their ϕPSII ratios (ϕPSII = 0.5-0.6). The ϕPSII and gas exchange measurements were taken at 24 and 30-33 days after germination, respectively. A decline in the photosynthetic rate of the anti-activase leaves in the period between which the chlorophyll fluorescence and gas exchange measurements were taken would account for the disparity between ϕPSII and assimilation rate.

A second series of ϕPSII measurements were taken after the gas exchange analysis had been carried out (Figure 6.2B). A comparison of the first and second series of ϕPSII measurements indicates a decline in ϕPSII in the anti-activase plants over development (Figures 6.2A and 6.2B). This result may reflect a developmental decline in photosynthetic rate, which would account for the disparity between ϕPSII #1 and assimilation rate in Figure 6.2A. The ϕPSII #2 generally indicated that the photosynthetic rates of the anti-activase plants were slightly higher than were measured in gas exchange (Figure 6.2B). This discrepancy between ϕPSII #2 and assimilation rate was large in two (out of nine) of the anti-activase plants. These two plants had ϕPSII ratios of 0.5 and assimilation rates of 4 μmol CO_2 $m^{-2}s^{-1}$. The slight disparity between assimilation rate and ϕPSII #2 in most of the anti-activase plants may be a product of how gas exchange and chlorophyll fluorescence were

measured. For instance, the leaves measured in gas exchange may have been slightly older than the leaves measured for chlorophyll fluorescence.

Thirty four days after germination and thereafter, none of the control, anti-SSU or anti-activase plants would open their stomates in gas exchange. This prevented further attempts at measuring CO_2 assimilation rate.

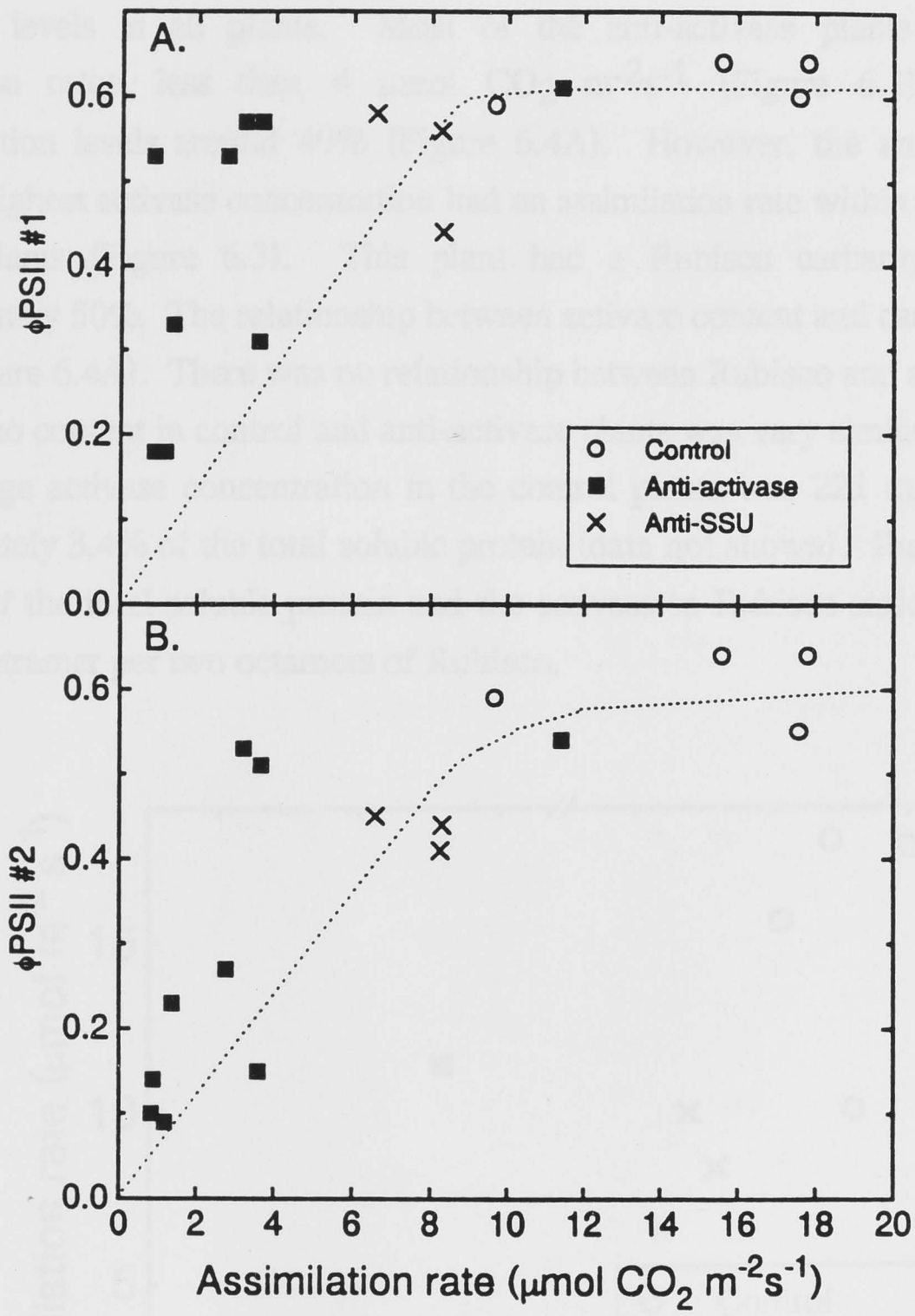

FIGURE 6.2: A comparison of photosynthetic rate measurements obtained using different methods. Chl fluorescence was measured at 0.03% CO_2 and 600 μmol quanta $m^{-2}s^{-1}$. ϕPSII was calculated according to the method of Genty et al.(1989). ϕPSII #1 (Figure 6.2A) was measured 24 days after germination, and ϕPSII #2 (Figure 6.2B) was measured 34 days after germination. The gas exchange measurements were made 30-33 days after germination at an irradiance of 1000 μmol quanta $m^{-2}s^{-1}$, the leaf temperature was 25°C, the leaf to air vapour pressure difference was 11 mbar, and the CO_2 partial pressure was 350 μbar. Both gas exchange and chlorophyll fluorescence were measured on the youngest, fully expanded leaves.

6.3.3 Relationship between activase content and assimilation rate, Rubisco carbamylation level and Rubisco content

On the basis of the ϕPSII measurements (Figure 6.1) a subset of anti-activase plants, covering a 0.2 - 0.6 range in ϕPSII, were assayed for activase and Rubisco content and carbamylation. The activase content in the anti-activase plants was below 20% of wild-type levels in all plants. Most of the anti-activase plants had very low assimilation rates, less than 4 μmol CO_2 $m^{-2}s^{-1}$ (Figure 6.3), and Rubisco carbamylation levels around 40% (Figure 6.4A). However, the anti-activase plant with the highest activase concentration had an assimilation rate within the range of the control plants (Figure 6.3). This plant had a Rubisco carbamylation level of approximately 50%. The relationship between activase content and carbamylation was weak (Figure 6.4A). There was no relationship between Rubisco and activase content; the Rubisco content in control and anti-activase plants was very similar (Figure 6.4B). The average activase concentration in the control plants was 221 mg m^{-2}; this was approximately 3.4% of the total soluble protein (data not shown). Rubisco accounted for 26% of the total soluble protein and the activase to Rubisco stoichiometry was 1 activase tetramer per two octamers of Rubisco.

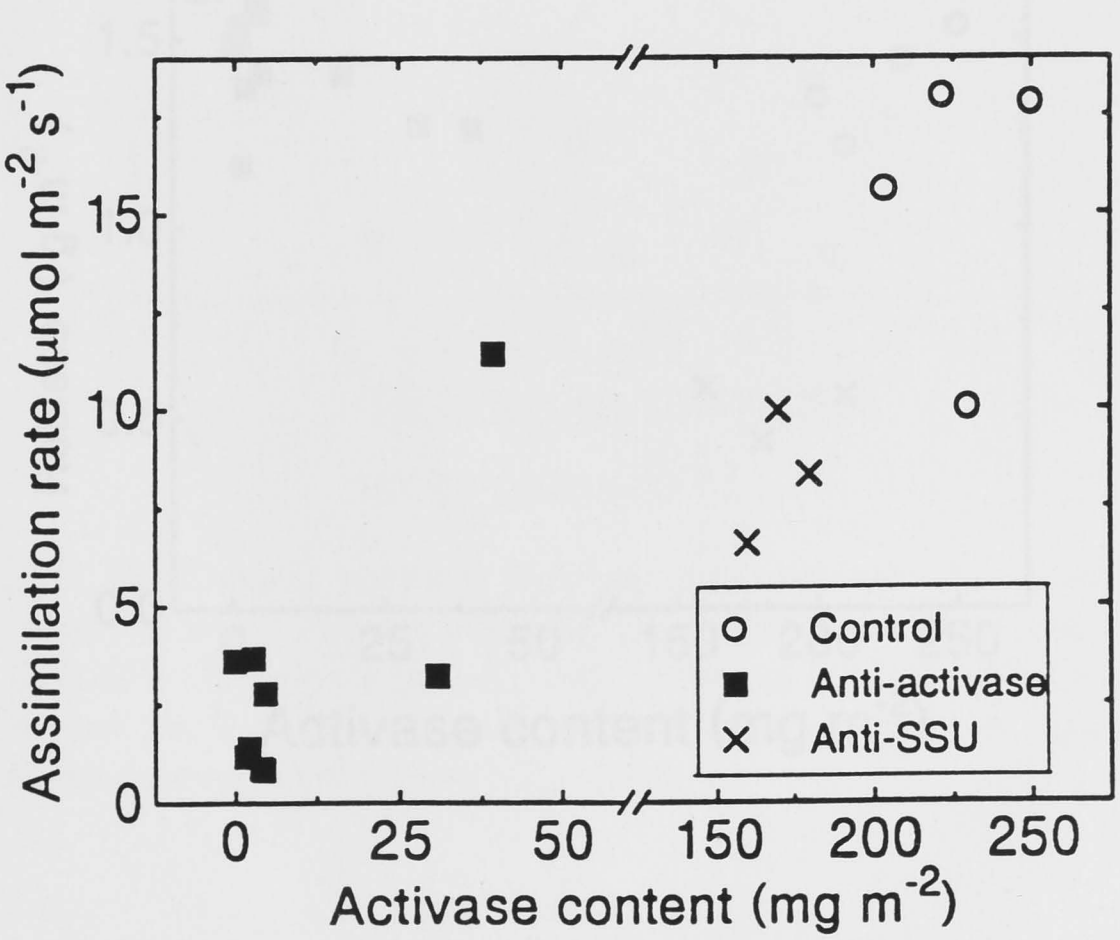

FIGURE 6.3: Relationship between assimilation rate and activase content. Activase content was measured by quantitative ECL immunoblot. Assimilation rate measurements were made 30-33 days after germination as described in Figure legend 6.2.

The anti-SSU plants had approximately the same activase content as the control plants (Figure 6.3). The assimilation rates of the anti-SSU plants were approximately half those of the controls (Figure 6.3). The Rubisco carbamylation level in the anti-SSU plants was similar to the controls (Figure 6.4A), but their Rubisco content was only 33% of wild-type levels (Figure 6.4B).

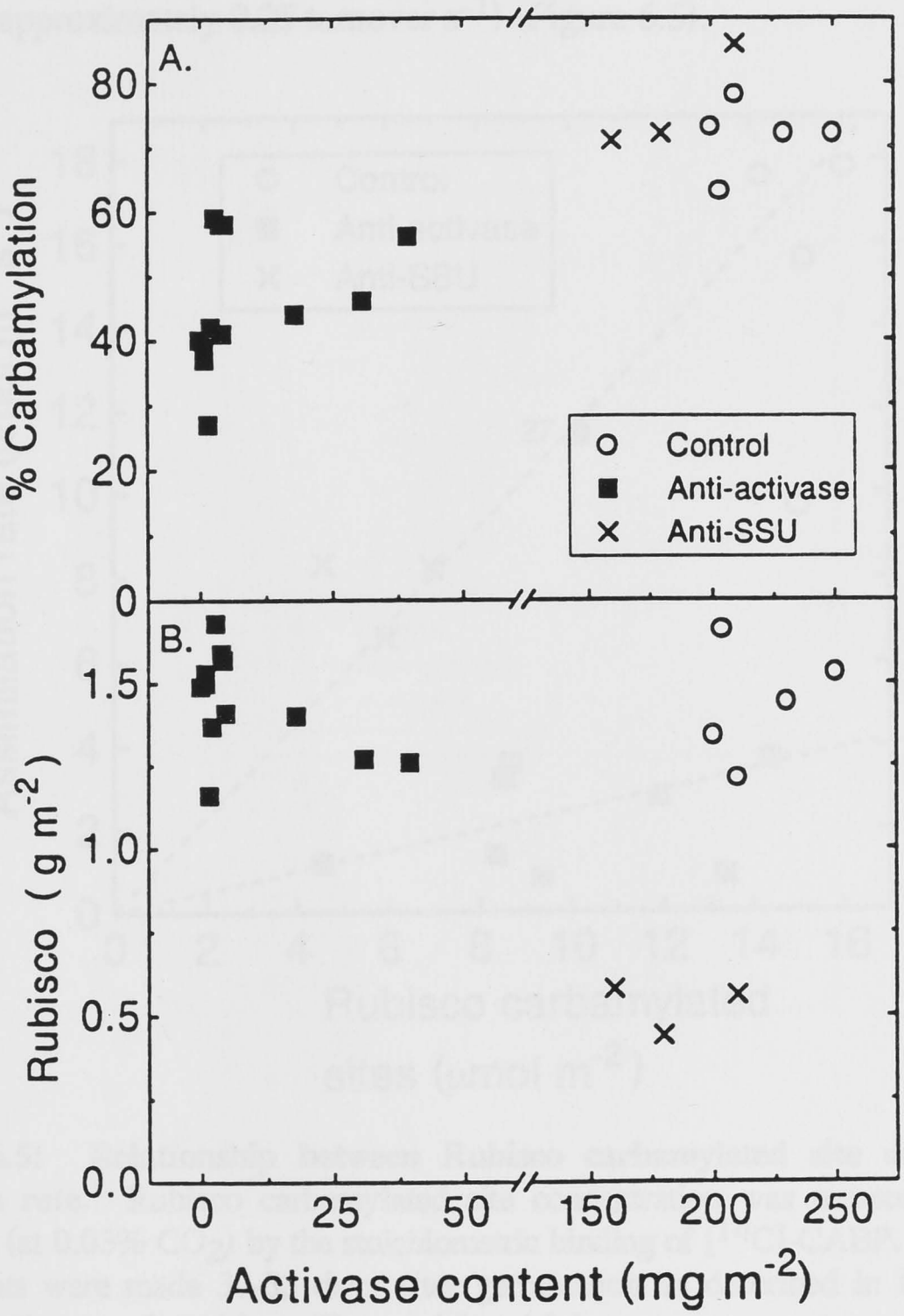

FIGURE 6.4: Relationship between activase content and Rubisco content and carbamylation. Activase content was measured by quantitative ECL immunoblot. Rubisco carbamylation and content were measured 28 days after germination (at 0.03% CO_2) by the stoichiometric binding of [^{14}C]-CABP.

6.3.4 Rubisco carbamylated sites

The relationship between assimilation rate and Rubisco carbamylated site concentration was linear for control and anti-SSU plants (Figure 6.5). However, only one of the anti-activase plants (#27) had the same assimilation rate / Rubisco carbamylated site ratio as the control and anti-SSU plants (averaging approximately 1.1 turnover s^{-1}). All the other anti-activase plants had much lower assimilation rates then expected based on their range of Rubisco carbamylated site concentrations (averaging approximately 0.25 turnover s^{-1}) (Figure 6.5).

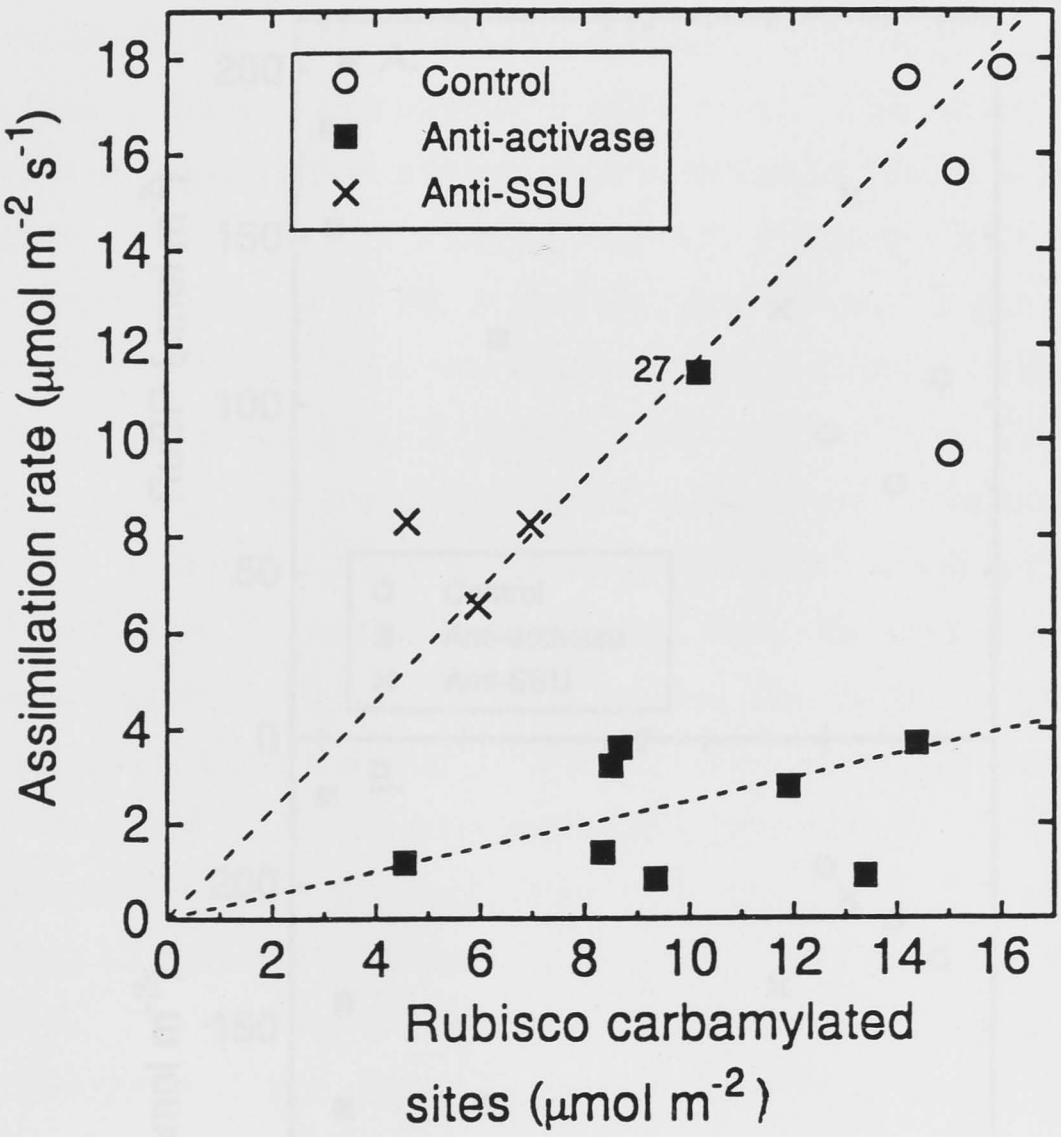

FIGURE 6.5: Relationship between Rubisco carbamylated site concentration and assimilation rate. Rubisco carbamylated site concentration was measured 28 days after germination (at 0.03% CO_2) by the stoichiometric binding of [^{14}C]-CABP. The gas exchange measurements were made 30-33 days after germination as described in Figure legend 6.2. This data has been replotted from Figures 6.3 and 6.4.

6.3.5 RuBP / PGA

The anti-activase and anti-SSU plants had higher RuBP concentrations than the control plants (Figure 6.6A). However, the anti-activase plant with the highest activase concentration had an RuBP concentration that was similar to the control plants. The anti-activase plants often had a lower PGA concentration then the control plants, but the PGA concentration in the anti-SSU plants was similar to the controls (Figure 6.6B). The average RuBP / PGA ratio in the controls was 0.46, in the anti-SSU plants it was 0.80 and in the anti-activase plants it was approximately 1.13.

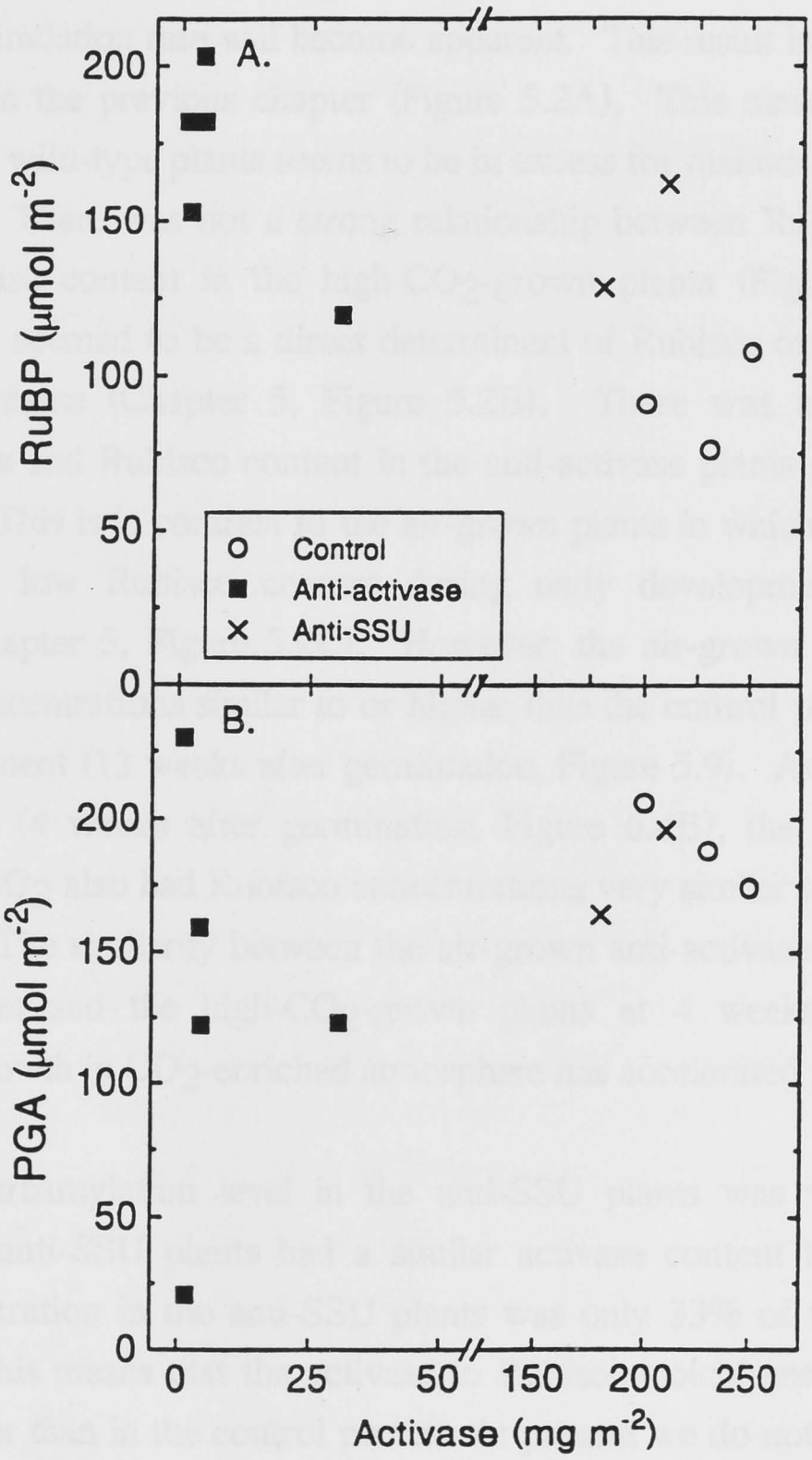

FIGURE 6.6: A comparison of RuBP and PGA concentration in control, anti-activase and anti-SSU plants. Activase content was measured by quantitative ECL immunoblot. RuBP and PGA were assayed from leaves which were sampled at 0.03% CO_2, 28 days after germination, using an enzyme-linked spectrophotometric assay.

6.4 DISCUSSION

6.4.1 Effect of activase concentration on ϕPSII, Rubisco carbamylation and Rubisco content

Almost all of the anti-activase plants had very low activase concentrations (0 - 12.5 mg m^{-2}) and low assimilation rates compared to the controls (Figure 6.3). One of the anti-activase plants had an 80% reduction in activase content compared to the control plants, and this caused only a 30% reduction in assimilation rate relative to controls. This result seems to indicate that large reductions in activase content can occur before an effect on assimilation rate will become apparent. This result is consistent with the low-CO_2 data in the previous chapter (Figure 5.2A). This means that the activase concentration in wild-type plants seems to be in excess for maintenance of steady-state photosynthesis. There was not a strong relationship between Rubisco carbamylation level and activase content in the high-CO_2-grown plants (Figure 6.4A), whereas activase content seemed to be a direct determinant of Rubisco carbamylation level in the air-grown plants (Chapter 5, Figure 5.2B). There was also no relationship between activase and Rubisco content in the anti-activase plants grown at high CO_2 (Figure 6.4B). This is in contrast to the air-grown plants in which low activase levels correlated with low Rubisco content during early development (9 weeks after germination, Chapter 5, Figure 5.2C). However, the air-grown anti-activase plants had Rubisco concentrations similar to or higher than the control plants when sampled later in development (13 weeks after germination, Figure 5.9). At the time they were initially assayed (4 weeks after germination, Figure 6.4B), the anti-activase plants grown at high CO_2 also had Rubisco concentrations very similar to the control plants (Figure 6.4B). The similarity between the air-grown anti-activase plants at 13 weeks after germination and the high-CO_2-grown plants at 4 weeks after germination indicates that growth in CO_2-enriched atmosphere has accelerated plant development.

The Rubisco carbamylation level in the anti-SSU plants was very similar to the controls. The anti-SSU plants had a similar activase content to controls but the Rubisco concentration in the anti-SSU plants was only 33% of that in the controls (Figure 6.4). This means that the activase to Rubisco stoichiometry in the anti-SSU plants was higher than in the control plants. At present we do not know what factors are involved in the light-regulation of Rubisco carbamylation (Chapter 1, Section 1.10). It is possible that activase activity may change in response to light, and that activase activity determines the Rubisco carbamylated site concentration. If this was

the case, we might expect the high activase to Rubisco stoichiometry in the anti-SSU plants to result in all of their Rubisco sites being carbamylated at relatively low light intensities. For instance, the activase activity required to carbamylate 30% of the Rubisco sites in the wild-type plants may be sufficient to carbamylate all of the Rubisco sites in anti-SSU plants (since their Rubisco site concentration is only 33% of wild-type). However, there was no evidence of this at the intermediate light intensity of 600 μmol quanta $m^{-2}s^{-1}$ (Figure 6.4A). The Rubisco carbamylation level in the control plants was approximately 70%. This is quite high, and it is similar to the Rubisco carbamylation levels of control plants sampled at saturating light intensties (1500 μmol quanta $m^{-2}s^{-1}$; Chapter 5, Figure 5.2B). Therefore, the Rubisco carbamylation levels in the high-CO_2-grown anti-SSU and control plants may have been approaching their high light maximum. In future experiments it may be interesting to assay the Rubisco carbamylation level of the anti-SSU and control plants at a lower light intensity (<600 μmol quanta $m^{-2}s^{-1}$). Under these conditions, the Rubisco carbamylation level in the control plants might be lower, thereby making an elevated Rubisco carbamylation level in the anti-SSU plants easier to detect.

6.4.2 Difference in activase content of controls grown in air and CO_2-enriched atmosphere

Interestingly, the high-CO_2-grown (0.3% CO_2) control plants accumulated higher concentrations of activase than did the air-grown (0.03% CO_2) control plants (Figures 6.3 and 5.2 respectively). The control plants grown in air had similar soluble protein and Rubisco content to the high-CO_2-grown control plants, and Rubisco accounted for approximately 31% of total soluble protein in the air-grown plants compared to 27% of total soluble protein in the high-CO_2-grown plants. Therefore, the lower activase content in the air-grown plants was not due to an overall decrease in protein concentration. It is interesting to speculate why these different groups of plants have accumulated different concentrations of activase. On first glance this data seems to indicate a greater requirement for activase at high CO_2 concentrations, but other differences in growth conditions need to be taken into account. The high-CO_2 plants were raised in growth cabinets, with a 12 h photoperiod, at an irradiance of 600 μmol quanta m^{-2} s^{-1}, whereas the low-CO_2 plants were raised in a glasshouse during the winter, with a typical midday irradiance of 600 μmol quanta m^{-2} s^{-1}. Therefore, the air-grown plants had much less total daily irradiance than did the high-CO_2-grown plants. Perhaps high concentrations of activase are advantageous at high light, in

facilitating quick increases in Rubisco carbamylation level in response to dark to high light conversions. Alternatively, high concentrations of activase may be beneficial at high CO_2. Perhaps large concentrations of an inhibitor to Rubisco accumulate at high CO_2, thereby necessitating higher concentrations of activase. *In vitro* studies indicate that activase may have an important role in removing inhibitory sugar phosphates from Rubisco's catalytic sites (Chapter 1, Section 1.6.1). Previous studies have shown that high CO_2 concentrations supress the Rubisco side-reaction that produces the fallover inhibitor, XuBP (Edmondson et al., 1990a). Therefore, XuBP would not accumulate at high CO_2. It is possible that other inhibitors, produced by another of Rubisco's side-reactions (Morell et al., in press), or by the effect of high CO_2 on stromal pH (John Andrews - personal communication), could accumulate at high CO_2, but this is purely speculation.

6.4.3 RuBP / PGA pool sizes

The high-CO_2-grown anti-activase plants had an elevated RuBP / PGA ratio compared to the controls, this was due to a simultaneous increase and decrease in RuBP and and PGA concentration, respectively (0.03% CO_2, Figure 6.6). The increase in the RuBP / PGA ratio in the air-grown anti-activase plants was entirely due to depletion of the PGA pool relative to controls (Chapter 5, Figure 5.6). The changes in both RuBP and PGA pool size in the high-CO_2-grown anti-activase plants may have been larger then in the air-grown anti-activase plants because plants with multiple T-DNA inserts were included in the analysis. Many anti-activase plants do not survive when grown in air (Chapter 5, Figure 5.1). Consequently, the analysis of air-grown anti-activase plants is probably restricted to those progeny with the highest activase content, and the least changes in RuBP / PGA pool size. The accumulation of high concentrations of RuBP, and depletion of the PGA pool in the anti-activase plants grown at high CO_2 is consistent with a Rubisco-limitation of photosynthesis. The elevated RuBP pool in the anti-SSU plants indicates that photosynthetic rate in these plants was also probably Rubisco-limited.

6.4.4 Observed photosynthetic rate of anti-activase plants was less than expected

All the anti-activase plants, except for one (#27), had much lower assimilation rates than expected based on their Rubisco carbamylated site concentrations (Figure 6.5). This disparity between observed and expected photosynthetic rate in the anti-activase plants has been observed previously at high CO_2 (Chapter 2). However, analysis of the anti-activase plants grown in air indicated that this disparity between observed and expected photosynthetic rate was minor (Chapter 5). Explanations for the disparity between observed and expected photosynthetic rate in the anti-activase plants have been discussed previously (Chapter 2). One of the possible explanations was the accumulation of an inhibitor at Rubisco's catalytic sites in the absence of activase. The Rubisco carboxylase reaction is subject to several abortive side-reactions. Some of these reactions result in the formation of compounds which bind to Rubisco's catalytic site and inhibit catalysis (Chapter 1, Section 1.4.4.3). *In vitro* experiments indicate that activase may have an important role in facilitating the release of these sugar phosphates (Chapter 1, Section 1.6.1). Therefore, it is possible that these compounds may accumulate at Rubisco's catalytic site when activase concentrations are low. However, if this is the cause for the disparity between observed and expected photosynthetic rate in the anti-activase plants, why is the disparity so much greater when the plants are grown at high CO_2 than when they are grown in air? In air, only a sub-population of anti-activase plants survive, whereas at high CO_2 the whole population survives. Perhaps the air-grown plants have sufficient activase to prevent the accumulation of high concentrations of this inhibitor, whereas the high-CO_2-grown plants have much lower concentrations of activase and cannot prevent the accumulation of this inhibitor(s).

If a tight-binding inhibitor was responsible for this difference in the photosynthetic rates of the control and anti-activase plants, we would expect to see a reduction in the k_{cat} of Rubisco in the anti-activase plants. Earlier experiments showed that the k_{cat} of Rubisco in control and anti-activase plants were very similar in the light (Chapter 3). Therefore, if an inhibitor is responsible, it must be loosely enough bound to be lost from Rubisco's catalytic sites during extraction and incubation with saturating CO_2 and Mg^{2+} concentrations *in vitro*. In the absence of inhibitors, the initial / total Rubisco activity ratio will approximate the Rubisco carbamylation level; and in the presence of inhibitors that bind to the carbamylated sites, the initial / total Rubisco activity ratio will under-estimate of the Rubisco carbamylation level. In the air-grown

anti-activase plants there was no evidence for an inhibitor remaning bound to Rubisco immediately after extraction. The initial rates measured as soon as possible after extraction were close to those predicted by the carbamylation levels estimated by [^{14}C]CABP binding (Figure 5.5). However, there may be a disparity between the initial / total Rubisco activity ratio and Rubisco carbamylation level in the anti-activase plants grown at elevated CO_2. It will be interesting to investigate this possibility in future experiments.

Another possible explanation for the disparity between observed and expected photosynthetic rate in the anti-activase plants was indirect inhibition of Rubisco by high RuBP concentrations, perhaps as a consequence of high stromal pH. High RuBP / PGA ratios promote stromal alkalinization, and the *Arabidopsis rca* mutant had very high RuBP pools, approximately four to eight-fold higher than the controls (Somerville et al. 1982; Salvucci et al., 1988). This abnormally high RuBP concentration could have considerable effect on the pH balance within the stroma. However, assays of metabolite pool sizes in control and anti-activase plants have shown that the RuBP concentration was not abnormally high in either air-grown or high-CO_2-grown anti-activase leaves (Figure 5.6 and 6.6, respetively). This means there must be some other explanation for the disparity between observed and expected photosynthetic rates in the activase-deficient plants.

6.4.5 Conclusions

All anti-activase progeny survived when grown at high CO_2, and this allowed several interesting observations, such as high RuBP concentrations and the disparity between observed and expected photosynthetic rate in the anti-activase plants. Unfortunately, gas exchange measurements were limited to the first 34 days after germination, due to subsequent closure of stomates. It would be beneficial in future to grow the plants at an intermediate CO_2 concentration, which might still ensure survival of all of the anti-activase progeny, but minimise difficulties with stomatal closure.

CHAPTER 7: Changes in Rubisco carbamylation level, Rubisco content and photosynthetic rate during development of activase-deficient tobacco plants grown in CO_2-enriched atmospheres

7.1 INTRODUCTION

Earlier analyses indicated that the high-CO_2-grown anti-activase plants partition progressively more of their soluble protein into Rubisco as they develop; whereas control plants partition a constant amount of their soluble protein into Rubisco throughout development (Chapter 2). The data presented in this chapter was collected in order to confirm these earlier results and also to examine the effect of plant age on other parameters, such as photosynthetic rate and Rubisco carbamylation level.

A decline in photosynthetic activity is one of the processes that characterise leaf senescence (Makino et al., 1983) and it usually occurs as a result of leaf ontogeny (nodal position on the plant) or high sink activity (Jiang et al., 1993). All the data presented in this chapter were collected by measuring or sampling the youngest, fully expanded leaves. Therefore, leaf senescence should not be a contributing factor to the changes in photosynthetic parameters.

Plant development is much faster when plants are grown at high CO_2 concentrations than it is when they are grown at low CO_2 concentrations. Therefore, developmental changes in Rubisco content become apparent over a much shorter period. An increase in partitioning of protein towards Rubisco has been observed in air-grown anti-activase plants (Chapter 5, Figure 5.9), but the difference between the anti-activase and control plants was not large, and the increase only became evident many weeks after germination. However, not all of the anti-activase plants survived when grown at low CO_2. The increase in Rubisco partitioning may have been subtle because only the anti-activase plants with relatively high activase concentrations were included in the analyses. Growth of the anti-activase plants at high CO_2 enables us to follow developmental changes in photosynthetic parameters in the entire range of progeny. Therefore, relatively subtle effects of activase-deficiency in the plants grown in air may be amplified by growth in CO_2-enriched atmosphere.

7.2 MATERIALS & METHODS

7.2.1 Plant material and growth conditions

Plant material and growth conditions were the same as described in Chapter 6.

7.2.2 Sampling procedures

Young, fully expanded leaves were sampled for determination of Rubisco and soluble protein content every 3-5 days over the period from 24 to 40 days after germination. The leaf punches taken at the second and final sampling (28 and 40 days after germination respectively) were also assayed for Rubisco carbamylation level. All leaf samples were taken 2-5 h after the onset of illumination.

7.2.3 ϕPSII

Chl fluorescence was measured using a fluorimeter (Pam 101; Waltz, Effeltrich, Germany). Measurements were taken at 24, 34 and 40 days after germination, under the growth conditions, except that the CO_2 concentration was lowered to 0.03% during measurement. The ϕPSII was calculated according to the method of Genty et al. (1989). ϕPSII is a measure of the quantum efficiency of PSII, and it reflects the activity of the light reactions of photosynthesis and the consumption of their products.

7.2.4 Biochemical assays

Rubisco content, carbamylation and soluble protein were assayed using the methods reported in Chapter 2, with the modifications described in Chapter 5.

7.2.5 Developmental stages

For the purpose of analysis, the period 24 to 28 days after germination is referred to as early development; the days 29-35 after germination are called intermediate development; and 35+ days after germination are referred to as late development.

7.3 RESULTS

7.3.1 Decline in ϕPSII over development

ϕPSII was used to detect changes in photosynthetic rate in the high-CO_2-grown plants during development (Figure 7.1). ϕPSII instead of assimilation rate was measured throughout development because of the difficulties encountered with gas exchange analysis. None of the high-CO_2-grown control, anti-activase or anti-SSU plants would open their stomates in the gas exchange chamber after the end of the fourth week after germination, ie. 34 days after germination. It is not known why the stomates would not open. ϕPSII was measured in the growth chamber whereas gas exchange was carried out in the laboratory. Perhaps there was a decline in humidity when the plants were transferred from the growth chamber to the laboratory. At this stage of development this may have provided sufficient stimulus for stomatal closure.

A small decrease in ϕPSII (25%) was observed in controls, anti-SSU and a sub-group of anti-activase plants (# 2, 27, 81 and 112) between early and late development (Figures 7.1A and 7.1B respectively). However, a much larger decrease in ϕPSII (80%) was observed in most of the anti-activase plants (Figure 7.1B).

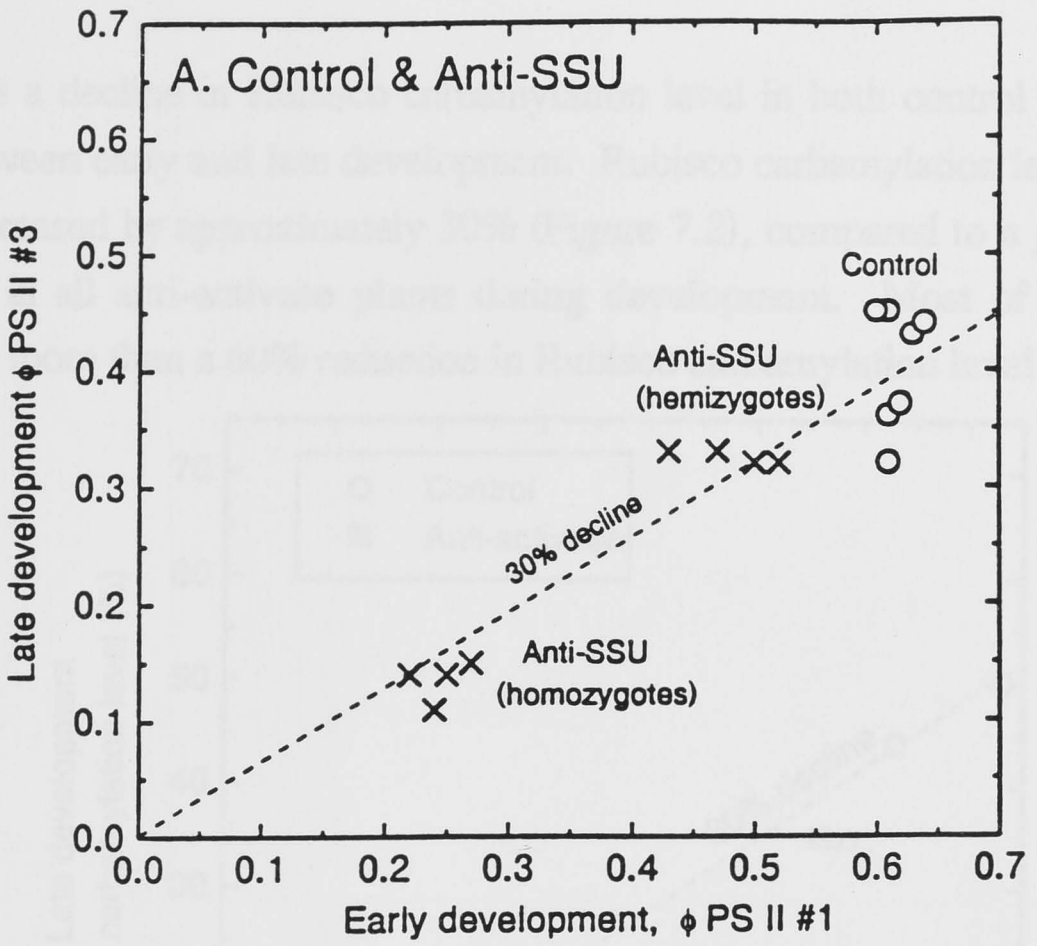

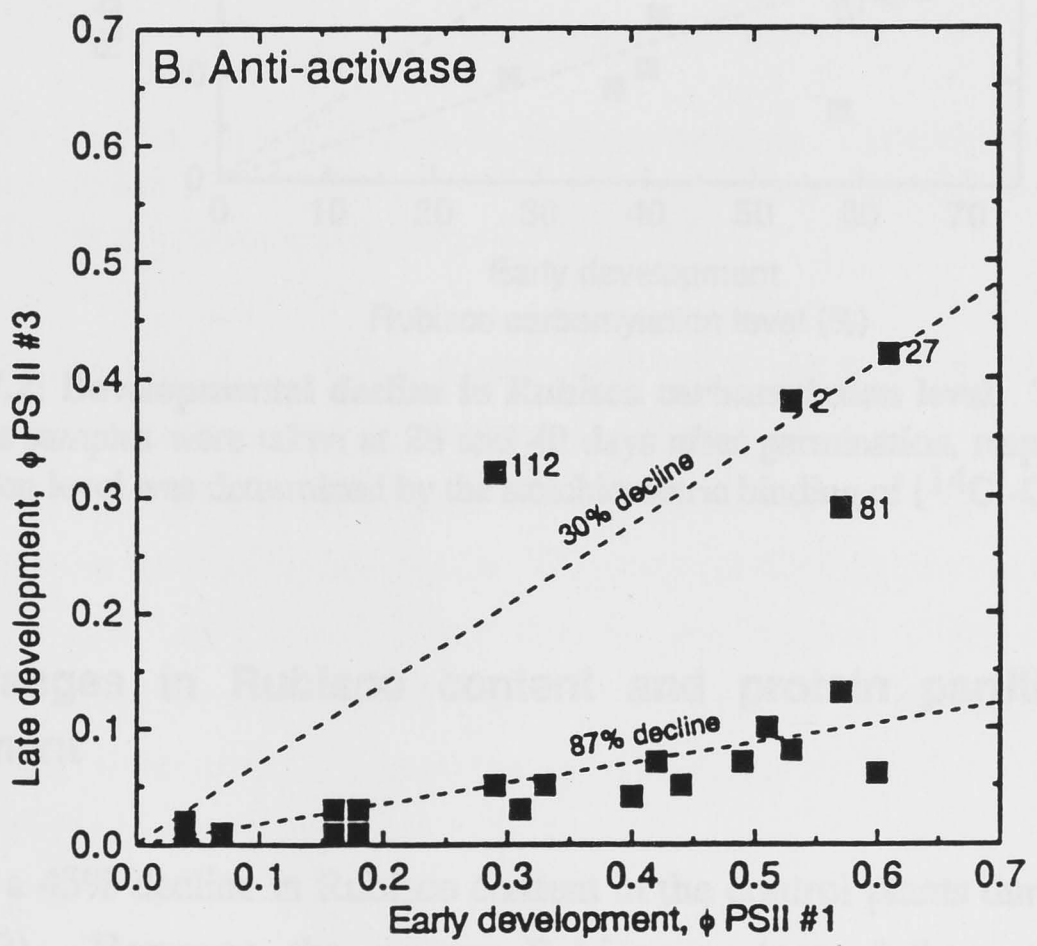

FIGURE 7.1: Developmental decline in ϕPSII. Chl fluorescence was measured at 0.03% CO_2 and 600 μmol quanta m^{-2} s^{-1}, at early (24 days after germination) and late (40 days after germination) development, ϕPSII #1 and #3 respectively. ϕPSII was calculated according to Genty et al. (1989). The hemizygote and homozygote anti-SSU plants in Figure 7.1A contain 1 and 2 T-DNA copies, respectively. The numbers in Figure 7.1B denote individual anti-activase plants.

7.3.2 Developmental decline in Rubisco carbamylation level

There was a decline in Rubisco carbamylation level in both control and anti-activase plants between early and late development. Rubisco carbamylation level in the control plants decreased by approximately 30% (Figure 7.2), compared to a greater then 30% reduction in all anti-activase plants during development. Most of the anti-activase plants had more than a 60% reduction in Rubisco carbamylation level (Figure 7.2).

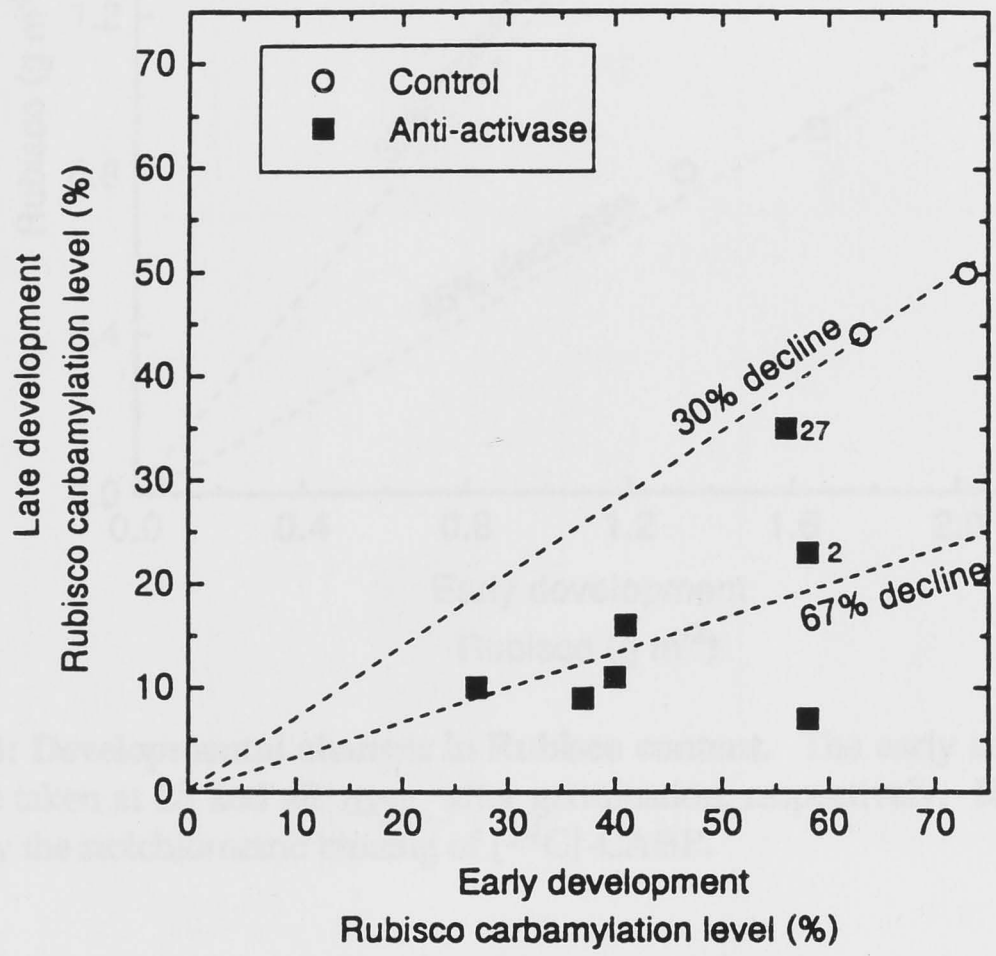

FIGURE 7.2: Developmental decline in Rubisco carbamylation level. The early and late development samples were taken at 28 and 40 days after germination, respectively. Rubisco carbamylation level was determined by the stoichiometric binding of [^{14}C]-CABP.

7.3.3 Changes in Rubisco content and protein partitioning during development

There was a 45% decline in Rubisco content in the control plants during development (Figure 7.3). However, the average Rubisco content of the anti-activase plants increased by approximately 35% during the same period (Figure 7.3). While there was little difference in the Rubisco content of the anti-activase and control leaves early in development, later the anti-activase plants had, on average, 2.5 times as much Rubisco as controls.

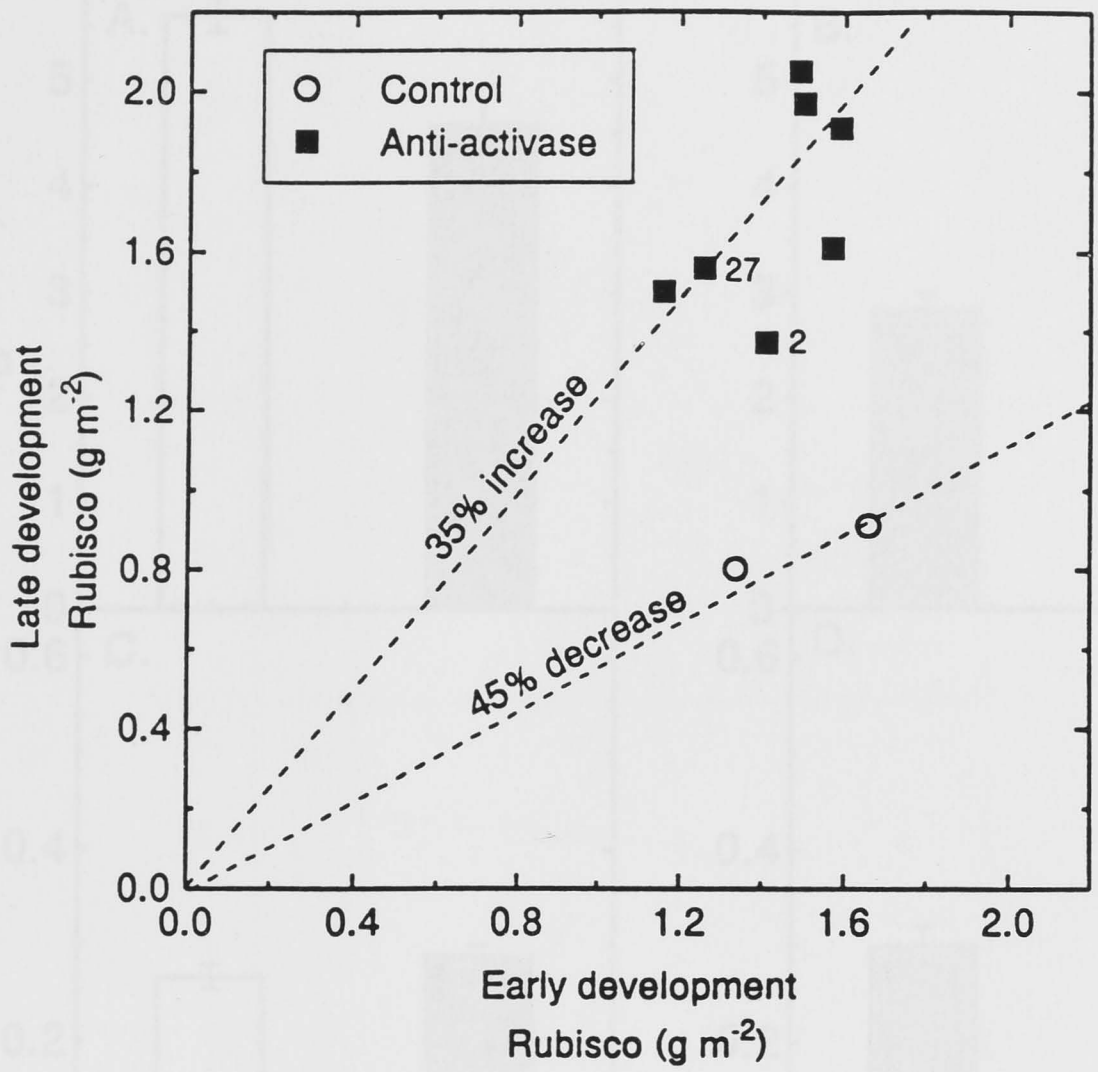

FIGURE 7.3: Developmental changes in Rubisco content. The early and late development samples were taken at 28 and 40 days after germination, respectively. Rubisco content was determined by the stoichiometric binding of [^{14}C]-CABP.

The average Rubisco and soluble protein content of control and anti-activase leaves was very similar at early development (Figures 7.3 and 7.4A, respectively), approximately 29% of leaf soluble protein was partitioned into Rubisco in both control and anti-activase leaves (Figure 7.4C). There was a 40% decline in soluble protein in both control and anti-activase plants during development (Figure 7.4B). At late development, Rubisco accounted for approximately 29% of leaf soluble protein in the control leaves, whereas it accounted for approximately 60% of leaf soluble protein in the anti-activase plants (Figure 7.4D).

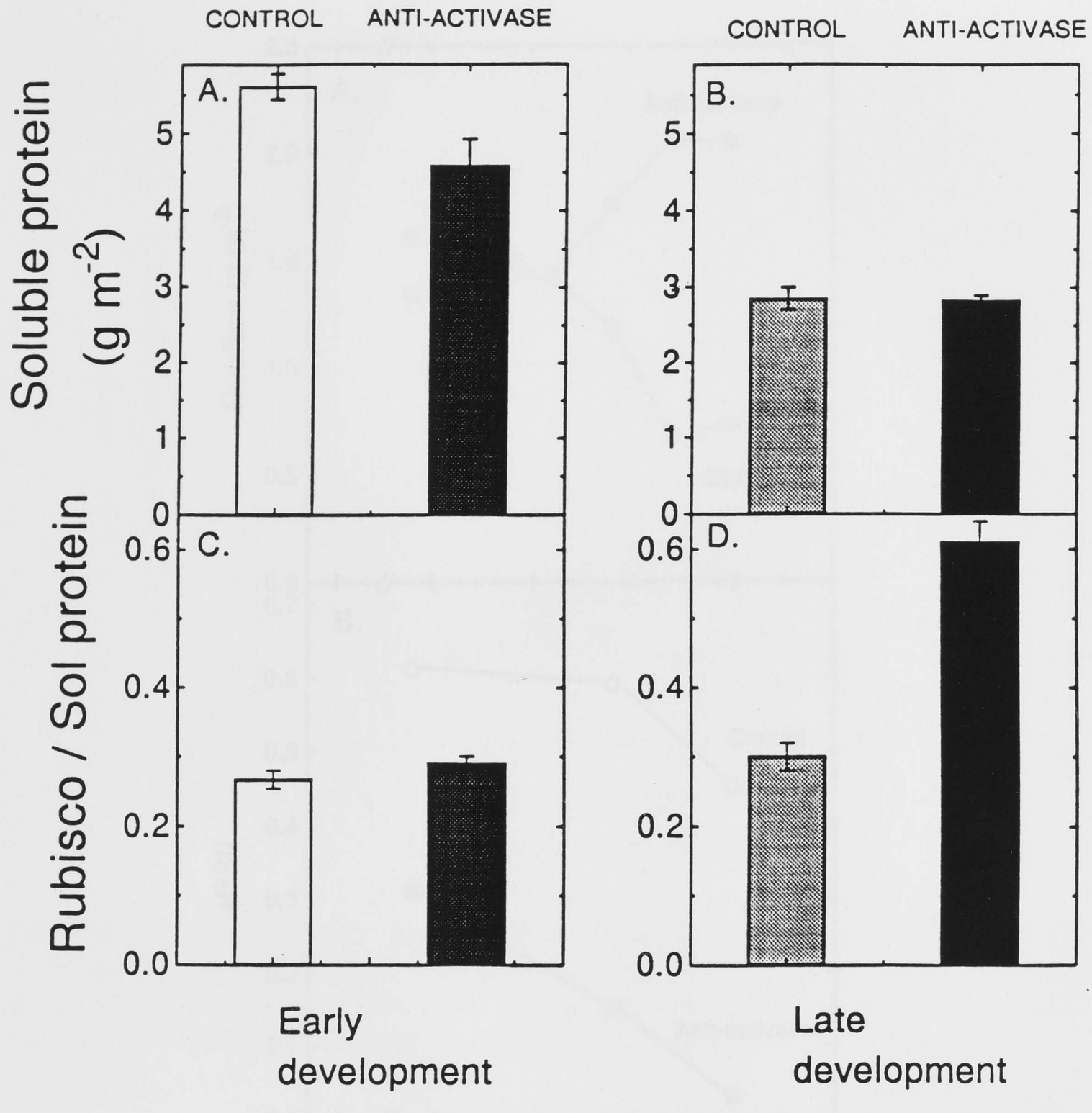

FIGURE 7.4: Developmental changes in soluble protein content and Rubisco partitioning. The early and late development samples were taken at 28 and 40 days after germination, respectively. Soluble protein content was assayed using Coomassie Blue dye, and Rubisco content was determined by the stoichiometric binding of [^{14}C]-CABP.

Changes in the Rubisco content and ϕPSII ratio of the uppermost, fully expanded leaf of a typical control and anti-activase plant were followed during development (Figure 7.5). Changes in Rubisco content became evident during intermediate development (29-35 days after germination), and became more obvious during late development (Figure 7.5A). The slight reduction in Rubisco content in the control plant during early and intermediate development did not affect its ϕPSII ratio (Figure 7.5B). The reduction in the ϕPSII ratio of the control plant occurred during intermediate and late development; whereas, there was a steady decline in the ϕPSII ratio of the anti-activase plant during early and late development (Figure 7.5B).

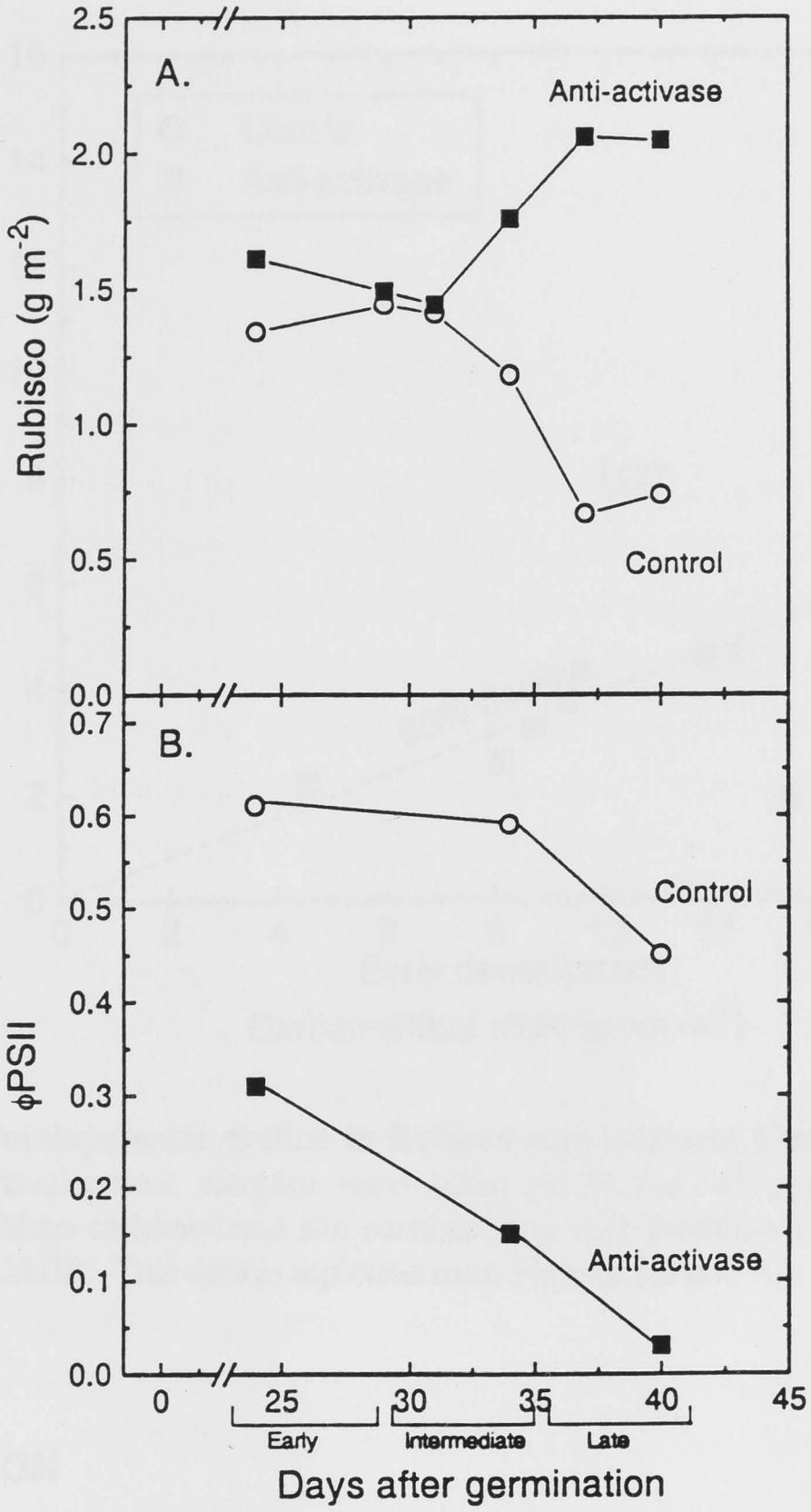

FIGURE 7.5: Rubisco content and ϕPSII in the uppermost fully expanded leaves of a typical control and anti-activase plant during development. In this figure; the first 24 to 28 days after germination are labelled as early development; 29-35 days after germination are labelled as intermediate development; and the 35+ days after germination are labelled as late development. Rubisco content was determined by the stoichiometric binding of [^{14}C]CABP, and ϕPSII was measured and calculated as outlined in Figure legend 7.1. The values given in this figure are for one control and one anti-activase plant only.

7.3.4 Decline in Rubisco carbamylated site concentration

There was a 60% decline in the Rubisco carbamylated site concentration in the leaves of control and most anti-activase plants between early and late development (Figure 7.6).

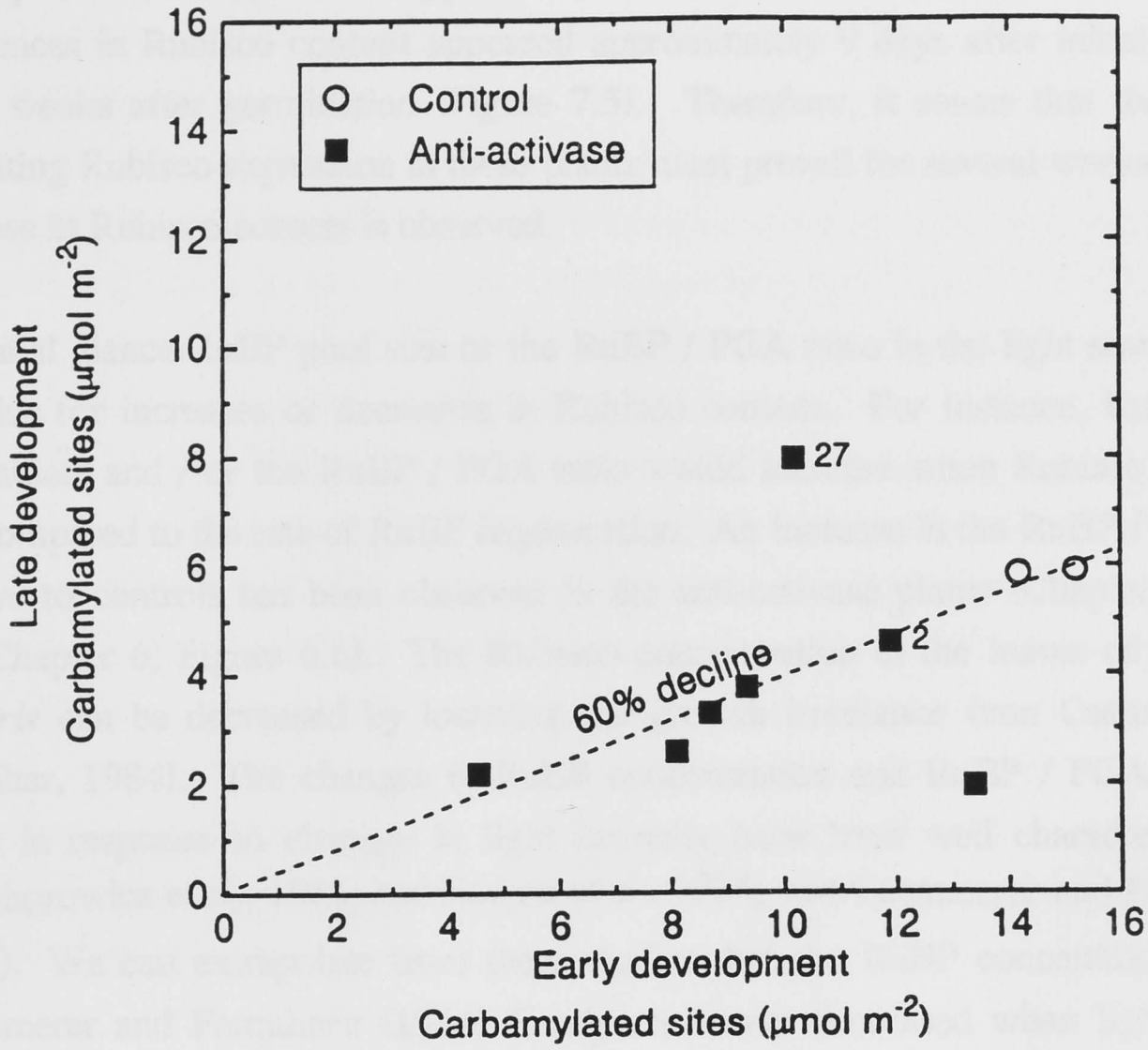

FIGURE 7.6: Developmental decline in Rubisco carbamylated site concentration. The early and late development samples were taken at 28 and 40 days after germination, respectively. Rubisco carbamylated site concentration was determined by the stoichiometric binding of [^{14}C]CABP. This data is replotted from Figures 7.2 and 7.3.

7.4 DISCUSSION

7.4.1 Rubisco increases with senescence

An increase in the partitioning of protein into Rubisco has been observed in both low-CO_2 (Chapter 5, Figure 5.9) and high-CO_2-grown (Chapter 2, Figure 2.5; Figure 7.4) anti-activase plants over time. It appears that the reduction in Rubisco carbamylation level in the anti-activase plants has been compensated by an increase in Rubisco site concentration. But what is the stimulus that allows the plants to 'sense' this and tells them to respond by increasing expression of the genes encoding Rubisco?

The increase in partitioning of soluble protein into Rubisco in the youngest, fully-expanded leaves of anti-activase plants became apparent quite late in plant

development. Assays of a typical anti-activase and control leaf indicated that differences in Rubisco content appeared approximately 9 days after initial sampling, i.e. 5 weeks after germination (Figure 7.5). Therefore, it seems that the stimulus regulating Rubisco expression in these plants must prevail for several weeks before an increase in Rubisco content is observed.

On initial glance RuBP pool size or the RuBP / PGA ratio in the light seems a likely stimulus for increases or decreases in Rubisco content. For instance, RuBP would accumulate and / or the RuBP / PGA ratio would increase when Rubisco activity is low compared to the rate of RuBP regeneration. An increase in the RuBP / PGA ratio relative to controls has been observed in the anti-activase plants (Chapter 5, Figure 5.6; Chapter 6, Figure 6.6). The Rubisco concentration in the leaves of *Phaseolus vulgaris* can be decreased by lowering the growth irradiance (von Caemmerer and Farquhar, 1984). The changes in RuBP concentration and RuBP / PGA ratio that occur in response to changes in light intensity have been well characterised (von (Perchorowicz et al., 1981; and Badger et al., 1984; von Caemmerer and Edmondson, 1986). We can extrapolate from these studies that the RuBP concentration in von Caemmerer and Farquhar's (1984) *P.vulgaris* leaves decreased when light intensity was lowered. Several days after the decrease in growth irradiance, von Caemmerer and Farquhar (1984) observed a decrease in the fully activated Rubisco activity of *Phaseolus vulgaris* leaves. Therefore, there was probably a correlation between changes in RuBP concentration and Rubisco content in these plants. A correlation between RuBP pool size and Rubisco content has been demonstrated in transgenic plants with antisense mRNA to glyceraldehyde 3-phosphate dehydrogenase. These plants have a range of RuBP concentrations in their leaves, and RuBP pool size is proportional to Rubisco content (Price et al., in press). Therefore, a strong correlation between RuBP pool size and Rubisco concentration can be demonstrated; but a cause-effect relationship has not yet been identified.

Sucrose has been identified as a potential regulator of photosynthetic parameters such as Rubisco concentration. Farrar (1992) has proposed a model in which this metabolite acts as a messenger between the source (leaves) and sink tissues (expanding leaves, elongating stems, fruit, etc.). Sucrose is well suited to this purpose because it is produced and exported by the source leaves and it is the substrate of sink metabolism. Therefore, sucrose concentration at the source and sink ends of the phloem will represent the capacity of the leaves to produce assimilate, and the capacity of the sink to utilise assimilate, respectively. In Farrar's model the plant would be able

to sense changes in sucrose concentration and as a result adjust sink and/or source strength. There are several examples in the literature that support this model of source / sink regulation.

Firstly, partial defoliation of soybean results in an increase in the Rubisco content of the remaining leaves a few days later (von Caemmerer and Farquhar, 1984). In terms of Farrar's model, partial defoliation would weaken source strength relative to the sinks, probably resulting in a decrease in sucrose concentration at both source and sink ends of the phloem. The increase in Rubisco content would increase the capacity of the leaves to produce assimilate, thereby matching the capacity for consumption of assimilate at the sinks. Conversely, a decrease in Rubisco concentration has been observed in response to high sugar concentrations in the transpiration stream (Krapp et al. 1991). Under these conditions, source strength is much greater than sink strength. According to Farrar's model, the plant may adjust the sucrose concentration by increasing the capacity of the sinks to accumulate sugars or by decreasing the production of assimilate at the source. In this example the photosynthetic capacity of the leaves was reduced.

According to this model of sink-source relations we would expect the increase in Rubisco partitioning in the anti-activase plants to be a response to low source strength, ie. a low capacity for carbohydrate production. However, if this was the case, we would not expect the increase in Rubisco content in the high-CO_2-grown anti-activase plants to be as large as the increase observed in the air-grown anti-activase plants. These plants were maintained at high CO_2 at all times except for the periods during which ϕPSII was measured and the leaf samples taken for assays of Rubisco carbamylation and content (five separate occassions of 3 - 24 hours duration). Past analysis indicates that, at high CO_2, the photosynthetic rates of the anti-activase plants are similar to those of the controls (Chapter 2, Table I) and this is consistent with the large starch pellets that were observed after extraction of the leaves from anti-activase plants grown at elevated CO_2 (data not shown) and on electron micrographs of anti-activase leaves (John Evans - personal communication). On the basis of these observations, we can assume that the carbohydrate concentration in the high-CO_2-grown anti-activase leaves was not unusually low. In source-sink terms this means that these plants were not strongly source-limited. However, there was a much larger increase in protein partitioning into Rubisco in these plants than there was in the air-grown anti-activase plants. This means that very low carbohydrate content was not the stimulus for the increase in Rubisco partitioning in these plants.

7.4.2 Decline in ϕPSII

There was a 60% reduction in the Rubisco carbamylated site concentration in control leaves during development (Figure 7.6), but their photosynthetic rate, as indicated by ϕPSII, only declined by 30% (Figure 7.1A). ϕPSII was measured at an intermediate light intensity, 600 μmol quanta m^{-2} s^{-1}. The data in the previous chapter indicates that the photosynthetic rate of the control plants during early development was limited by light at this irradiance (Chapter 6, Figure 6.2). This means that during early development the control leaves would have had more Rubisco carbamylated sites then they required to maintain maximal levels of photosynthesis at 600μmol quanta $m^{-2}s^{-1}$. The initial 30% reduction in Rubisco carbamylated site concentration probably caused a change in the limitation on photosynthetic rate in control leaves, from light-limitation to Rubisco-limitation, without necessarily reducing photosynthetic rate. If this was the case, the subsequent 30% reduction in Rubisco carbamylated site concentration would entirely account for the 30% decline in photosynthetic rate (Figure 7.1A).

Measurements of ϕPSII indicate that there was an 87% decline in the photosynthetic rate of most anti-activase leaves during development (Figure 7.1B). The 67% reduction in Rubisco carbamylated site concentration cannot account for this decline in photosynthetic rate (Figure 7.6). This raises the question, what other factor accounts for the the remaining 20% reduction in ϕPSII over time? Possible explanations for the disparity between Rubisco carbamylated site concentration and observed photosynthetic rate in the high-CO_2-grown anti-activase plants have been discussed previously (Chapter 6, Section 6.4.4). One of these possibilities was the accumulation of an inhibitor at Rubisco's catalytic sites. Inhibitor compounds are produced by Rubisco's abortive side-reactions. These compounds can bind to Rubisco's sites and block catalysis, but appear to be removed by activase (Chapter 1, Section 1.6). Perhaps these compounds accumulate in the leaves of anti-activase plants during development, thereby contributing to the decline in photosynthetic rate.

It is interesting to note that the decline in photosynthetic rate was much more severe in the anti-activase plants than it was in the anti-SSU plants (Figure 7.1). The anti-SSU plants had relatively low ϕPSII ratios at early development and photosynthesis in these plants was probably limited by their Rubisco carbamylated site concentration (as indicated by an elevated RuBP / PGA ratio compared to controls, see Chapter 6, Section 6.4.3). However, as these plants aged they only showed a 25% decline in

photosynthetic rate over time, which is approximately the same as the rate of decline in the controls. The slower rate of decline in photosynthetic rate in the anti-SSU plants than the anti-activase plants is probably due to a lesser reduction in Rubisco carbamylated site concentration during development, but unfortunately the Rubisco carbamylated site concentration in the anti-SSU plants was not measured.

7.4.3 What stimulates reductions in Rubisco carbamylation level during development?

High concentrations of starch were accumulated in the leaves of both control and activase-deficient plants grown in CO_2-enriched atmosphere (data not shown). This may have been the result of sink strength being relatively low compared to source strength. The overproduction of sugars and starch at high CO_2 may have stimulated a reduction in source strength, resulting in the 30% decline in Rubisco carbamylation level and 45% decline in Rubisco content in the control plants during development. Sawada et al. (1990) observed that Rubisco deactivates in sink-limited leaves, probably due to depletion of the inorganic phosphate pool. Low inorganic phosphate concentrations may also have been responsible for the decline in Rubisco carbamylation in the control leaves grown at high CO_2. However, the reduction in Rubisco carbamylation level in the anti-activase plants was much larger then in the controls (60% decline, Figure 7.2). Therefore, it is unlikely that the reduction in Rubisco carbamylation level in anti-activase leaves was entirely due to high source strength (ie. overproduction of sugars and starch).

The large decline in photosynthetic rate in the anti-activase plants may be due to a reduction in the stoichiometry of activase to Rubisco. Analysis of plants early in development has shown that Rubisco carbamylation is only reduced in those plants with a greater than 80% reduction in activase content (Chapter 6, Figure 6.4A). However, as the anti-activase plants aged, the Rubisco content in some plants increased and, as a result, higher concentrations of activase might be needed to maintain the levels of Rubisco carbamylation observed earlier in development. The anti-activase plants would be unable to produce more activase under these conditions due to the effect of the antisense gene(s). The decline in soluble protein and the increase in partitioning of soluble protein into Rubisco also would have contributed to the decrease in the relative concentration of activase to Rubisco. Alternatively, the reduction in Rubisco carbamylation level in the anti-activase plants may be due to the

accumulation of an inhibitor that binds more tightly to Rubisco's inactive sites then it does to Rubisco's carbamylated sites. In the absence of activase, this may shift the equilibrium of the carbamylation reaction towards the inactive form.

7.4.4 Conclusions

The large increase in Rubisco content in the leaves of anti-activase plants grown at elevated CO_2 during development raises many questions about the processes regulating protein partitioning. It is difficult to draw conclusions about the type and intensity of stimulus required to produce changes in Rubisco content based on our current knowledge. However, a future comparison of the high-CO_2-grown and air-grown anti-activase plants and quantitative analysis of their reducing sugar and triose-phosphate concentrations may elucidate the key metabolites involved in regulating Rubisco content.

CHAPTER 8: Future research directions

Reduction of activase levels in tobacco by antisense RNA and the subsequent analyses of these plants has enabled us to answer several questions about the roles and mechanisms of activase. For example, we now know that activase has an important role in accelerating the release of the inhibitor, CA1P, from Rubisco's carbamylated sites with the onset of illumination (Chapter 3); and we also know that activase is a catalyst of sugar phosphate release from Rubisco, rather then a ligand or missing subunit of Rubisco (Chapter 5). However, the analyses of the activase-deficient plants have also raised several interesting questions about the processes regulating Rubisco activity *in vivo*.

Rubisco activity *in vivo* can be modulated by Rubisco carbamylation level, Rubisco content and the concentration of inhibitors, such as CA1P, which bind to Rubisco's sites and inhibit catalysis. In the late stages of plant development, the activase-deficient plants accumulated higher concentrations of Rubisco, and partitioned more of their protein into Rubisco then did the control plants (Chapters 5 and 7). These results indicated that the low Rubisco carbamylation level in the activase-deficient plants may have been compensated by an increase in Rubisco site concentration. We have not yet identified the signal that resulted in this increase in partitioning of protein into Rubisco. However, future analysis of these plants may enable us to identify this 'signal' and allow study of the processes regulating the expression of the gene encoding Rubisco.

The observed photosynthetic rates of the activase-deficient plants grown at elevated CO_2 were much less than expected based on measures of Rubisco carbamylated site content (Chapters 2 and 6). It is interesting to speculate on the possible explanations for this result. *In vitro* studies indicate that activase's role is to remove sugar phosphates from Rubisco's catalytic sites (Chapter 1, Section 1.6). Therefore, the disparity between observed and expected photosynthetic rates in the activase-deficient plants may be due to the accumulation of an inhibitor at Rubisco's carbamylated sites. The maximum catalytic turnover rate (k_{cat}) in the control and anti-activase plants was similar in the light (Chapter 3). Therefore, if an inhibitor is responsible, it must be loosely enough bound to be lost from Rubisco's catalytic sites during extraction and subsequent incubation with high concentrations of CO_2 and Mg^{2+}. This means that the tight-binding fallover inhibitor, XuBP, is not likely to be responsible for the disparity between observed and expected photosynthetic rate in the activase-deficient plants. However, recent studies indicate that Rubisco's abortive side-reactions produce other compounds (Morell et al., in press). These might remain associated

with Rubisco in the absence of activase. This possibility could be investigated using high pressure liquid chromatography (HPLC) techniques which have already been developed (Morell et al., in press).

There are several aspects of the light-regulation of Rubisco carbamylation that we have not yet investigated using the anti-activase plants. Relatively little is known about the factors regulating changes in Rubisco carbamylation level (Chapter 1, Section 1.10). However, one of the possibilities is that activase activity is a direct determinant of Rubisco carbamylation level. In Chapter 6, Section 6.4.1., I discussed how the anti-SSU plants could be used to investigate this possibility. The anti-activase plants also provide us with a useful tool for investigating the processes regulating Rubisco carbamylation level. In future experiments, it would be interesting to measure Rubisco carbamylation levels and photosynthetic rates of activase-deficient plants over a range of irradiances. This may provide some insight into the importance of activase in the light-regulation of carbamylation. It will also be interesting to study the effect of activase-deficiency on Rubisco carbamylation level under non-steady state conditions. The results presented in Chapter 5 indicated that activase was present at twenty-fold excess to the concentration required to maintain steady-state Rubisco carbamylation levels. However, the apparently high concentrations of activase in the wild-type plants may be beneficial in facilitating quick changes in Rubisco carbamylation under non steady-state conditions.

Future experimentation with these plants will enable us to learn more about the role of activase in the light-regulation of carbamylation and the maintenance of Rubisco activity *in vivo*.

BIBLIOGRAPHY

Andrews TJ, Lorimer GH (1987) Rubisco: Structure, mechanisms and prospects for improvement. *In* MD Hatch, NK Boardmen, eds, The Biochemistry of Plants, Academic Press, New York, pp 132-219

Badger MR, Sharkey TD, von Caemmerer S (1984) The relationship between steady-state gas exchange of leaves and the levels of carbon reduction cycle intermediates. Planta **160**: 305-313

Badger MR, Lorimer GH (1981) Interaction of sugar phosphates with the catalytic site of ribulose-1,5-bisphosphate carboxylase. Biochem **20**: 2219-2225

Brändén CI (1990) Founding fathers and families. Nature **346**: 607-608

Brooks A (1986) Effects of phosphorus nutrition on ribulose-1,5-bisphosphate carboxylase activation, photosynthetic quantum yield and amounts of some Calvin cycle metabolites in spinach leaves. Aust J Plant Physiol **13**: 221-237

Brooks A, Portis AR, Jr., Sharkey TD (1988) Effects of irradiance and methyl viologen treatment on ATP, ADP and activation of ribulose bisphosphate carboxylase in spinach leaves. Plant Physiol **88**: 850-853

Brugnoli E, Hubick KT, von Caemmerer S, Wong SC, Farquhar GD (1988) Correlation between the carbon isotope discrimination in leaf starch and sugars of C_3 plants and the ratio of intercellular and atmospheric partial pressure of carbon dioxide.. Plant Physiol **88**: 1418-1424

Buchanan BB (1980) Role of light in the regulation of chloroplast enzymes. Annu Rev Plant Physiol Plant Mol Biol **31**: 341-374

Butz ND, Sharkey TD (1989) Activity ratios of ribulose bisphosphate carboxylase accurately reflect carbamylation ratios. Plant Physiol **89**: 735-739

Campbell WJ, Ogren WL (1990a) A novel role for light in the activation of ribulosebisphosphate carboxylase/oxygenase. Plant Physiol **92**: 110-115

Campbell WJ, Ogren WL (1990b) Electron transport through photosystem I stimulates light activation of ribulose bisphosphate carboxylase/oxygenase by rubisco activase. Plant Physiol **94**: 470-484

Campbell WJ, Ogren WL (1992) Light activation of Rubisco by Rubisco activase and thylakoid membranes. Plant Cell Physiol **33(6)**: 751-756

Collatz GJ, Badger MR, Smith C, Berry JA (1978) A radioimmune assay for RuP2 carboxylase protein. Carnegie Inst Wash Year Book **78**: 171-175

Curmi PMG, Schreuder H, Cascio D (1991) Rubisco- X-ray snapshots of nature's carbon fixating enzyme. Today's Life Science **3**: 24-32.

Does MP, Dekker BMM, de Groot MJA, Offringa R (1991) A quick method to establish the T-DNA copy number in transgenic plants at an early stage after transformation, using inverse PCR. Plant Molecular Biology **17**: 151-153

Edmondson D, Kane HJ, Andrews TJ (1990a) Substrate isomerization inhibits ribulosebisphosphate carboxylase-oxygenase during catalysis. FEBS Lett **260**: 62-66

Edmondson DL, Badger MR, Andrews TJ (1990b) Slow inactivation of ribulosebisphosphate carboxylase during catalysis is caused by accumulation of a slow, tight-binding inhibitor at the catalytic site. Plant Physiol **93**: 1390-1397

Ellis RJ (1979) The most abundant protein in the world. Trends Biochem Sci **4**: 241-244

Esau B, Snyder G, Portis AR, Jr., Ogren WL (1991) Abstracts of the American Society of Plant Physiologists: Localization of the two activities of spinach activase (#332). Plant Physiol **96**: Supplement p.50

Farrar JF (1992) The whole plant: carbon partitioning during development. *In* CJ Pollock, JF Farrar, AJ Gordon, eds, Carbon partitioning, within and between organisms, BIOS Scientific Publishers Lmtd., Environmental Plant Biology Series, pp 163-179

Flaherty KM, DeLuca-Flaherty C, McKay DB (1990) Three-dimensional structure of the ATPase fragment of a 70K heat-shock cognate protein. Nature **346**: 623-628

Genty B, Briantais JM, Baker NR (1989) The relationship between the quantum yield of photosynthetic electron transport and quenching of chlorophyll fluorescence. Biochim Biophys Acta **990**: 87-92

Grierson D (1993) Possible mechanisms for the inhibition of plant gene expression with sense and antisense genes. Abstracts of the Australian Society for Biochemistry and Molecular Biology **25**: 79

Harlow E, Lane D 1988 *Antibodies: A laboratory manual.* Cold Spring Harbour Publications, NY.

Hatch AL, Jensen RG (1980) Regulation of ribulose-1,5-bisphosphate carboxylase from tobacco: changes in pH response and affinity for CO_2 and Mg^{2+} induced by chloroplast intermediates. Arch Biochem Biophys **205**: 587-591

Heber U, Takahama U, Neimanis S, Shimizu-Takahama M (1982) Transport as the basis of the Kok effect. Levels of some photosynthetic intermediates and activation of light regulated enzymes during photosynthesis of chloroplasts and green leaf protoplasts. Biochem Biophys Acta **679**: 289-299

Heldt HW, Chon CJ, Lorimer GH (1978) Phosphate requirement for the light activation of ribulosebisphosphate carboxylase in intact spinach chloroplasts. FEBS Lett **92**: 234-240

Herrera-Estrella L, Simpson J (1988) Foreign gene expression in plants. *In* CH Shaw ed, Plant Molecular Biology. A Practical Approach., IRL Press, Oxford, pp 131-160

Hewitt EJ, Smith TA (1975) Plant Mineral Nutrition. English University Press: England

Hudson GS, Dengler RE, Hattersley PW, Dengler NG (1992a) Cell-specific expression of Rubisco small-subunit and Rubisco activase genes in C_3 and C_4 species of *Atriplex*. Aust J Plant Physiol **19**: 89-96

Hudson GS, Evans JR, von Caemmerer S, Arvidsson YBC, Andrews TJ (1992b) Reduction of ribulose-1,5-bisphosphate carboxylase/oxygenase content by antisense RNA reduces photosynthesis in transgenic tobacco plants. Plant Physiol **98**: 294-302

Jackson RB, Woodrow IE, Mott KA (1991) Non-steady state photosynthesis following an increase in photon flux density (PFD). Effects of magnitude and duration of initial PFD. Plant Physiol **95**: 498-503

Jefferson RA, Kavanagh TA, Bevan MW (1987) GUS fusions: β-glucuronidase as a sensitive and versatile gene fusion marker in higher plants. EMBO J **6**: 3901-3907

Jensen RG, Bahr JT (1977) Ribulose 1,5-bisphosphate carboxylase-oxygenase. Annu Rev Plant Physiol **28**: 379-400

Jiang CZ, Rodermel SR, Shibles RM (1993) Photosynthesis, Rubisco activity and amount, and their regulation by transcription in senescing soybean leaves. Plant Physiol **101**: 105-112

Jordan DB, Chollet R (1983) Inhibition of ribulose bisphosphate carboxylase by substrate ribulose-1,5-bisphosphate. J Biol Chem **258**: 13752-13758

Jordan DB, Chollet R, Ogren WL (1983) Binding of phosphorylated effectors by active and inactive forms of ribulose-1,5-bisphosphate carboxylase. Biochem **22**: 3410-3418

Jordan DB, Ogren WL (1981) A sensitive assay procedure for simultaneous determination of ribulose-1,5-bisphosphate carboxylase and oxygenase activities. Plant Physiol **67**: 237-245

Kirschbaum MUF, Pearcy RW (1988) Gas exchange analysis of the relative importance of stomatal and biochemical factors in photosynthetic induction in *Alocasia macrorrhiza*. Plant Physiol **86**: 782-785

Kobza J, Seemann JR (1988) Mechanisms for light-dependent regulation of ribulose-1,5-bisphophate carboxylase activity and photosynthesis in intact leaves. Proc Natl Acad Sci USA **85**: 3815-3819

Krapp A, Quick WP, Stitt M (1991) Ribulose-1,5-bisphosphate carboxylase / oxygenase, other Calvin-cycle enzymes, and chlorophyll decrease when glucose is supplied to mature spinach leaves via the transpiration stream. Planta **186**: 58-69

Laing WA, Christeller JT (1976) A model for the kinetics of activation and catalysis of ribulose 1,5-bisphosphate carboxylase. Biochem J **159**: 563-570

Lan Y, Mott KA (1991) Determination of apparent K_m values for ribulose-1,5-bisphosphate carboxylase/oxygenase activase using the spectrophotometric assay of rubisco activity. Plant Physiol **95**: 604-609

Lan Y, Woodrow IE, Mott KA (1992) Light-dependent changes in ribulose bisphosphate carboxylase activase activity in leaves. Plant Physiol **99**: 304-309

Leegood RC, von Caemmerer S (1988) The relationship between contents of photosynthetic metabolites and the rate of photosynthetic carbon assimilation in the leaves of *Amaranthus edulis* L. Planta **174**: 253-262

Leff SE, Rosenfeld MG, Evans RM (1986) Complex transcriptional units: diversity in gene expression by alternative RNA processing. Annu Rev Biochem **55**: 1091-1117

Lorimer GH (1979) Evidence for the existence of discrete activator and substrate sites for CO_2 on ribulose-1,5-bisphosphate carboxylase. J Biol Chem **254**: 5599-5601

Lorimer GH, Badger MR, Andrews TJ (1976) The activation of ribulose-1,5-bisphosphate carboxylase by carbon dioxide and magnesium ions. Equilibria, kinetics, a suggested mechanism, and physiological implications.. Biochem **15**: 529-536

Lorimer GH, Miziorko HM (1980) Carbamate formation on the ϵ-amino group of a lysyl residue as the basis for the activation of ribulose bisphosphate carboxylase by CO_2 and Mg^{2+}. Biochem **19**: 5321-5328

Mächler F, Nösberger J (1980) Regulation of ribulose bisphosphate carboxylase activity in intact wheat leaves by light, CO_2, and temperature. J Expt Bot **31**: 1485-1491

Mächler F, Nösberger J (1984) Influence of inorganic-phosphate on photosynthesis of wheat chloroplasts. II. Ribulose-bisphosphate carboxylase activity. J Expt Bot **35**: 488-494

Makino A, Mae T, Ohira K (1983) Photosynthesis and ribulose-1,5-bisphosphate carboxylase in rice leaves. Changes in photosynthesis and enzymes involved in carbon assimilation from leaf development through senescence. Plant Physiol **73**: 1002-1007

Miziorko HM (1979) Ribulose bisphosphate carboxylase. Evidence in support of the existence of distinct CO_2 activation and CO_2 substrate sites.. J Biol Chem **245**: 270-272

Miziorko HM, Lorimer GH (1983) Ribulose-1,5-bisphosphate carboxylase / oxygenase. Ann Rev Biochem **5**: 507-535

Morell MK, Paul K, Kane HJ, Andrews TJ (1992) Rubisco: Maladapted or misunderstood? Aust J Bot **40**: 431-441

Morell MK, Paul K, O'Shea NJ, Kane HJ, Andrews TJ (in press) Mutations of an active site threonyl residue promote β-elimination and other side reactions of the enediol intermediate of the ribulose bisphosphate carboxylase reaction. J Biol Chem

Mott KA, Jensen RG, O'Leary JW, Berry JA (1984) Photosynthesis and ribulose 1,5-bisphosphate concentrations in intact leaves of *Xanthium strumarium* L.. Plant Physiol **76**: 968-971

Mott KA, Woodrow IE (1993) Effects of O_2 and CO_2 on nonsteady-state photosynthesis. Further evidence for ribulose-1,5-bisphosphate carboxylase/oxygenase limitation. Plant Physiol **102**: 859-866

Orozco BM, Robertson-McClung C, Werneke JM, Ogren WL (1993) Molecular basis of the ribulose-1,5-bisphosphate carboxylase/oxygenase activase mutation in *A.thaliana* is a guanine-to-adenine transition at the 5'-splice junction of intron 3. Plant Physiol **102**: 227-232

Osmond CB (1981) Photo-respiration and photoinhibition, some implications for the energetics of photosynthesis. BIOC BIOP A **639**: 77-98

Parry MAJ, Keys AJ, Foyer CH, Furbank RT, Walker DA (1988) Regulation of ribulose-1,5-bisphosphate carboxylase activity by the activase system in lysed spinach chloroplasts. Plant Physiol **87**: 558-561

Perchorowicz JT, Raynes DA, Jensen RG (1981) Light limitation of photosynthesis and activation of ribulose bisphosphate carboxylase in wheat seedlings. Proc Natl Acad Sci USA **78**: 2985-2989

Porter MA, Milanez S, Stringer CD, Hartman FC (1986) Purification and characterisation of ribulose-5-bisphosphate kinase from spinach. Arch Biochem Biophys **245**: 14-23

Portis AR, Jr. (1990) Rubisco activase. Biochem Biophys Acta **1015**: 15-28

Portis AR, Jr. (1992) Regulation of ribulose 1,5-bisphosphate carboxylase/oxygenase activity. Annu Rev Plant Physiol **43**: 415-437

Portis AR, Jr., Salvucci ME, Ogren WL (1986) Activation of ribulosebisphosphate carboxylase/oxygenase at physiological CO_2 and ribulosebisphosphate concentrations by rubisco activase. Plant Physiol **82**: 967-971

Price GD, Evans JR, von Caemmerer S, Yu J, Badger MR (in press) Specific reduction of chloroplast glyceraldehyde-3-phosphate dehydorgenase activity by antisense RNA reduces CO_2 assimilation via a reduction in RuBP regeneration in trangenic tobacco plants. Planta

Qian J, Rodermel SR (1993) Ribulose-1,5-bisphosphate carboxylase/oxygenase activase cDNAs from *Nicotiana tabacum*. Plant Physiol **102**: 683-684

Robinson SP, Portis AR, Jr. (1988a) Release of the nocturnal inhibitor, carboxyarabinitol-1-phosphate, from ribulose bisphosphate carboxylase/oxygenase by rubisco activase. FEBS Letters **233**: 413-416

Robinson SP, Portis AR, Jr. (1988b) Involvement of stromal ATP in the light activation of ribulose-1,5-bisphosphate carboxylase-oxygenase in intact isolated chloroplasts.. Plant Physiol **86**: 293-298

Robinson SP, Portis AR, Jr. (1989a) Ribulose-1,5-bisphosphate carboxylase/oxygenase activase protein prevents the in vitro decline in activity of ribulose-1,5-bisphosphate carboxylase/oxygenase. Plant Physiol **90**: 968-971

Robinson SP, Portis AR, Jr. (1989b) Adenosine triphosphate hydrolysis by purified rubisco activase. Arch Biochem Biophys **268**: 93-99

Robinson SP, Streusand VJ, Chatfield JM, Portis AR, Jr. (1988) Purification and assay of Rubisco activase from leaves. Plant Physiol **88**: 1008-1014

Rodermel SR, Abbott MS, Bogorad L (1988) Nuclear-organelle interactions: Nuclear antisense gene inhibits ribulose bisphosphate carboxylase enzyme levels in transformed tobacco plants. Cell **55**: 673-681

Roitt, I. 1980 *Essential Immunlogy*. Blackwell, Oxford, England, Ed.4. pp 173-196

Rundle SJ, Zielenski RE (1991) Organization and expression of two tandemly oriented genes encoding ribulosebisphosphate carboxylase/oxygenase activase in barley. J Biol Chem **266**: 4677-4685

Sage RF, Sharkey TD, Seemann JR (1990) Regulation of ribulose-1,5-bisphosphate carboxylase activity in response to light intensity and CO_2 in the C_3 annuals *Chenopodium album* L. and *Phaseolus vulgaris* L.. Plant Physiol **94**: 1735-1742

Saghai-Maroof MA, Soliman KM, Jorgensen RA, Allard RW (1984) Ribosomal DNA spacer-length polymorphisms in barley: Mendelian inheritance, chromosomal location, and population dynamics. Proc Natl Acad Sci USA **81**: 8014-8018

Salvucci ME (1992) Subunit interactions of Rubisco activase: Polyethylene glycol promotes self-association, stimulates ATPase and activation activities and enhances interactions with Rubisco. Arch Biochem Biophys **298**: 688-696

Salvucci ME, Portis AR, Jr., Ogren WL (1986) Light and CO_2 response of ribulose-1,5-bisphosphate carboxylase/oxygenase activation in *Arabidopsis* leaves. Plant Physiol **80**: 655-659

Salvucci ME, Portis AR, Jr., Ogren WL (1985) A soluble chloroplast protein catalyzes ribulose-bisphosphate carboxylase/oxygenase activation *in vivo*. Photosynth Res **7**: 193-201

Salvucci ME, Werneke JM, Ogren WL, Portis AR, Jr. (1987) Purification and species distribution of Rubisco activase. Plant Physiol **84**: 930-936

Sawada S, Usada H, Hasegawa Y, Tsuki T (1990) Regulation of ribulose-1,5-bisphosphate carboxylase activity in response to changes in the source / sink balance in single-rooted soybean leaves: the role of inorganic orthophosphate in activation of the enzyme. Plant Cell Physiol. 31 (5): 697-704

Schneider G, Lindqvist Y, Brändén C (1992) Rubisco: Structure and Mechanism. Ann Rev Biophys Biomol Struct **21**: 119-143

Seemann JR, Berry JA, Freas SM, Krump MA (1985) Regulation of ribulose-bisphosphate carboxylase activity *in vivo* by a light-modulated inhibitor of catalysis. Proc Natl Acad Sci USA **82**: 8024-8028

Seemann JR, Kobza J, Moore B (1990) Metabolism of 2-carboxyarabinitol 1-phosphate and regulation of ribulose-1,5-bisphosphate carboxylase activity. Photosynth Res **23**: 119-130

Servaites JC (1990) Inhibition of ribulose 1,5-bisphosphate carboxylase/oxygenase by 2-carboxyarabinitol-1-phosphate. Plant Physiol **92**: 867-870

Shen JB, Orozco EM, Jr., Ogren WL (1991) Expression of the two isoforms of spinach ribulose 1,5-bisphosphate carboxylase activase and essentiality of the conserved lysine in the consensus nucleotide-binding domain. J Biol Chem **266**: 8963-8968

Smith CJS, Watson C, F., Bird CR, Ray J, Schuch W, Grierson D (1988) Antisense RNA inhibition of polygalacturonase gene expression in transgenic tomatoes. Nature **334**: 724-726

Smith DB, Johnson KS (1981) Single-step purification of polypeptides expressed in Ecoli as fusions with glutathione S-transferase. Gene **67**: 31-40

Somerville CR, Portis AR, Jr., Ogren WL (1982) A mutant of *Arabidopsis thaliana* which lacks activation of RuBP carboxylase *in vivo*. Plant Physiol **70**: 381-387

Streusand VJ, Portis AR, Jr. (1987) Rubisco activase mediates ATP-dependent activation of ribulose bisphosphate carboxylase. Plant Physiol **85**: 152-154

von Caemmerer S, Edmondson DL (1986) Relationship between steady-state gas exchange, *in vivo* ribulose bisphosphate carboxylase activity and some carbon reduction cycle intermediates in *Raphanus sativus*. Aust J Plant Physiol **13**: 669-688

von Caemmerer S, Evans JR, Hudson GS, Andrews TJ (in press) The kinetics of Rubisco *in vivo* inferred from measurements of photosynthesis in leaves of transgenic tobacco with reduced Rubisco content. Planta

von Caemmerer S, Farquhar GD (1981) Some relationships between the biochemistry of photosynthesis and the gas exchange of leaves. Planta **153**: 376-387

von Caemmerer S, Farquhar GD (1984) Effects of partial defoliation, changes of irradiance during growth, short-term water stress and growth at enhanced p(CO_2) on the photosynthetic capacity of leaves of *Phaseolus vulgaris* L.. Planta **160**: 320-329

Vu CV, Allen LH, Bowes G (1984) Dark/Light modulation of ribulose bisphosphate carboxylase activity in plants from different photosynthetic categories. Plant Physiol **76**: 843-845

Vu CV, Allen LH, Jr., Bowes G (1983) Effects of light and elevated atmospheric CO_2 on the ribulose bisphosphate carboxylase activity and ribulose bisphosphate level of soybean leaves. Plant Physiol **73**: 729-734

Wang Z, Portis AR, Jr. (1992) Dissociation of ribulose-1,5-bisphosphate bound to ribulose-1,5-bisphosphate carboxylase/oxygenase and its enhancement by ribulose-1,5-bisphosphate carboxylase/oxygenase activase-mediated hydrolysis of ATP. Plant Physiol **99**: 1348-1353

Wang Z, Ramage B, Portis AR, Jr. (1991) Abstracts of the American Society of Plant Physiologists: Specificity in the interaction between Rubisco activase and Rubisco from different species (#330). Plant Physiol **96** Supplement p.49

Wang Z, Snyder GW, Esau BD, Portis AR, Jr., Ogren WL (1992) Species-dependent variation in the interaction of substrate-bound ribulose-1,5-bisphosphate carboxylase/oxygenase (Rubisco) and Rubisco activase. Plant Physiol **100**: 1858-1862

Weir, D.M. 1986 *Handbook of Experimental Immunology. Volume 3. Genetics and Molecular Immunlogy*. Blackwell Scientific Publications, Oxford, England, Ed.4. pp 98.7

Werneke JM (1989) Thesis **Uni. of Ilinois**: Urbana-Illinois

Werneke JM, Zielenski RE, Ogren WL (1988) Structure and expression of spinach leaf cDNA-encoding ribulosebisphosphate carboxylase oxygenase activase. Proc Natl Acad Sci USA **85**: 787-791

Werneke JM, Chatfield JM, Ogren WL (1989) Alternative mRNA splicing generates the two ribulosebisphosphate carboxylase/oxygenase activase polypeptides in spinach and *Arabidopsis*. The Plant Cell **1**: 815-825

Werneke JM, Ogren WL (1989) Structure of an *Arabidopsis thaliana* cDNA encoding rubisco activase. Nucl Acids Res **17**: 2871

Woodrow IE, Berry JA (1988) Enzymatic regulation of photosynthetic CO_2 fixation in C_3 plants. Annu Rev Plant Physiol Plant Mol Biol **39**: 533-594

Woodrow IE, Mott KA (1992) Biphasic activation of ribulose bisphosphate carboxylase in spinach leaves as determined from non steady-state CO_2 exchange. Plant Physiol **99**: 298-303

Zhu G, Jensen RG (1991) Xylulose bisphosphate synthesized by ribulose bisphosphate carboxylase/oxygenase during catalysis binds to decarbamylated enzyme. Plant Physiol **97**: 1348-1353

Zielinski RE, Werneke JM, Jenkins ME (1989) Coordinate expression of rubisco activase and rubisco during barley leaf cell development. Plant Physiol **90**: 516-521